UNIVERSITI SAINS MALAYSIA

Laporan Akhir Projek Penyelidikan Jangka Pendek

Pilot Plant Studies For Treatment Of Palm Oil Mill Effluent (POME) Using Membrane Technology

by
Prof. Abdul Latif Ahmad
Prof. Subhash Bhatia

2007

LAPORAN AKHIR PROJEK PENYELDIKAN

Tajuk Projek

Pilot Plant Studies For Treatment Of Palm Oil Mill Effluent (POME) Using Membrane Technology

Ketua Projek

PROF. ABDUL LATIF AHMAD

Ahli-Ahli

PROF. SUBHASH BHATIA

Pusat Pengajian Kejuruteraan Kimia
Kampus Kejuruteraan
Universiti Sains Malaysia

2007

ACKNOWLEDGEMENT

Special Thanks

to

YAYASAN FELDA

for their financial support of this project

TABLE OF CONTENT

ABSTRACT

The discharge of Palm Oil Mill Effluent (POME) into the environment leads to serious pollution problems and the membrane based POME treatment process has been suggested as the solution. The present research proposed an optimized industrial scale membrane based POME treatment plant design based on the experimental data obtained from the pilot plant study.

The proposed direct flocculation process has proven that the organic dual polymers could replace Alum in POME treatment with 3.6 times lower cost. The optimum cationic polymer dosage was 300mg/L at stirring of 200rpm for 3min and the optimum anionic polymer dosage was 50mg/L at stirring of 150rpm for 1min. The direct flocculation shows high treatment efficiency with 99.7%, 58.0%, 99.7% and 82.1% of suspended solids, Chemical Oxygen Demand (COD), oil & grease removal and water recovery respectively.

POME was considered as a multiple solute system and the transport models developed for the multiple solutes system include (1) Population Balance Model for direct flocculation, (2) coupled model of Homogeneous Surface Diffusion with Adsorbed Solution Theory for granular activated carbon adsorption, (3) coupled model of Back Transport Analysis with Filtration theory for ultrafiltration (UF) membrane system and (4) coupled model of Extended Spiegler-Kedem Model with Concentration Polarization Model for reverse osmosis (RO) membrane system. The model parameters were evaluated from the experimental data obtained from the pilot plant study. The simulation results show a good agreement with the experimental data.

portion of the COD and BOD are contributed by the dissolved organic solutes of carbohydrate constituents, protein and ammoniacal nitrogen. The total nitrogen includes the nitrogenous compound of protein and ammoniacal nitrogen.

From the environmental point of view, the discharge of untreated POME characterized by the extremely high content of degradable organic matters based on the characteristic as shown in Table 1.1 into the water streams or rivers will definitely lead to severe pollution to the rivers, destruction to the aquatic habitats and deterioration of ecosystem. In addition, the conventional biological POME treatment of anaerobic ponding system produces unpleasant odor of biogas which contains methane, carbon dioxide, hydrogen sulphide and other gasses (Mahabot and Harun, 1986). Thus, proper POME treatment is urgently needed to ensure the sustainable economic growth of palm oil industry in Malaysia besides protecting the environment.

1.1 Environmental Regulatory Control for POME Discharge

The Environmental Quality (Prescribed Premises) (Crude Palm Oil) Regulations 1977, promulgated under the enabling powers of Section 51 of the EQA 1974, are the governing regulations and contain the effluent discharge standards. Other regulatory requirements are to be imposed on the individual palm oil mills through conditions of license. The current effluent discharge standards ordinarily applicable to crude palm oil mills are shown in Table 1.2 (Environmental Quality Act 1974, 2005).

Table 1.2: Effluent discharge standards for crude palm oil mills (Environmental Quality Act 1974, 2005)

Parameter		Parameter Limits (Second Schedule)	Remarks
Biological Oxygen Demand (BOD; 3-Day, 30°C)	mg/L	100	
Chemical Oxygen Demand (COD)	mg/L	*	
Total Solids	mg/L	*	
Suspended Solids	mg/L	400	
Oil and Grease	mg/L	50	
Ammoniacal Nitrogen	mg/L	150	Value of filtered sample
Total Nitrogen	mg/L	200	Value of filtered sample
pH	-	5 – 9	
Temperature	°C	45	

Note: *No discharge standard after 1984

1.2 Conventional Biological Treatment System for POME

The biological treatment system with emphasis on anaerobic digestion is the most conventional POME treatment system adopted in most of the palm oil mills in Malaysia. However, coping with the increasing production in most palm oil mills, the under-sized biological treatment system is unable to cope with the increased volume of POME (Ismail, 2005). The biological treatment relies on bacteria to break down the organic matters into simple end products of methane, carbon dioxide, hydrogen sulphide and water. The organic matters digestion by the bacteria requires long treatment period and thus, large treatment area is required. Unfortunately, size/capacity upgrade for biological treatment system is often failed to be implemented because the mills have only limited space.

Therefore, an efficient treatment system is urgently desired to replace the conventional biological treatment to ensure the final discharge of the treated water is meeting the effluent discharge standards imposed by the DOE, Malaysia.

1.3 Membrane based POME Treatment Pilot Plant

Membrane separation technology is recognized as an efficient, economical and reliable technology that exhibits high potential to be applied in POME treatment to replace the conventional biological treatment system (Ismail, 2005). POME contains valuable plant nutrients in substantial amount. The membrane separation technology coupled with pretreatment recovers these nutrients as fertilizer and recycle clean water to achieve zero discharge. Consequently, the treatment of POME using membrane technology will be efficient, innovative and attractive to the mill owners.

The investigation on the feasibility and suitability of the membrane separation technology in POME treatment is carried out in a pilot plant with the capacity of 450L/hr (Ismail, 2005). This pilot plant was designed and fabricated locally; consists of two stages of treatment. This includes series of pretreatment processes followed by the membrane separation processes. The Process Flow Diagram (PFD) of the membrane based POME treatment pilot plant is shown in Fig. 1.1. As shown from Fig. 1.1, the pretreatment processes in the pilot plant involve coagulation by using Aluminum Sulfate (Alum), flocculation by using cationic polymer (flocculent), sludge dewatering by filter press and granular activated carbon (GAC) adsorption. The membrane separation processes in the pilot plant involve ultrafiltration (UF) membrane system and reverse osmosis (RO) membrane system.

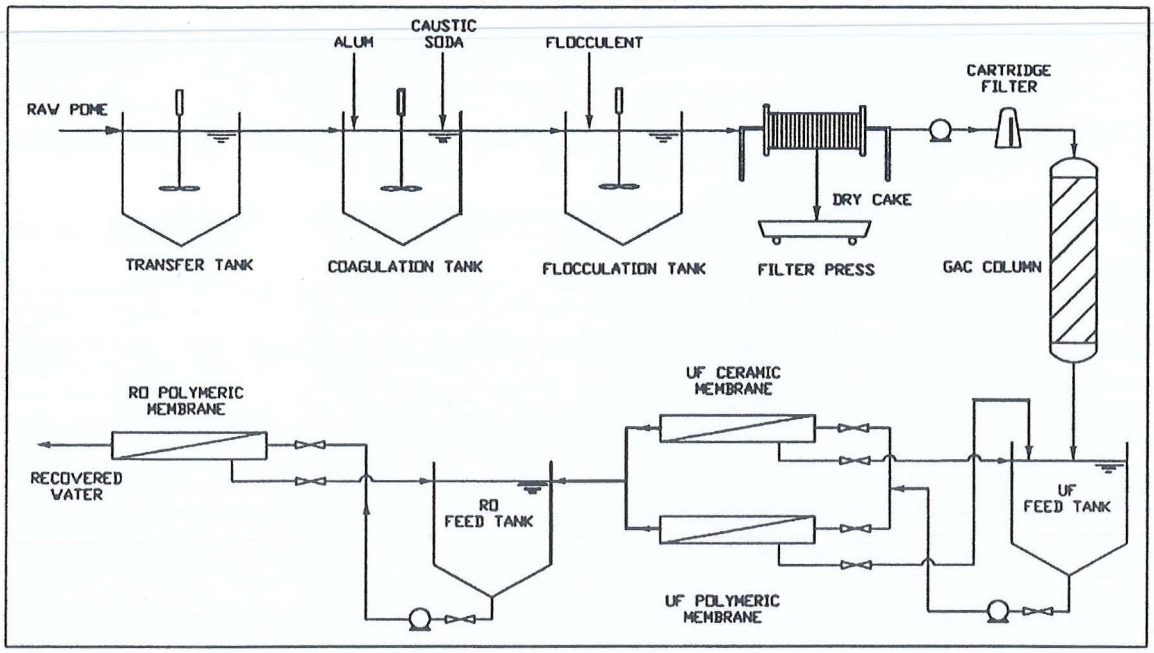

Fig. 1.1: Process Flow Diagram (PFD) for the membrane based POME treatment pilot plant

The overall performance of the membrane based POME treatment pilot plant shows a very promising result. The recovered water/treated POME not only complied with the effluent discharge standards set by the DOE of Malaysia, but the recovered water was crystal clear and could be recycled. The high content of organic nutrient in the dry cake from the filter press could be converted into organic fertilizer (Ismail, 2005).

1.4 Research Objectives

The research objectives for the present study are as follows:

1. To obtain reliable and reproducible process data over a wide range of conditions using the pilot plant fabricated from the earlier Yayasan Felda grant.
2. To study and identify appropriate method to overcome membrane fouling problem.
3. To develop a suitable model for membrane separation process used in pilot plant.
4. To optimize total treatment system.
5. To obtain the necessary design process parameters for industrial scale up.

LITERATURE REVIEW

2.1 Pretreatment Process and Membrane Technology in Effluent Treatment

The pretreatment processes employed for POME treatment in the present research are the coagulation and flocculation, sludge dewatering and granular activated carbon (GAC) adsorption. These processes are integrated in the membrane based POME treatment pilot plant to reduce the suspended solids content to an acceptable level in order to ensure the success of membrane separation technology. The pretreatment process is used to mitigate membranes fouling and degradation due to suspended solids loading during the operation and thus the membrane lifespan is prolonged (Ahmad *et al.*, 2005).

Membrane technology is found to be successful in removing suspended solids, oil & grease, heavy metals, Biological and Chemical Oxygen Demand (BOD and COD), salts and biological contamination from the wastewaters (Cheryan, 1998). It has been widely employed by various industries such as chemical, cosmetics, textile, transportation, pulp and paper, dairy, food, beverage and many other industries (Ismail, 2005). In the present research, the scope is focused on the membrane processes of ultrafiltration (UF) and reverse osmosis (RO). The UF is used as the pretreatment to RO while RO is used to achieve the desired treatment efficiency.

2.2 Process Design via Modeling, Simulation and Optimization

Process design refers to planning the routine steps of a process aside from the expected result and the processes are treated as a product of design, not the method of design (Wikipedia, 2006). Thus, process design is the devising of a system or process to meet a stated objective based on mathematics, basic science, engineering science, and flavored by the humanities and social science (Biegler *et al.*, 1999).

2.2.1 Modeling and Simulation

Modeling is the use of mathematical language to describe the behaviour of a system. Simulation is an attempt to model a real-life system or process so that behavior of the system or process can be studied and examined. By changing the variables, predictions may be made about the behaviour of the system. Therefore, simulation has become a useful part of modeling many systems in engineering to gain insight into the operation of those systems (Wikipedia, 2006).

The transport models provide fundamental understanding of the system or process. In the present research, the transport models are developed for direct flocculation, sludge dewatering, granular activated carbon (GAC) adsorption, UF and RO membrane system. Overview and background of these transport models are discussed in the following sections.

2.2.1(a) Direct Flocculation Process

The direct flocculation (i.e. without addition of coagulants) using cationic and anionic polymers offers the possibility to completely replace the inorganic coagulants with water-soluble organic polymers in POME pretreatment under a constant applied shear. The flocculation process can be classified into the single and dual polymer systems. The single polymer system utilizes the medium charge density with high molecular weigh cationic polymer. The cationic polymer served as double acting polymer by first neutralizing the negative charge of the particles (charge neutralization) and then visible flocs formation by bridging. The dual polymer system is employed when the single polymer system failed to achieve the desired flocculation. In this system, the cationic polymer is first added for charge neutralization and bridging. The bridging-type long chain anionic polymer

is then added to further enhance the bridging effects by mechanically bridging the flocs into larger and rapid settling flocs (dense flocs).

The polymer-induced flocculation efficiency is commonly evaluated by water recovery, suspended solids, COD and oil & grease removal. However, these are only indirect indicators of the effectiveness of flocculation. These indirect indicators are unable to ascertain the dominant mechanism of flocculation of whether it is charge neutralization, bringing or both. The most explicit and direct measure of flocculation efficiency is floc size distribution. The Population Balance Modeling (PBM) has been used extensively to simulate the evolution of floc size distribution with time to investigate the efficiency of the flocculation process (Somasundaran and Runkana, 2003; Runkana *et al.*, 2004; Runkana *et al.*, 2006; Ding *et al.*, 2006; Nere and Ramkrishna, 2006; Gerstlauer *et al.*, 2006).

Somasundaran and Runkana (2003) proposed a complete flocculation model for colloidal mineral suspensions using the PBM. The influence of surface forces in the presence of salts and polymers was incorporated into the PBM to obtain an analytical solution for the collision efficiency. The collision efficiency is an important parameter in PBM and it is previously employed as a fitting parameter. Runkana *et al.* (2004; 2006) also proposed a mathematical model based on PBM for processes involving polymer induced flocculation via simple charge neutralization using the modified DLVO (Derjaguin Landau Verwey Overbeek) theory. The effect of adsorbed polymer layers on van der Waals attraction was included. The investigation was also extended by considering the effects of bridging attraction or steric repulsion due to the adsorbed polymer layers based on scaling theory.

However, the PBM for polymer induced flocculation by charge neutralization and bridging attraction presented in the literature focused on perikinetic aggregation of Brownian motion and differential sedimentation. Orthokinetic aggregation due to applied shear is commonly applied to accelerate the flocculation process. Therefore, the PBM suitable for polymer-induced flocculation by charge neutralization and bridging under applied shear is proposed in the present research to investigate the efficiency of the flocculation process in POME pretreatment. Besides, the current investigation attempt for the first time to correlate the information of floc size distribution from the PBM to the indirect indicators of COD, suspended solids and oil & grease.

2.2.1(b) Sludge Dewatering Process

In the present research, flocculated sludge from the POME using direct flocculation has to be separated from the supernatant before the supernatant can be further treated. In the pilot plant analysis, the flocculated sludge is dewatered by using the filter press due to low solids loading with batch mode operation. In the industrial scale design, a Dry Solids Decanter is employed due to the continuous high solids loading and high cake solids concentration needs to be achieved. In fact, maximum dryness level needs to be achieved because the subsequent processing involves thermal drying using a sludge dryer to convert the sludge into fertilizer. Thermal energy is much more expensive than mechanical energy.

In the present research, the transport models are developed for modeling and simulation of industrial scale membrane based POME treatment plant. Therefore, the process modeling for Dry Solids Decanter instead of filter press is being considered. The transport models developed in the literature are based on a capacity scaling factor which can be only obtained based on the experimental data of a reference decanter (Walker,

2000; Walker, 2000a; Leung, 1998). In other words, the transport models are used for sizing and scale up of a decanter based on a reference decanter with the capacity scaling factor. The capacity scaling factor is only applicable when both decanters are of similar type and they are used to dewater the feed slurry with similar characteristics. Thus, in the present research, the process modeling of the decanter is presented as the sizing equations in the Sizing and Costing section.

2.2.1(c) Granular Activated Carbon (GAC) Adsorption

The design and operation of a fixed-bed GAC adsorption column require an accurate modeling for the breakthrough curve prediction. The breakthrough curve is an S-shaped curve indicating the effluent concentration history (Perry, 1997). One of the most widely used model for the breakthrough curve prediction is the Homogeneous Surface Diffusion Model (HSDM) developed by Mathews and Weber (1976). The HSDM was used extensively for breakthrough curves prediction of acid dye adsorption system (Lee *et al.* 2005), synthetic organic chemicals (SOCs) adsorption system (Lo and Alok, 1996), trinitrotoluene (TNT) adsorption from wastewater (Lee *et al.*, 2006) and metal ions adsorption system (Ko *et al.*, 2005).

The most common simulation model used for the prediction of GAC adsorption in multiple solutes system is based on the incorporation of Ideal Adsorbed Solution Theory (IAST) into kinetic models (Tien, 1994). Lo and Alok (1996) proposed a simulation model based on the incorporation of the IAST into the HSDM to make it possible to predict the effluent concentration of synthetic organic chemicals (SOCs) from groundwater. Ko *et al.* (2005) applied the incorporation of IAST into the HSDM to predict the binary metal ions adsorption on fixed-bed system. By using the IAST, the single-solute behavior represented

by the Freundlich adsorption isotherm can be related to the HSDM for predicting the multiple solutes adsorption (Lo and Alok, 1996; Tien, 1994; Hand *et al.*, 1997).

In the present research, information on the removal efficiency of the organic solutes from pretreated POME using GAC is important for pilot-scale investigation and industrial scale application. Adsorption of dissolved organic solutes of pretreated POME using GAC involves complex solutions system. Thus, the HSDM is utilized in predicting the breakthrough curves for the complex system of pretreated POME by using the incorporation of IAST. The IAST application needs single-solute data, and the model allows multiple solutes calculations to be performed using the single-solute isotherm relationships. Due to the complexity of the pretreated POME system, the single-solute isotherm for each component is obtained by using synthetic sample where the representative solute was added into the pure water.

2.2.1(d) Ultrafiltration (UF) Membrane System

A number of mathematical models are available in the literature to describe the transport mechanism through the UF membranes by considering the gel polarization phenomena. The most common model used in describing the UF is the resistance-in-series model (Tansel *et al.*, 2000; Kumar *et al.*, 2004; Gehlert *et al.*, 2005 and Bhattacharjee and Datta, 2003). The resistance-in-series model assumes that the flux of permeate is proportional to the trans membrane pressure and inversely proportional to the viscosity of the suspending solution where the parameter of hydraulic resistance is being introduced. The hydraulic resistance is the total resistance exerted by the membrane and solutes.

However, the models proposed in the literature are only suitable to predict the performance of UF with the single solute system. When multiple solutes system is used, these models can only predict the total permeate concentration of the system. In the industrial application, multiple solutes systems are often encountered and the mass transport of each solute in the multiple solutes system is important. Therefore, a time-dependent mathematical model predicting the performance of an UF process in the separation of multiple solutes system of pretreated POME is developed in the present research. The model is based on the mass balance analysis coupled with the filtration theory (osmotic pressure model, Darcy's law, resistance-in-series and gel polarization models).

2.2.1(e) Reverse Osmosis (RO) Membrane System

The mathematical models for RO available in the literature are based either on transport mechanisms or irreversible thermodynamics. The models based on transport mechanisms include solution-diffusion, solution-diffusion imperfection, Kimura-Sourirajan and extended Nerst-Planck model while the model based on irreversible thermodynamics is the Spiegler-Kedem model (Bhattacharya and Ghosh, 2004).

The Spiegler-Kedem model has been extensively used in predicting the data of the transport of single solute and solvent through the membrane in the RO system (Jain and Gupta, 2004; Gauwbergen and Baeyens, 1998; Sutzkover *et al.*, 2000). Bhattacharya *et al.* (2004) used the Spiegler-Kedem model while Fukuda *et al.* (2003) used the Kedem-Katchalsky model in predicting the binary solute system when an impermeable ion is present in the salt-water solution. Wadley *et al.* (1995) used the Spiegler-Kedem model combined with the film theory to predict the performance of binary solutes system (sodium chloride and organic compounds). However, this model is not suitable for other multiple

solutes system because only membrane-solute and solute-solvent interactions were considered and the solute-solute interactions were neglected.

The extended Spiegler-Kedem model suitable for multiple solutes system of pretreated POME; which contains complex dissolved organic solutes (namely carbohydrate constituents, protein and ammoniacal nitrogen) in RO membrane separation with the consideration of solute-solute interactions is developed in the present research. On the other hand, unsteady-state simulation by the incorporation of extended Spiegler-Kedem model with the concentration polarization to depict multiple solutes and water transfer through RO membranes is also developed.

2.2.2 Optimization Study

The optimization of the membrane based POME treatment plant in the present research is mainly focused on the minimization of total treatment cost subjects to a set of constraints to obtain the optimum operating conditions, design parameters and configuration of membrane modules distribution, i.e., the number of membrane modules in series and in parallel, and the number of stages in series. Similar optimization study of the membrane system is presented by Geraldes *et al.* (2005). According to this study, an optimization of two-stage seawater RO desalination system with spiral-wound modules was investigated. The modules configuration and operating conditions for RO desalination system was optimized based on the transport model of mass momentum coulpled with the cost model (constrained nonlinear problem) via Generalized Reduced Gradient Algorithm to obtain the minimum product water cost.

The previous literature review clearly shows that the optimization was only focused on the membrane system without considering the optimization of pretreatment process. In

addition, most of the previous optimization studies were only focused on RO desalination plants. In contrast, the large scale optimization of industrial scale membrane based POME treatment plant in the present research includes the optimization of pretreatment process and membrane system which consists of UF and RO membranes. The integrated transport models representing the unit operations in the flowsheets are used to optimize the operating conditions, design parameters and membrane modules configurations in order to obtain the minimum total treatment cost.

2.2.3 Computer Tool for Modeling, Simulation and Optimization

The flowsheets modeling, simulation and optimization deal with numerous equations which involves algebraic and differential equations. Thus, advanced computer tools are required. In the present research, the modeling system of Matlab and Simulink from The MathWorks, Inc. is used for designing the industrial scale membrane based POME treatment plant. The Matlab and Simulink is chosen because it allows the transport models developed for the POME system to be coded in its user-defined model library for flowsheet synthesis, modeling, simulation and optimization.

3.2 POME Characteristic Analysis and Correlations

The high COD of the POME can be divided into two major portions which are the insoluble COD and soluble COD. The insoluble COD constitutes more than half of the total COD and is closely related to the concentration of suspended solids. By assuming that the insoluble COD is solely contributed by the suspended solids concentration (C_{ss}), the suspended solids can be correlated to the total COD (COD_{total}) of the suspension as:

$$COD_{total} = b_{ss}\, C_{ss} + COD_{soluble} \tag{3.1}$$

where the term $COD_{soluble}$ is the soluble COD concentration in the system and b_{ss} is the dimensionless coefficient. Suspended solids concentration can also be correlated to the oil & grease concentration ($C_{O\&G}$) by using the correlation as:

$$C_{O\&G} = b_{O\&G}\, C_{ss} \tag{3.2}$$

where the term $b_{O\&G}$ is the dimensionless coefficient.

The soluble COD are contributed by three major groups of dissolved organic solutes, which are carbohydrate constituents, protein and ammoniacal nitrogen. A correlation is used in the present studies to relate the concentrations of all dissolved organic solutes in the system with the soluble COD as follows (Miorin, 1997)

$$COD_{soluble} = \sum_{i=1}^{n} b_i C_i \quad \text{for} \quad i = 1,2,3 \tag{3.3}$$

where the term C_i is the concentration of the dissolved organic solute i in the system ($i = 1$ for carbohydrate constituents, $i = 2$ for protein and $i = 3$ for ammoniacal nitrogen) and b_i is the dimensionless coefficient. As the total nitrogen is present in the form of

organic nitrogen of protein and ammoniacal nitrogen, the summation of both concentrations will give the indication to the total nitrogen concentration.

As the COD is used to assess the total amount of organics present, the gross fraction of the total amount of organic measured as COD; which can be biodegraded, can be identified as the BOD. Thus, the COD value can be correlated approximately with the BOD value (Perry, 1999) and the correlation is given as:

$$BOD = b_{BOD}\, COD \tag{3.4}$$

where the term BOD is the BOD concentration, COD is the COD concentration in the system and b_{BOD} is the dimensionless coefficient.

Consequently, the POME forms a multiple solutes system of suspended solids, carbohydrate constituents, protein and ammoniacal nitrogen. These solutes are utilized in all the transport models to predict and evaluate the performance of the processes or systems in the pilot plant. Once the concentration of these solutes are obtained, the concentration of oil & grease, COD, BOD and total nitrogen will be calculated based on the Eqs. (3.1) to (3.4).

3.2 Population Balance Model for Flocculation Process

Population Balance Model (PBM) of Smoluchowski (Kumar and Ramkrishna, 1996) is used for modeling aggregation phenomena in colloidal suspensions. In the aggregation-fragmentation processes, fragmentation is generally assumed to take place only due to fluid stress and not due to collisions between different aggregates, though it is also possible. Based on the geometric discretization techniques (Spicer and Pratsinis, 1996),

the rate of change of particle or aggregate number concentration during the simultaneous aggregation and fragmentation is given by the following discretized and lumped PBM:

$$\frac{dN_i}{dt} = \frac{1}{2}\alpha_{i-1,i-1}\beta_{i-1,i-1}N_{i-1}^2 + N_{i-1}\sum_{j=1}^{i-2}2^{j-i+1}\alpha_{i-1,j}\beta_{i-1,j}N_j$$
$$- N_i\sum_{j=1}^{i-1}2^{j-i}\alpha_{i,j}\beta_{i,j}N_j - N_i\sum_{j=i}^{\max_1}\alpha_{i,j}\beta_{i,j}N_j - S_iN_i + \sum_{j=i}^{\max_2}\gamma_{i,j}\,S_j\,N_j \quad (3.5)$$

where N_i is number concentration of particles or aggregates in section i, t is flocculation time, α is collision efficiency factor, β is collision frequency factor, S is the specific rate constant of fragmentation, γ is breakage distribution function, $\max_1$ is maximum number of sections used to represent the complete aggregate size spectrum and $\max_2$ corresponds to the largest section from which flocs in the current section are produced by fragmentation. The first and second terms on the right of Eq. (3.5) account for growth, while the third and fourth terms account for loss of aggregates by aggregation, fifth term accounts for the loss of aggregates due to fragmentation and the last term account for generation of smaller aggregates due to breakage or erosion. The flocculation can be visualized as a three-step process: aggregate transport represented by the collision frequency factor, $\beta_{i,j}$, attachment given by the collision efficiency, $\alpha_{i,j}$ and aggregates breakage represented by the specific rate constant of fragmentation, S_i and breakage distribution function $\gamma_{i,j}$.

3.2.1 Collision frequency

In the wastewater treatment system, orthokinetic aggregation (aggregation due to applied shear) is often preferred. In the pretreatment of POME, shear is applied by the stirring motion of impeller to accelerate aggregation process. The collision frequency factor of orthokinetic (Somasundaran and Runkana, 2003) is given by:

$$\beta_{i,j}^{sh} = \frac{4}{3} G \left(\sqrt{E_{fi}} r_{ci} + \sqrt{E_{fj}} r_{cj} \right)^3 \tag{3.6}$$

where G is the global average fluid velocity gradient or shear rate, r_{ci} or r_{cj} is the floc collision radius, and E_f is the fluid collection efficiency of an aggregate. The E_f is in the range of $0 \leq E_f \leq 1$. The collision frequency factor for permeable aggregates can be reverted to those for rigid spheres (rectilinear model) by setting E_f equal to 1. If the E_f is less than 1, it is curvilinear model (Thill *et al.*, 2001; Bushell *et al.*, 2002).

3.2.2 Collision efficiency

The collision efficiency factor is computed as the reciprocal of the Fuchs' stability ratio, W between the primary particles (Somasundaran and Runkana, 2003):

$$W_{i,j} = \left(r_{oi} + r_{oj} \right) \int_{r_{oi}+r_{oj}}^{\infty} \frac{\exp\left(V_T / K_B T \right)}{s^2} ds \tag{3.7}$$

where V_T is net interaction energy between two primary particles of radii r_{oi} and r_{oj}, s is the distance between particles centers ($s = r_{oi} + r_{oj} + h_o$), h_o is the minimum separation distance between particle surfaces, K_B is the Boltzmann constant and T is the suspension temperature.

In the DLVO (Derjaguin Landau Verwey Overbeek) theory (Somasundaran and Runkana, 2003; Runkana *et al.*, 2004; Runkana *et al.*, 2006), the net interaction energy between two primary particles, V_T is equal to the sum of Van der Waals energy V_{vdw}, electrical double layer repulsion V_{edl} and energy of steric repulsion or bridging attraction V_s.

$$V_T = V_{vdw} + V_{edl} + V_s \tag{3.8}$$

3.2.2(a) Van der Waals Energy

In the case where polymer is used, the adsorbed polymer layers on the particles should be considered. The expression for the Van der Waals energy for the case of two solids of the same kind with equal adsorbed polymer layer thickness is (Somasundaran and Runkana, 2003; Vincent, 1973):

$$\begin{aligned} -12V_{vdw}^{V} = {} & H_{si\,sj}\left(A_{si}^{1/2} - A_m^{1/2}\right)\left(A_{sj}^{1/2} - A_m^{1/2}\right) + H_{pi\,pj}\left(A_{pi}^{1/2} - A_{si}^{1/2}\right)\left(A_{pj}^{1/2} - A_{sj}^{1/2}\right) \\ & + H_{pi\,sj}\left(A_{pi}^{1/2} - A_{si}^{1/2}\right)\left(A_{sj}^{1/2} - A_m^{1/2}\right) + H_{pj\,si}\left(A_{pj}^{1/2} - A_{sj}^{1/2}\right)\left(A_{si}^{1/2} - A_m^{1/2}\right) \end{aligned} \tag{3.9}$$

where A_p, A_m, A_s is the Hamaker constant of the solids, solvent and polymer respectively across vacuum, $H_{(x,y)}$ is the unretarded geometric functions.

3.2.2(b) Electrical Double Layer Repulsion

The interaction energy due to the electrical double layers between two spheres of radii, (r_{oi} and r_{oj}) and surface potentials, ψ_{oi} and ψ_{oj} is given by (Bell *et al.*, 1970):

$$V_{edl} = 64\pi\varepsilon_o\varepsilon_r\left(\frac{K_BT}{z_ce}\right)^2\left(\frac{r_{oi}r_{oj}}{r_{oi}+r_{oj}}\right)\tanh\left(\frac{z_ce\psi_{oi}}{4K_BT}\right)\tanh\left(\frac{z_ce\psi_{oj}}{4K_BT}\right)\exp(-\mathrm{K}h_o) \tag{3.10}$$

where e is the elementary charge, z_c is the valence of counter ion, ε_o, ε_r are the dielectric constant of vacuum and the solvent and K is the Debye-Hückel parameter.

3.2.2(c) Bridging Attraction

The interaction energy due to bridging attraction (V_s) is dependant on the adsorbed polymer layers. It is important to understand the electrochemical changes brought by the adsorbed polymer on particle surfaces. The scaling theory (Genes, 1981; Genes, 1982) is

used to compute forces due to adsorbed polymer layers. It was chosen because it permits derivation of analytical formulas for interaction between spherical particles. The scaling theory is based on minimization of a surface free energy functional subject to the constraint that total amount of polymer adsorbed is fixed in the region between two surfaces having adsorbed layers. The interaction energy due to bridging attraction between two unequal polymer-coated spheres can be computed as (Runkana *et al.* 2006):

$$V_s = \left(\frac{2\pi r_{oi} r_{oj}}{r_{oi} + r_{oj}}\right)\left(\frac{\alpha_{Sc} K_B T}{a_m^3}\right)\Phi_{so}^{9/4} D_{Sc} \times \left\{-\frac{16\Gamma D_{Sc}}{\Gamma_o}\ln\left(\frac{2\delta}{h_o}\right) + \frac{4D_{Sc}^{5/4}}{2^{5/4}}\left(\frac{8\Gamma}{\Gamma_o}\right)^{9/4}\left[\frac{1}{h_o^{1/4}} - \frac{1}{(2\delta)^{1/4}}\right]\right\} \quad (3.11)$$

where δ is adsorbed polymer layer thickness, α_{Sc} is numerical constant which can be obtained from osmotic pressure and light scattering experiments on polymer solution, a_m is effective monomer size, Γ is total amount of polymer adsorbed on a single surface, D_{sc} is the scaling length, Φ_{so} is polymer concentration at a single saturated surface and Γ_o is adsorbed amount at saturation.

3.2.3 Aggregates Breakage

The increase of collision frequency by applying shear does not necessary result in high rates of flocculation. Aggregates breakage or fragmentation often occurs due to shear stress especially at high stirring speed. The parameters used to compute the aggregates breakage is the specific rate constant of fragmentation, S_i and the breakage distribution function, $\gamma_{i,j}$. The specific rate constant of fragmentation, S_i is defined as (Somasundaran and Runkana, 2003; Flesh, 1999):

$$S_i = \left(\frac{4}{15\pi}\right)^{\frac{1}{2}} \left(\frac{\bar{\varepsilon}}{\nu}\right)^{\frac{1}{2}} \exp\left(\frac{-\varepsilon_{b,i}}{\bar{\varepsilon}}\right) \tag{3.12}$$

where $\varepsilon_{b,i}$ is the critical turbulent energy dissipation rates at which floc breakage takes place. The breakage distribution function, $\gamma_{i,j}$ is a fitting parameter.

3.3 Coupled model of Homogeneous Surface Diffusion Model (HSDM) with Ideal Adsorbed Solution Theory (IAST) for Granular Activated Carbon (GAC) Adsorption

The rate of mass transfer of the adsorbate (organic solutes) onto the adsorbent (fixed-bed GAC) is based on the diffusion of adsorbate from the bulk solution through the stagnant film surrounding the particle external surface (external film mass transfer). Once reaching the surface, adsorption occurs instantaneously and equilibrium is established between the adsorbate in the fluid and that on the adsorbent surface. The adsorbed material then diffuses into the pores in the adsorbed state (Lo and Alok, 1996; Lee *et al.*, 2005).

In the fixed bed operation, the mass transfer of the single-solute adsorption is described by the mathematical model of HSDM developed by previous researchers (Lee *et al.*, 2005). The HSDM considers the mass balance on the liquid phase and GAC particle. The liquid phase mass balance describes the spatial and temporal variations of the adsorbate concentration in the solution. The mass balance on liquid phase which contains only solute i in the fixed-bed GAC adsorption system is represented as:

$$\frac{\partial C_i}{\partial t} = -V_s \frac{\partial C_i}{\partial z} - \frac{3}{R} \frac{(1-\varepsilon)}{\varepsilon} k_{fi} (C_i - C_{si}) \tag{3.13}$$

where C_i is the bulk liquid phase concentration of the adsorbate i, t is the time parameter, z is the coordinate along the longitudinal bed axis, ε is the porosity of the

GAC bed, R is the adsorbent particle radius, k_{fi} is the external mass transfer coefficient of adsorbate i, C_{si} is the equilibrium concentration of adsorbate i and V_s is the influent approach velocity. The initial and boundary conditions of Eq. (3.13) are

$$t = 0, \qquad 0 \le z \le L, \qquad C_i = 0 \tag{3.14a}$$

$$t > 0, \qquad z = 0, \qquad C_i = C_{fi} \tag{3.14b}$$

$$t > 0, \qquad z = L, \qquad \frac{\partial C_i}{\partial z} = 0 \tag{3.14c}$$

where L is the bed length and C_{fi} is the concentration of the adsorbate i in the feed.

For the HSDM, the internal mass balance on the GAC particle is as follows (Lee *et al.*, 2005):

$$\frac{\partial q_i}{\partial t} = \frac{D_{si}}{r^2}\frac{\partial}{\partial r}\left(r^2 \frac{\partial q_i}{\partial r}\right) \tag{3.15}$$

where q_i is the solid phase loading of adsorbate i on the GAC particle, D_{si} is the surface diffusivity coefficient of adsorbate i, r is the radial axis of GAC particle. The initial and boundary conditions of Eq. (3.15) are

$$t = 0, \qquad 0 \le z \le L, \ 0 \le r \le R, \qquad q_i = 0 \tag{3.16a}$$

$$t > 0, \qquad r = 0, \qquad \frac{\partial q_i}{\partial r} = 0 \tag{3.16b}$$

$$t > 0, \qquad r = R, \qquad k_{fi}\left(C_i - C_{si}\right) = \rho_p D_{si}\left(\frac{\partial q_i}{\partial r}\right)_{r=R} \tag{3.16c}$$

where ρ_p is the GAC particle density.

The mathematical model of HSDM describes the mass transfer of the single solute system of adsorbate i. The incorporation of the IAST into the HSDM allows the prediction of multi-component adsorption system. The IAST model is based on the thermodynamic equivalence of the spreading pressure of each solute at equilibrium. The term 'spreading pressure', π, is defined as the difference between the interfacial tension of the pure solvent-solid interface and that of the solution-solid interface at the same temperature. The spreading pressure of a single solute will remain unchanged when it is mixed with other components in an adsorption system (Tien, 1994). Thus, the spreading pressure of the adsorbate i, π_i is equal to that of each individual component and to that of the mixture.

The Freundlich adsorption isotherm is the most widely used empirical equation for describing an equilibrium behavior of a solute in a single component aqueous-solid system (Lo and Alok, 1996) and is expressed as:

$$q_{e_i} = K_i C_{e_i}^{1/n_i} \tag{3.17}$$

where q_{e_i} is the solid phase surface loading at equilibrium for adsorbate i, C_{e_i} is the equilibrium liquid phase concentration of adsorbate i, K_i is the Freundlich capacity parameter and $1/n_i$ is the Freundlich intensity parameter.

Based on the Freundlich isotherm of Eq. (3.17), a relationship for predicting multi-component adsorption can be derived (Crittenden *et al.*, 1985). The equilibrium concentration of adsorbate i in the presence of other competing organic solutes (C_{si}) is expressed in term of the solid phase loading of adsorbate i (q_i) on the GAC particle at $r = R$ through the Freundlich parameters of K_i and n_i.

$$C_{si} = \frac{q_i}{\sum_{j=1}^{N} q_j} \left(\frac{\sum_{j=1}^{N} n_j q_j}{n_i K_i} \right)^{n_i} \quad (i = 1 \; to \; N) \tag{3.18}$$

By incorporating the IAST of Eq. (3.18) into the kinetic model of HSDM (Eqs. (3.13)-(3.16)), the effluent concentration of the dissolved organic solutes (carbohydrate constituents, protein and ammoniacal nitrogen) in the multi-component (pretreated POME) adsorption system can be predicted. Solution of the equations will give the breakthrough curves for the complex system of pretreated POME in terms of the effluent concentration of each adsorbate as a function of the operation time of GAC bed.

3.4 Coupled Model of Back Transport Analysis with Filtration Theory for Ultrafiltration (UF) Membrane System

A mathematical model is developed to provide a conceptual framework for understanding the phenomenon responsible for flux decline for the multiple solutes system in the UF process. During filtration process, the solvent is transported by pressure-driven convective flow through the pores. Separation occurs because the solvent is filtered through some of the pores in the membrane. The UF membrane rejects the solutes by sieving action.

The total volume flux of permeate, J_v can be calculated by using the osmotic pressure model (Karode, 2001).

$$J_v = \frac{1}{A}\frac{dV_p}{dt} = \frac{\Delta P - \Delta \pi}{\mu (R_H)} \tag{3.19}$$

where ΔP is the transmembrane pressure, $\Delta \pi$ is the osmotic pressure difference across the membrane, μ is the viscosity of the bulk, R_H is the hydraulic resistance of the system.

The hydraulic resistance, R_H is the sum of the membrane resistances, R_m and the gel layer resistance, R_g (Kumar et al., 2004). Thus, the Eq. (3.19) can be written as:

$$J_v = \frac{1}{A}\frac{dV_p}{dt} = \frac{\Delta P - \Delta\pi}{\mu(R_m + R_g)} \tag{3.20}$$

The total volume flux of permeate can also be calculated by the Darcy's law (Bhattacharjee and Datta, 2003):

$$J_v = \frac{1}{A}\frac{dV_p}{dt} = P_m\left(\frac{\Delta P_c}{\mu H}\right) \tag{3.21}$$

where ΔP_c is the pressure drop across the gel layer, P_m is the permeability coefficient and H is the effective filtration thickness. Thus, the resistance-in-series model can be obtained by combining the Eqs. (3.20) and (3.21).

$$J_v = \frac{\Delta P - \Delta\pi}{\mu\left(R_m + z/P_m\right)} \tag{3.22}$$

Substitution of z into Eq. (3.22) and rearrange in terms of $1/J_v$ gives:

$$\frac{1}{J_v} = \frac{\mu R_m}{\Delta P - \Delta\pi} + \frac{\mu}{AP_m\left(\Delta P - \Delta\pi\right)}\frac{\sum_{i=1}^{n}\left(C_{bi} - C_{pi}\right)}{\sum_{i=1}^{n}\left(C_{gi} - C_{bi}\right)}V_p - \frac{\mu vt}{AP_m\left(\Delta P - \Delta\pi\right)}\frac{\sum_{i=1}^{n}K_{bi}C_{gi}}{\sum_{i=1}^{n}\left(C_{gi} - C_{bi}\right)} \tag{3.23}$$

or,

$$\frac{1}{J_v} = a_1 + a_2 V_p - a_3 t \tag{3.24}$$

where,

$$a_1 = \frac{\mu R_m}{\left(\Delta P - \Delta\pi\right)} \tag{3.25}$$

$$a_2 = \frac{\mu}{AP_m(\Delta P - \Delta\pi)} \frac{\sum_{i=1}^{n}(C_{bi} - C_{pi})}{\sum_{i=1}^{n}(C_{gi} - C_{bi})} \tag{3.26}$$

$$a_3 = \frac{\mu v}{AP_m(\Delta P - \Delta\pi)} \frac{\sum_{i=1}^{n} K_{bi} C_{gi}}{\sum_{i=1}^{n}(C_{gi} - C_{bi})} \qquad \text{for} \quad i = 1,2,3...n \tag{3.27}$$

The Eqs. (3.24)-(3.26) represent the volume flux of permeate in the multiple solutes system of the continuous cross-flow UF system with n solutes ($i = 1,2,3,...n$) in a solvent.

The concentrations of each solute in the permeate, C_{pi} of the multiple solutes system of the continuous cross-flow UF system can be written as:

$$C_{pi} = C_{bi} - \frac{K_{bi} v C_{gi}}{A J_{v,ss}} \qquad \text{for} \qquad i = 1,2,3...n \tag{3.27}$$

where the symbol $J_{v,ss}$ is the volume flux of permeate at the steady-state condition. Eq. (3.27) is the equation used to estimate the concentration of solute i in the permeate, C_{pi} of the multiple solutes system of continuous cross-flow UF system. However, in order to calculate the concentration of solute i in the permeate, the concentration of solute i in the gel layer, C_{gi} must be known. The concentration of solute i in the gel layer can be estimated by using the gel polarization model (Bhattacharjee and Datta, 2003).

$$\frac{(C_{gi} - C_{pi})}{(C_{bi} - C_{pi})} = \exp\left(\frac{J_{v,ss}}{k_i}\right) \tag{3.28}$$

where the term k_i is the mass transport coefficient of solute i in the system. The mass transport coefficient, k_i describe the solutes transport in the gel layer based on concentration gradient (diffusion coefficient) and flow velocity (hydrodynamic properties).

Therefore, mass transport coefficient, k_i exhibits a close relationship with the back transfer coefficient, K_{bi}. When the mass transport coefficient, k_i increases, the back transfer coefficient will also increase, K_{bi}. However, mass transport coefficient, k_i describes the solutes transport which are bounded to the gel layer only.

The Eqs. (3.24)-(3.26) and (3.27)-(3.28) define the multiple solutes system for continuous cross-flow UF. Once the operating parameters (ΔP, v, C_b, C_{bi}) and the membrane parameters (R_m, $\Delta\pi$, P_m, μ, K_{bi}, k_i) are known, the volume flux of permeate, concentration of the each solutes in the permeate and the gel layer resistance can be predicted.

3.6 Coupled Model of Extended Spiegler-Kedem Model with Concentration Polarization Model for Reverse Osmosis (RO) System

A serious limitation in the operation of the RO process is the progressive deterioration in permeate flux with time due to the fouling phenomena of concentration polarization. Unsteady-state modeling in permeation flux and quality is important to accomplish efficient and economical process design, achieving effective up-scaling to full scale operation (Tu *et al.*, 2001). The overall task of simultaneously predicting the unsteady-state permeation flux and rejection of organics solutes of a mixture involves a coupled solution of two transport models. The first model describes the transport phenomena of organic solutes across the membrane based on extended Spiegler-Kedem model, while the second model deals with the transport phenomena in the concentration polarization boundary layer on the feed side adjacent to the membrane yielding the true rejection of the organic solutes. The extended Spiegler-Kedem model is coupled to the model of concentration polarization through the membrane surface boundary conditions.

The coupled solution of the extended Spiegler-Kedem model and the model of concentration polarization provides simultaneous predictions of the unsteady-state permeate flux and observed rejection of the organic solutes.

3.5.1 Extended Spiegler-Kedem Model

In the multiple solutes system of reverse osmosis, there are $(n+1)$ components system with n solutes ($i = 1, 2, 3.....n$) in a solvent (e.g. water). In case of large volume flows and high concentration gradients, the changing concentration profile at different flow rates has to be taken into account. Consider a homogeneous membrane that is broken down into differential elements, separated by uniform solution segments which are in equilibrium with two contiguous membrane faces. The permeate flux becomes,

$$J_v = L_p\left[\Delta P - \sum_{i=1}^{n} \sigma_i\, a_i\, R_i\, C_{mi}\right] \tag{3.29}$$

The L_p is the hydraulic permeability constant, ΔP is the trans membrane pressure, σ_i is the reflection coefficient, a_i is 'the Vant Hoff's equation' parameter (Pastagia *et al.*, 2003), C_{mi} is the concentration of solute at the wall of feed side and the term R_i is the true rejection. Using the relation of $C_{pi} = J_i / J_v$ for the multiple solutes system of $i = 1, 2, 3, 4.....n$ and $[j = 1, 2, 3, 4.....n \;\&\; j \neq i]$; which gives:

$$\frac{C_{pi} - C_{mi}(1-\sigma_i)}{C_{pi}\sigma_i} = F_i \qquad \text{where;} \tag{3.30}$$

$$F_i = \exp\left[\frac{-J_v(1-\sigma_i)}{P_{ii}}\left(1 + \sum_{j=1}^{n} A_j\right)\right] \qquad \text{with;} \tag{3.31}$$

$$A_j = \frac{P_{ij}\left(C_{pj} - C_{bj}\right)\exp\left(\frac{J_v}{k_j}\right)}{J_v\left[C_{pi} - (1-\sigma_i)C_i\right]} \tag{3.32}$$

The term C_{bj} is the solute bulk concentration, C_{pi} is the solute concentration at the permeate side, P_{ii} is the solute permeability coefficient of solute i with the consideration of the interaction of solute i and the P_{ij} is the solute permeability coefficient of solute i with the consideration of the interaction of solute j.

Using the rejection fractions instead of concentrations, the Film Theory Model can be expressed as (Kimura, 1995; Slezak *et al.*, 1989):

$$\frac{R_{oi}}{1-R_{oi}} = \frac{R_i}{1-R_i}\exp\left(\frac{-J_v}{k_i}\right) \tag{3.34}$$

where R_{oi} is the observed rejection of solute. The Film Theory Model of Eq. (3.34) gives:

$$\frac{R_{oi}}{1-R_{oi}} = \frac{\sigma_i\left(1-F_i\right)}{1-\sigma_i}\exp\frac{-J_v}{k_i} \tag{3.35}$$

The Eqs. (3.29), (3.31)-(3.32) and (3.35) are the global equations (integrated over the membrane thickness) of the extended Spiegler-Kedem model developed in the present study for the multiple solutes system with the consideration of solute-solute interactions.

3.5.2 Concentration Polarization Model

The concentration polarization layer adjacent to the membrane surface can be schematically represented as shown in Fig. 3.1. Within the concentration polarization layer, the governing equation for the concentration of each solute i is based on the unsteady-state differential material balance (Karode, 2001).

$$\frac{\partial C_i}{\partial t} = -J_v \frac{\partial C_i}{\partial x} + D_{bi} \frac{\partial^2 C_i}{\partial x^2} \tag{3.36}$$

where C_i is the solute concentration in the polarization layer , t is the filtration time and x is the coordinate perpendicular to the membrane as shown in Fig. 3.1.

Eq. (3.36) is solved with the following initial and boundary conditions.

$$t = 0, \qquad 0 \le x \le \delta_{pol}, \qquad C_i = C_{bi_o} \tag{3.37a}$$

$$t > 0, \qquad x = 0, \qquad C_i = C_{bi} \tag{3.37b}$$

$$t > 0, \qquad x = \delta_{pol} \qquad J_v C_i \Big|_{x=\delta_{pol}} = D_{bi} \frac{\partial C_i}{\partial x} \Big|_{x=\delta_{pol}} \tag{3.37c}$$

where, C_{bi_o} is the initial solutes bulk feed concentration and C_{bi} is the solutes bulk feed concentration.

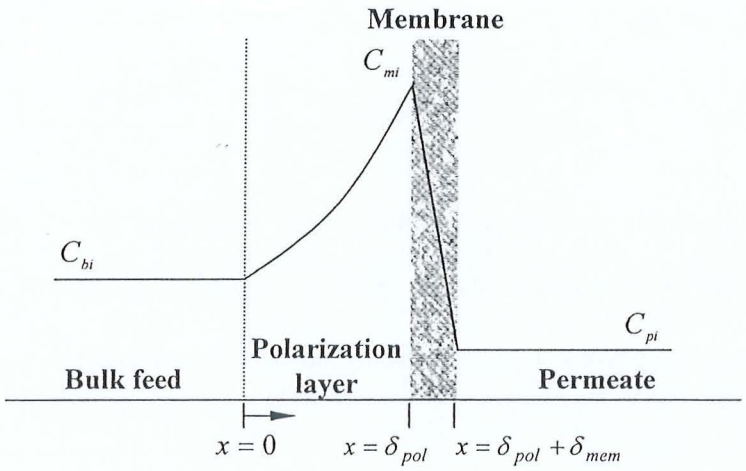

Fig. 3.1: Schematic diagram of a concentration polarization boundary layer.

4.1 Process Description

During the flowsheet simulation, each process represented by its own transport model is placed in different orientation to form specific process configuration. The connectivity between the processes of the flowsheet is represented by the mass balance analysis. In the present study, three different process configurations for POME treatment plant design namely Design A, Design B and Design C are being proposed and investigated.

4.1.1 Design A

The POME treatment system (Fig. 4.1) is divided into two sections, (a) pretreatment system (b) membrane filtration system. The pretreatment system consists of equalization, cationic polymer coagulation and flocculation, anionic polymer flocculation, sludge dewatering by using Dry Solids Decanter and granular activated carbon (GAC) adsorption. The equalization is used to reduce variation in the POME characteristics such as flow rate and the solutes/contaminants concentration. The effective pretreatment is essential to reduce the membrane fouling and to increase the membrane lifespan. The membrane separation system consists of ceramic type ultrafiltration (UF) membrane and polymeric type reverse osmosis (RO) membrane with tubular module. The UF membrane serves as pretreatment to the RO membrane.

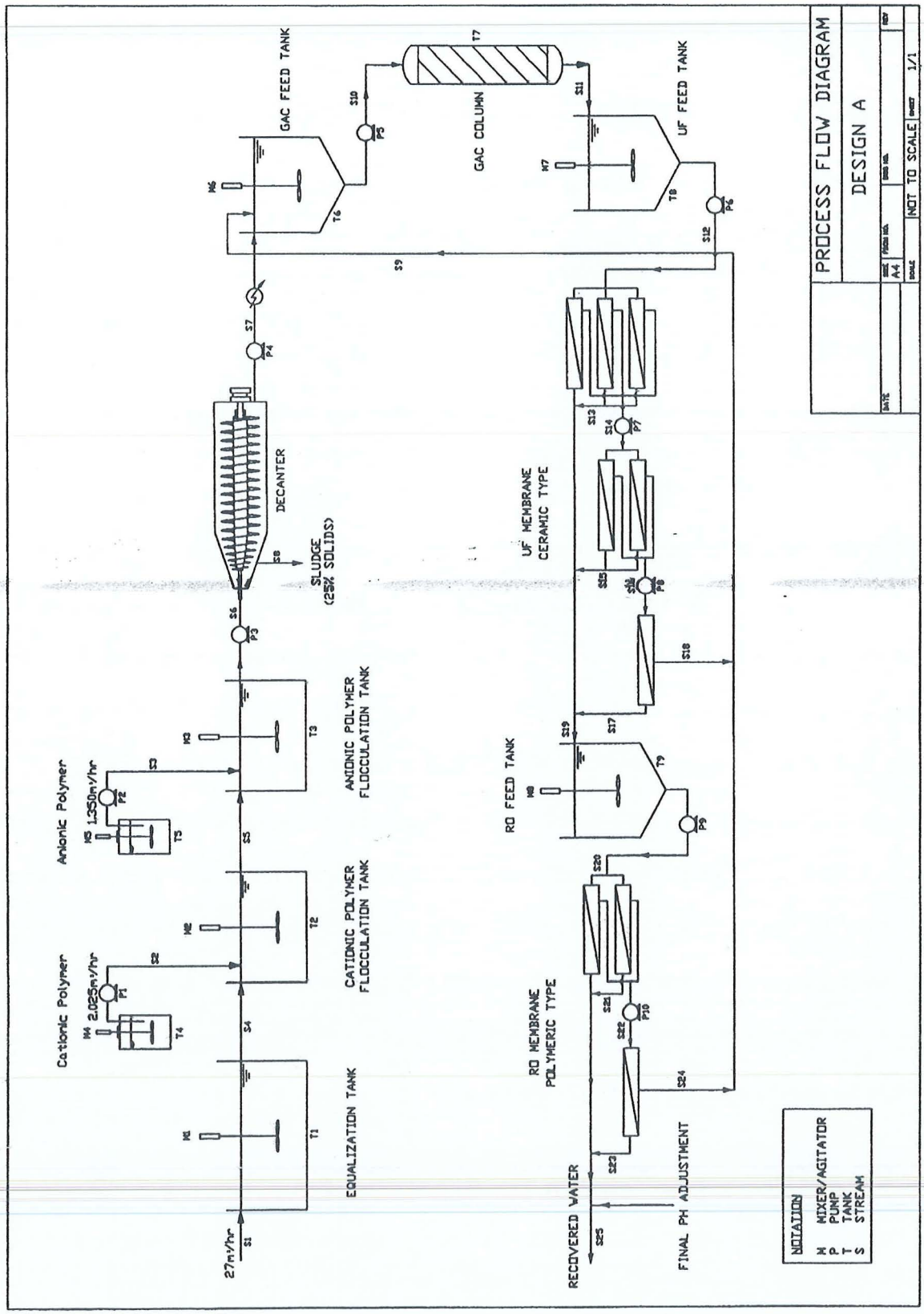

Fig. 4.1: Process Flow Diagram (PFD) of membrane based POME treatment system for Design A

4.1.2 Design B

The pretreatment system of raw POME in Design B as depicted in Fig. 4.2 is identical with Design A. The difference between both designs is the ceramic type UF membrane of Design A is replaced by the polymeric type UF membrane in the Design B.

4.1.3 Design C

By using the same pretreatment method as Designs A and B, this design eliminates the use of UF system and adopts the two-pass RO system as shown in Fig. 4.3. For the first pass RO system, the pretreated POME is pressurized and distributed to the pressure vessels/modules in parallel in the first RO stage. The first stage outlet retentate is distributed to the pressure vessels/modules in parallel in the subsequent stage until the final stage. The permeate blend of every RO stage in the first pass serves as the feed stream to the second pass RO system. The feed stream is pressurized and distributed in parallel to every stage of the second pass RO system in the identical manner as the first pass. The feed stream from the first pass is clean and thus the second pass system can operate at a relatively high average permeate flux and high recovery rate. The treated water will be the blending of the RO permeate in the second pass. The outlet retentate of first and second pass RO system is recycled back to the GAC feed tank. The dissolved contaminant in the outlet retentate from the second pass is usually lower than the outlet retentate from the first pass. Therefore, blending both streams will dilute the contaminant concentration of the outlet retentate in the first pass RO system.

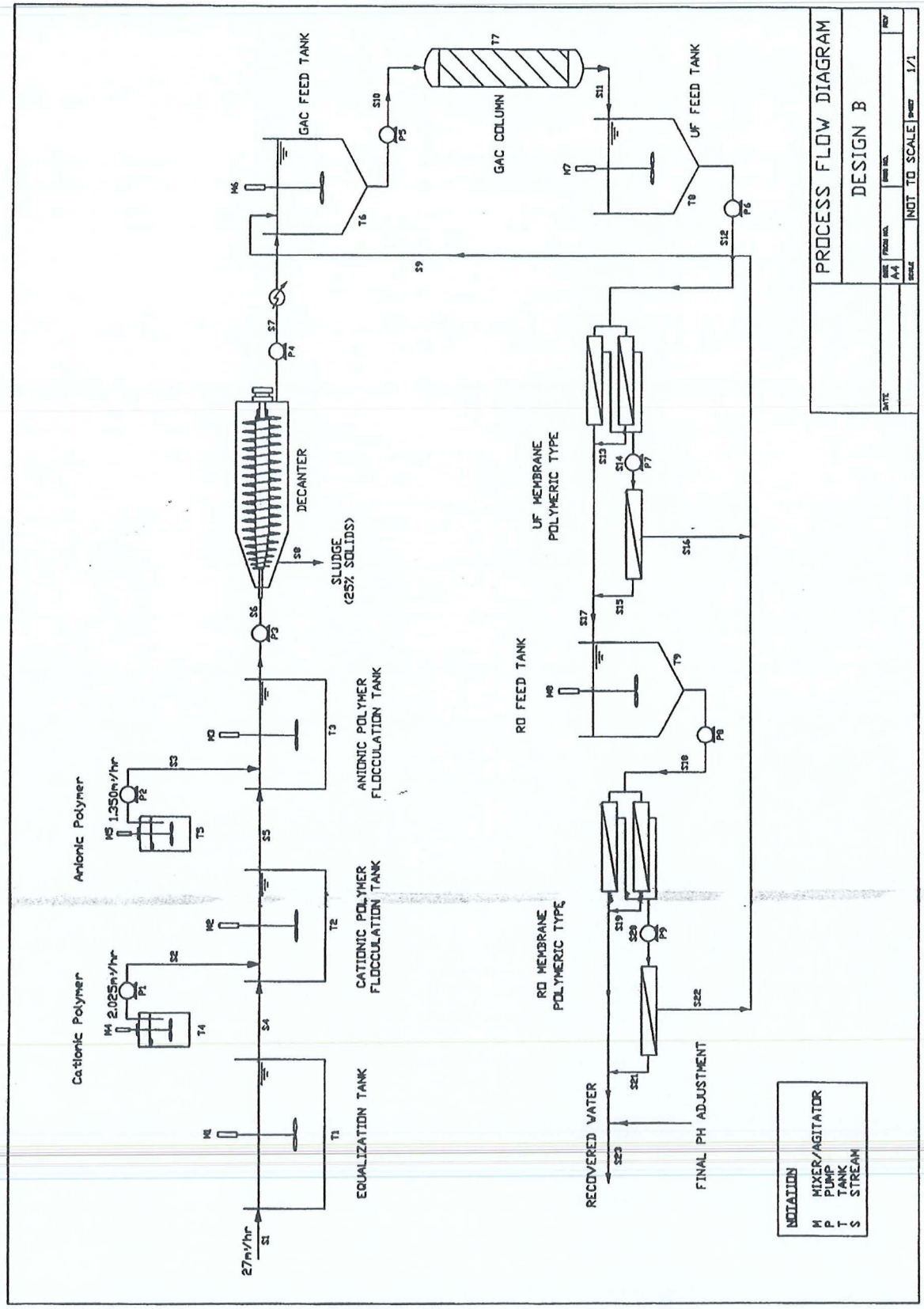

Fig. 4.2: Process Flow Diagram (PFD) of membrane based POME treatment system for Design B

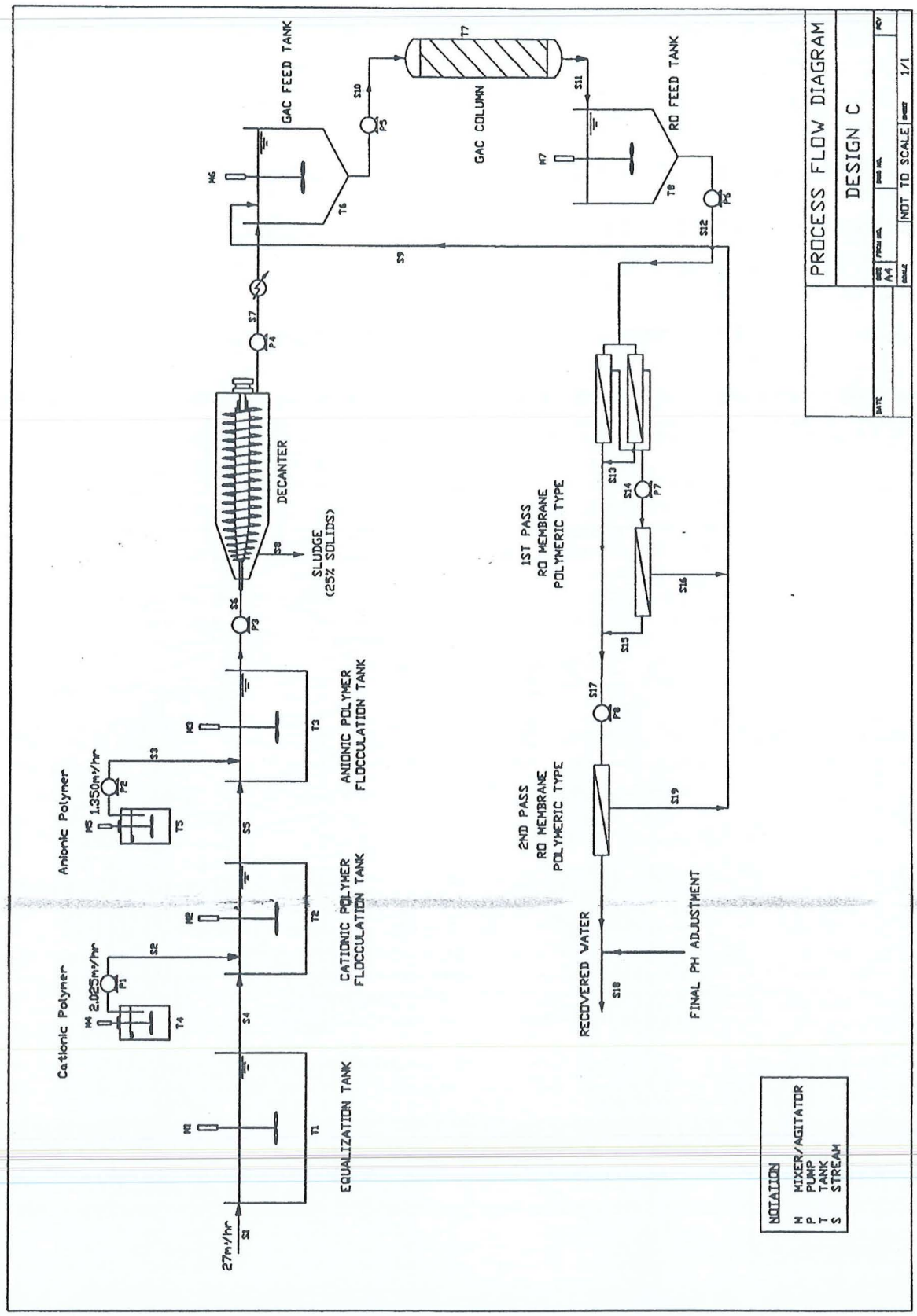

Fig. 4.3: Process Flow Diagram (PFD) of membrane based POME treatment system for Design C

Each of the proposed Designs A, B and C poses its specific advantages and disadvantages as summarized in Table 4.1. Consequently, based on the qualitative comparison as shown in Table 4.1, the best design for the membrane based POME treatment is difficult to evaluate unless an optimization study is conducted so that the cost effectiveness for each design at the optimum condition is compared.

Table 4.1: Comparison between the type of membrane used and the design of the process.

Membrane type	UF ceramic	UF Polymeric	RO polymeric
Advantages	Offers long durability which can withstand excessive strong chemicals and high temperature, requires low trans membrane pressure.	Easy availability, offer larger effective filtration area, simple CIP procedure, cheap, requires low trans membrane pressure.	Much cheaper, well established, high pollutant rejection, large effective filtration area, simple CIP procedure and requires little cleaning reagent.
Disadvantages	Very expensive, small effective filtration area, require complex CIP procedure and much cleaning reagent.	Cannot withstand excessive strong chemicals and high temperature, not durable.	Cannot withstand excessive strong chemicals and high temperature, requires very high trans membrane pressure, not durable.
Design	**A**	**B**	**C**
Membrane system			
1st System	UF Ceramic	UF Polymeric	RO Polymeric
2nd System	RO Polymeric	RO Polymeric	RO Polymeric
Advantages	Require low energy cost, has long membrane life.	Require little membrane cleaning and low energy cost.	Low investment cost, requires very little membrane cleaning, produce very good water quality.
Disadvantages	Require very high investment cost and excessive membrane cleaning, produce only acceptable water quality.	Require high investment cost, produce only acceptable water quality, has short membrane life.	Require very high energy cost and has short membrane life.

4.2 Mass Balance Analysis

In the mass balance calculations, constant average feed flow rate and solutes concentrations are used. The solutes considered in the mass balance calculation were suspended solids, carbohydrate constituents, protein and ammoniacal nitrogen. Once the mass balance is obtained, the COD, BOD, oil & grease and total nitrogen concentrations

are obtained based on the correlation equations of Eqs. (3.1) to (3.4). A typical feed flow rate of $27m^3$/hr based on the palm oil mill capacity of 36 tons/hr (181,400 tons/yr) Fresh Fruit Bunch (FFB) processed is chosen. The flocculation and sludge dewatering process is implemented at the POME inlet temperature of 70°C. The centrate from the decanter is cooled to room temperature before GAC adsorption by using a heat exchanger.

4.3 Sizing and Costing

4.3.1 Sizing

The sizing of tanks, agitators, pumps, membrane systems, GAC column and heat exchanger are based on the method presented by Geankoplis (1993) and Perry (1997). The sizing of the decanter is discussed in detail.

Consider the steady-state condition in the cylindrical section of a Dry Solids Decanter bowl filled with a consolidating or compacting cake. Cake is continuously being scrolled and pressed out under the BD disk (the barrier mounted between bowl and beach - see Fig. 4.2). Liquid is continuously being expelled as the cake compacts, and new wet cake is continuously being "deposited" on the top of the cake, corresponding to the feed slurry rate entering the centrifuge. Since a steady-state condition has been assumed, the radial liquid flow, Q_L is constant throughout the cake and can be calculated by using a constant average permeability (k_{avg}) through the height of the cake as:

$$Q_L = \frac{\pi L k_{avg}}{\eta \ln(r_2 / r_1)} (\rho_{cake} - \rho_L)(r_2^2 - r_1^2)\omega^2 \quad \text{or} \quad (4.1)$$

$$Q_L = K.\pi L \frac{(r_2^2 - r_1^2)}{\ln(r_2 / r_1)} \omega^2 \quad (4.2)$$

where

system. The Indirect Capital Cost (ICC) is taken as 10% of the DCC and thus the Total Capital Cost (TCC) is the summation of DCC and ICC.

The exponential method calculates the cost of equipment by using capacity-ratio exponents based on existing cost data of a company or drawn from published correlations. If the cost of a piece of equipment q_1 is C_1, then the cost C_2 of a similar piece of equipment q_2 can be calculated from

$$C_2 = C_1\left(\frac{q_2}{q_1}\right)^{\zeta} \tag{4.7}$$

where the value of the exponent ζ depends on the type of equipment. Table 4.2 gives typical values of ζ for the equipment required for Design A, B and C. The Table 4.2 also includes the base cost of the equipment, C_1; which is obtained from the quotation of EnviLab Sdn. Bhd. for the pilot plant fabrication in year 2007.

Table 4.2: Typical exponents (Perry, 1997) and base cost (EnviLab Sdn. Bhd.) for equipment cost estimation.

Equipment	Size	Unit	Base Cost	Exponent
Tanks: atm, vertical cylinder, concrete	0.55	m^3	1500	0.3
Tanks: atm, vertical cylinder, HDPE	0.69	m^3	546	0.3
Tanks: atm, vertical cylinder, SS	0.55	m^3	3000	0.3
Agitator, turbine, top entry, open	0.37	kW	1700	0.45
Centrifugal pump	0.32	kW	5000	0.67
Piston pump	27.73	kW	14600	0.67
Dosing pump	0.04	kW	1400	0.10
Heat exchanger, shell-tube, floating head, C/S	1	m^2	460	0.59
UF membrane module, ceramic , SS housing	0.36	m^2	16533	1
UF membrane module, polymeric , SS housing	0.9	m^2	4500	1
RO membrane module, polymeric, SS housing	0.9	m^2	2250	1

Note: All costs are based on Malaysian Ringgit (RM)

The costs of framework, labor and piping, valves & fittings are calculated in the similar manner as in Eq. (4.7) by assuming the exponent ζ equal to unity. The base costs

for the framework, labor and piping, valves & fitting as listed in Table 4.3 are different for different unit operation or system depending on its application in the process.

Table 4.3: Base costs for the framework, labor and piping, valves & fitting (EnviLab Sdn. Bhd.).

Unit operation/system	Size, q_1	Base Cost, C_1		
		framework	labor	Piping, valves & fittings
Equalization	0.55m^3	300	200	nil*
Feed tanks	0.55 m^3	500	100	nil*
Cationic Polymer Flocculation	0.55 m^3	1000	500	nil*
Anionic Polymer Flocculation	0.55 m^3	1000	500	nil*
GAC Adsorption	0.55 m^3	100	50	nil*
Heat exchanger	1.00 m^2	25	10	15
UF membrane system, ceramic type	0.36 m^2	50	42	27
UF membrane system, polymeric type	0.90 m^2	50	42	27
RO membrane system, polymeric type	0.90 m^2	50	42	27

Note: All costs are based on Malaysian Ringgit (RM)
* The cost is already inclusive in the framework cost

The CIP or back-flush for membrane system is assumed 2% of the membrane module cost and the control & automation cost is calculated based on the summation of total instruments, control panel and wiring used in the system. As the membrane system requires efficient control so that the membrane system can be operated at a designated trans membrane pressure, the automation in term of pressure control is essential while for the other system, manual control is adequate. The unit cost for each instrument used for the control & automation cost estimation is listed in Table 4.4. The activated carbon granular used to fill up the GAC column for GAC adsorption system is required in the initial installation of the treatment plant and therefore, the material cost for activated carbon granular must be included in the capital cost calculation. The material cost needed can be estimated by multiplying the volume of activated carbon granular needed.

Table 4.4: Unit cost for each instrument used for the control & automation cost estimation (EnviLab Sdn. Bhd.).

Instrument	Unit	Cost
Flow meter, digital type	RM/unit	3000
Flow meter, analog type	RM/unit	155
Pressure indicator, analog type	RM/unit	120
Pressure control system (indicator, transmitter, controller)	RM/unit	4100
Agitator inverter	RM/unit	1700
Temperature indicator	RM/unit	1400
Control panel	RM/unit	9600
Wiring	RM/unit	6500

Once the costs of equipment, C_{equip}, framework, C_{frame}, labor, C_{labor}, control & automation, $C_{control}$, piping, valves & fittings, $C_{piping\ \&\ valves}$, material, $C_{material}$ and Clean In Place (CIP) or back-flush for the membrane system, C_{CIP} are estimated, the Direct Capital Cost (DCC) of a process plant can be obtained as:

$$DCC = C_{equip} + C_{frame} + C_{labor} + C_{control} + C_{piping\ \&\ valves} + C_{material} + C_{CIP} \quad (4.8)$$

The Indirect Capital Cost (ICC) is given as (Helal *et al.*, 2003):

$$ICC = 0.1\,DCC \quad (4.9)$$

Thus, the Total Capital Cost (TCC) is

$$TCC = DCC + ICC \quad (4.10)$$

In the present study, the operating cost of the system includes electrical cost, maintenance cost, chemical cost, chemical cleaning cost for membrane system, activated carbon granular and membrane replacement cost. The fertilizer generated from the pretreatment process is an added advantage in reducing the total treatment cost through the profit generated from the fertilizer sale. The sale can either be to external or internal customers (including local savings achieved via reduction of imported fertilizer for plantation). As FELDA owns the major palm oil plantation in Malaysia, sale of fertilizer internally can be easily achieved.

4.3.2(b) Total Cost

Ultimately, the total cost is an important parameter to be considered in the process design for the present study. By considering the plant life of N_{yr} years with the interest rate, i of 4%, the capital recovery factor, CRF is:

$$CRF = \frac{i(1+i)^{N_{yr}}}{[(1+i)^{N_{yr}} - 1]} \tag{4.11}$$

The annualized capital cost, ACC then is calculated as:

$$ACC = TCC \cdot CRF \tag{4.12}$$

The total cost, C_{total} is the summation of the annualized capital cost, the operating cost, $C_{operating}$ and subtraction of the profit gained via fertilizer sale, C_{Fert} as:

$$C_{total} = ACC + C_{operating} - C_{Fert} \tag{4.13}$$

Thus, the total treatment cost per cubic meter of POME treated, c_{total} is calculated as:

$$c_{total} = \frac{C_{total}}{Q_{in}\, t_d\, t_h} \tag{4.14}$$

where the term Q_{in} is taken as the feed flow rate of the plant.

4.4 Optimization and Constraints

The present study investigates the complete optimization of membrane based POME treatment system of proposed Designs A, B and C, including the configuration of the membrane system and operating conditions using constrained nonlinear optimization. Each of the Design A, B and C is optimized respectively, and the results pertaining to process economics in term of total costs are compared to identify the optimal process design. The objective of the optimization is to minimize total treatment cost per cubic meter of POME treated, c_{total} for the membrane based POME treatment system. Thus the

objective function to be minimized based on Eq. (4.14); which is subjected to a set of decision variables, x is presented mathematically by:

$$\min f(x) = c_{total} = \frac{ACC + C_{operating} - C_{Fert}}{Q_{in}\, t_d\, t_h} \tag{4.15}$$

The minimization of the objective function of Eq. (4.15) involves determination of the annual capital cost (ACC), operating cost ($C_{operating}$) and profit gained from fertilizer sale (C_{Fert}). Determination and optimization (minimization) of these cost values are subjected to the calculation of transport models, mass balance, sizing and costing of the equipments.

The upper limit and the lower limit allowed for each variable is the constraint imposed in the optimization calculation. For the membrane based POME treatment system, the constraints as listed in Table 4.5 are the operating conditions and physical limitations of the pretreatment and membrane system as well as the water quality requirement imposed by the DOE. As shown in the Table 4.5, the range of the constraints $C_{ss,out}$, $P_{out,j}$, $N_{s,j}$ and v_j are the physical limitations of the membrane systems supplied by the membrane manufacturer, PCI-Memtech, UK. The water recovery in every stage of membrane system should not be more than 55% in order to prevent serious membrane fouling (Maskan *et al.*, 2000). The objective function of Eq. (4.15) also depends on the parameters, which are regarded as constants during the optimization calculation. The parameters used in the optimization calculations are mainly the feed flow rate and the raw POME characteristic, the cost parameters and the properties of membrane modules as listed in Tables 4.6 and 4.7 respectively.

The system models for Design A, B and C were coded in MATLAB respectively and the constrained nonlinear problems are optimized using the sequential quadratic

programming method (Maskan, *et al.*, 2000). The systems are minimized through the single-objective function which is total treatment cost per cubic meter, c_{total} of Eq. (4.15), subject to the constraints imposed on the variables as listed in Table 4.5. The optimal values of the optimization variables were determined by the optimization tool of MATLAB. To increase the chance to obtain a global minimum of the total cost, the optimization procedure is repeated with several initial values of the optimization variables.

Table 4.5: The range of constraints used for optimization

Variable/Constraint	Range	Reason
Pretreatment		
i) Cationic Polymer Flocculation		
- Polymer dosage, d_s	<=600 mg/L	To avoid high chemical cost
- Stirring speed, N	<=250 rev/min	To avoid flocs breakage
- Suspended solids concentration, $C_{ss,out}$	<=100 mg/L	To avoid irreversible fouling in the membrane system.
ii) Anionic Polymer Flocculation		
- Polymer dosage, d_s	<=60 mg/L	To avoid high chemical cost
- Stirring speed, N	<=250 rev/min	To avoid flocs breakage
- Suspended solids concentration, $C_{ss,out}$	<=50 mg/L	To avoid irreversible fouling in the membrane system.
iii) Sludge Dewatering		
- G-force	<=3574G	To meet the manufacturer specification
iv) GAC Adsorption		
-Residence time, τ	<=30 min	To avoid large vessel/too many vessels
Membrane System		
i) UF Membrane Ceramic Type		
- Outlet pressure, $P_{out,j}$	1-6 bar	To avoid membrane rupture
- Number of module in series, $N_{s,j}$	<=25	To avoid large pressure drop
- Cross flow velocity, v_j	>=0.5m/s	To ensure sufficient turbulence
- Water recovery, r_j	<=55%	To avoid irreversible fouling
ii) UF Membrane Polymeric Type		
- Outlet pressure, $P_{out,j}$	1-6 bar	To avoid membrane rupture
- Number of module in series, $N_{s,j}$	<=25	To avoid large pressure drop
- Cross flow velocity, v_j	>=0.2m/s	To ensure sufficient turbulence
- Water recovery, r_j	<=55%	To avoid irreversible fouling
iii) RO Membrane Polymeric Type		
- Outlet pressure, $P_{out,j}$	20-50 bar	To avoid membrane rupture
- Number of module in series, $N_{s,j}$	<=25	To avoid large pressure drop
- Cross flow velocity, v_j	>=0.3m/s	To ensure sufficient turbulence
- Water recovery, r_j	<=55%	To avoid irreversible fouling
Recovered Water Quality		
- Biological Oxygen Demand, BOD_{final} (BOD; 3 days, 30°C)	<=100mg/L	To meet discharge standards
- Chemical Oxygen Demand, COD_{final}	Not Required	To meet discharge standards
- Suspended Solids, $C_{ss,final}$	<=400 mg/L	To meet discharge standards
- Oil and Grease, $C_{O\&G,final}$	<=50 mg/L	To meet discharge standards
- Ammoniacal Nitrogen, $C_{i,final}$; $i=3$	<=150 mg/L	To meet discharge standards
- Total Nitrogen, $C_{i,final}$; $i=2$	<=200 mg/L	To meet discharge standards
- pH	5-9	To meet discharge standards
- Temperature, T_{ho}	<=45°C	To meet discharge standards

Table 4.6: Cost parameters used for total cost minimization

Parameters	Value
Plant life, N_{yr}	20 years
Operation hours, t_h	16 hrs/day
Operation days, t_d	315 days/yr
Interest rate, i	4%
Capital recovery factor, CRF	0.0736
Maintenance cost, $C_{maintenance}$	6% of the annualized capital cost.
CIP for membrane system	2% of membrane cost
Indirect capital cost, ICC	10% of the direct capital cost, DCC
Electricity rate, c_{elec}	RM 0.258/kWh
Unit cost for cationic polymer, c_{chem}	RM 13.50/kg
Unit cost for anionic polymer, c_{chem}	RM 12.70/kg
Unit cost for activated carbon granular, c_{GAC}	RM 1700/m^3
Unit cost of UF membrane, ceramic type, c_{memb}	RM 45,925/m^2
Unit cost of UF membrane, polymeric type, c_{memb}	RM 3889/m^2
Unit cost of RO membrane, polymeric type, c_{memb}	RM 1389/m^2
Unit cost for sodium hydroxide, c_{NaOH}	RM 0.80/kg
Unit cost for nitric acid, c_{HNO_3}	RM 1.50/kg
Selling price for fertilizer, c_{Fert}	RM 0.60/kg

Table 4.7: Properties of membrane small modules from PCI-Memtech, UK

Property	UF membrane		RO membrane
Material	Ceramic	Polymeric	Polymeric
Module Type	Tubular	Tubular	Tubular
$N_{memb,yr}$ or ARR_{memb}	5 years	50%	50%
Effective membrane area, A	0.36 m^2	0.90 m^2	0.91 m^2
Area of membrane channel, $A_{channel}$	0.03 m^2	0.05 m^2	0.05 m^2
Inner diameter of membrane tube, d	0.006 m	0.013 m	0.013 m
Number of membrane tubes, n	19	18	18
Membrane length, L	1.00 m	1.25 m	1.27 m
Number of membrane cleaning cycle, $N_{cleaning}$	48/yr	24/yr	24/yr[a] / 12/yr[b]
Amount of caustic needed for CIP, m_{NaOH}	0.3 kg/module	0.3 kg/module	Not Required
Amount of acid needed for CIP, m_{HNO_3}	0.3 kg/module	0.3 kg/module	0.042 kg/module

[a] for RO membrane of Design A & B and first pass RO membrane of Design C.
[b] for second pass RO membrane of Design C.

Raw POME and Analysis

The sample analysis was done to determine the physical, chemical and biochemical composition of POME and the treated POME. The sample was analyzed immediately after the collection to avoid any interference (APHA, 1999). Two liters of the sample was collected and continuously stirred to maintain the homogeneous condition. All analysis was carried out in triplicate to obtain the average data. The parameters involved in the analysis include temperature, pH, viscosity, suspended solids, particle size distribution, Chemical Oxygen Demand (COD), Biological Oxygen Demand (BOD), Oil and Grease, Carbohydrate Constituents (Dubois et al., 1956), Protein (BCA Protein Assay, Pierce, USA), Ammoniacal Nitrogen and Zeta Potential. All analysis is based on the Standard Method (APHA, 1999) unless it is mentioned other wise.

5.2 Bench Scale Study

5.2.1 Flocculation Process

Raw POME was collected from United Palm Oil Mill, Sungai Kecil Nibong Tebal, Penang, Malaysia at an average temperature of 70°C. The cationic polymer used was the medium charge density with high molecular weight (Polyfloc KP 9650) while the anionic polymer used was the high charge density with high molecular weight (Polyfloc AP 8350). Both polymers were provided by Dia-Chemical Sdn. Bhd. In all experimental tests, the appropriate mass of cationic and anionic polymer was dissolved in water to give 0.4% w/v and 0.1% w/v feedstock solution respectively. These feedstock solution concentrations were recommended by their manufacturers in order to ensure the optimum performance of the polymers.

5.2.1(a) Jar Test Procedure

Experiments were carried out in a jar test apparatus (Flocculator SW1, Stuart Scientific, UK) equipped with six beakers of 1L volume. The experiment was carried out on site and in the case where the raw POME sample was transferred to the in house laboratory of Universiti Sains Malaysia, the raw POME was maintained at desired temperature by using a water bath (Julabo, SW22). The sample was stirred thoroughly for re-suspension of possible settled solids and analyzed. The sample was transferred into the 400mL beakers. The appropriate dosage of cationic and anionic polymers was added into the samples while stirring at varying stirring speed and stirring time respectively. The sample was left to settle for 1 min and the supernatant from the sample was taken and analyzed.

5.2.2 Granular Activated Carbon (GAC) Adsorption

The adsorbent used in the present study was granular activated carbon (GAC) manufactured from coconut shell, supplied by Envilab Sdn. Bhd. with the following properties: apparent density, 498 kgm^{-3}; particle density, 740 kgm^{-3}; porosity, 0.50. The particle size distribution of the GAC was determined by sieve analysis (Sotelo *et al.*, 2004). The average particle size of 1.75mm was obtained. In order to remove any fines attached to the GAC particles and any leachable matter, the GAC was further washed several times with distilled water. The activated carbon was considered fit for use when the distilled water obtained after washing was visibly clear. After washing the GAC, it was air dried at room temperature. After the GAC was completely dried, it was stored in a glass bottle until use. The pretreated POME used in the GAC adsorption study was obtained by the flocculation process using polymers to remove the suspended solids and oil & grease from the raw POME.

5.2.2(a) Fixed-Bed Adsorption Study

In the fixed-bed adsorption study, the complex solution of pretreated POME (ternary system) was used. The pretreated POME was pumped through a flowmeter into a GAC column. The bed porosity and the inner diameter of column were 0.5 and 50mm respectively. The desired residence time, τ was maintained by maintaining the feed flow rate using a peristaltic pump at the desired bed length. The effluent samples were taken at every time interval and the concentrations were subsequently analyzed. A typical adsorption experimental run time was between 60 – 70 hours.

5.3 Pilot Plant Study

Throughout the pilot plant study, the pilot plant was operated based on the Standard Operating Procedure (SOP). The flocculation and GAC adsorption process were conducted based on the optimum condition obtained from the bench scale study. The results obtained from the pilot plant study must be corresponding with the results obtained from the bench scale study at the variation not more than 5%.

5.3.1 Flocculation Process

The flocculation process was conducted in Chemical Treatment Tank. 400L of raw POME sample at ~70°C was mixed at 200rev/min mixing speed to create a homogeneous condition. Cationic Polymer, Polyfloc KP 9650 prepared at the concentration of 0.4% w/v was added to the sample with the dosage of 300mg/L and stirred for 3 minutes at 200rev/min. Anionic Polymer, Polyfloc AP 8350 (0.1% w/v) was then introduced with the dosage of 50mg/L and the mixer speed was immediately reduced to 150rev/min. The mixture was mixed for 1 minute. The suspended solids of the supernatant was frequently

checked to ensure the value was below 50mg/L before it was pumped to the next process. The analyses of the effluent samples were carried out accordingly.

5.3.2 Sludge Dewatering using Filter Press

After the flocculation process was completed, the sludge and supernatant of the process were pumped using Blagdon air operated double diaphragm pump, United Kingdom, to the filter press unit for separation process which leads to higher supernatant recovery. The plate and frame filter press model LES 250, composed of filter plates with dimension of 250 mm x 250 mm made of polypropylene. PP 2816 (black) filter cloth with 15 L/dm^2/min were inserted between the filter plates and hydraulic hand pump system was applied to tighten the plates and cloths. Filter frame made of fabricated steel with cold rolled steel sidebars. The operating pressure is up to 700 kg/cm^2. There are 6 chambers of the filter press with 7.86 liter of press volume and cake thickness of 30mm. The filtrate was collected in the 10 liters sample bottles before being transferred to the next process. After the collection of the filtrate was completed, the filtrate samples were analyzed accordingly.

5.3.3 Granular Activated Carbon (GAC) Adsorption

The supernatant collected from the filter press was left until the temperature was reduced to room temperature (28-30°C). The supernatant was fed via a pump using downward flow into a fixed bed of granular activated carbon. The activated carbon containing column was made of perspex (250 mm diameter x 1300 mm height) and used for removing of dissolved organic solutes, colour and odour. The flow rate was adjusted to maintain the residence time of 22.5 minutes. The analyses of the effluent samples were carried out.

5.3.4 Ultrafiltration (UF) Membrane System

The UF membranes used in the pilot plant were the tubular modules of ceramic and polymeric type with stainless steel housing. The ceramic (TiO_2) membrane module P16-60 (PCI-Memtech) had a nominal molecular weight cut-off (MWCO) of 10 kg/mole with 19 flow channels. The inner diameter of each tube was 6.0mm and its length was 1m. The effective area for filtration was 0.36m^2 and could be operated up to maximum pressure of 6bar. The polymeric (Polyvinylidene Diflouride (PVDF)) membrane module (PCI-Memtech) had a nominal molecular weight cut-off (MWCO) of 200 kg/mole with 18 flow channels. The inner diameter of each tube was 13mm and its length was 1.25m. The effective area for filtration was 0.90m^2 and could be operated up to maximum pressure of 6bar.

The pretreated POME from GAC adsorption unit was placed in the feed tank of the membrane system. The feed was pumped through the membrane module (ceramic or polymeric type) using a centrifugal pump (Grundfos CRN-8-50). The required cross-flow rate and trans membrane pressure were adjusted using the pressure control valves (Gemu-diaphragm type). The inlet and outlet pressures of the module were measured using the pressure gauges. The turbine function flowmeter (Burkert) was used to measure cross-flow rate of the feed. The required cross-flow velocity, v was calculated from the feed flow rate, Q_F using the following equation:

$$v = \frac{Q_F}{A_{sc}} \tag{5.1}$$

where A_{sc} is the cross sectional area of the membrane module. The trans membrane pressure, ΔP was calculated as the average of the inlet pressure, P_{in} and outlet pressure, P_{out} as

$$\Delta P = \frac{(P_{in} + P_{out})}{2} - P_{ap} \quad (5.2)$$

where the term P_{ap} is the atmospheric pressure. The permeate and the retentate streams were recycled back to the feed tank (total recycle mode) to maintain a constant feed concentration. During the experiments, permeate flow rate of each membrane was periodically measured. The permeate flux (J_v) was calculated by the following equation:

$$J_v = \frac{Q_p}{A} \quad (5.3)$$

where Q_p is the permeate flow rate and A is the effective filtration area of the membrane. Each of the experiment was repeated twice and the average values were recorded. The data were reproducible within an error of $\pm 5\%$.

5.3.5 Reverse Osmosis (RO) Membrane System

The RO membrane used in the pilot plant was the polymeric (Polyvinylidene Diflouride (PVDF)) membrane module B1 (PCI-Memtech) with stainless steel (SS 316) housing. The membrane module had a rejection of 99.9% NaCl with 18 flow channels. The inner diameter of each tube was 12.7mm and its length was 1.2m. The effective area for filtration was 0.90m^2 and could be operated up to maximum pressure of 60bar.

The types of feed to the reverse osmosis system investigated in the present studies were based on two different mode of operation, which were:

(a) GAC-UF-RO mode. In this mode, the feed to the RO membrane system was obtained from the permeate of UF membrane system,

(b) GAC-RO-RO mode. In this mode, two types of feed to the RO membrane system were investigated. The first type of feed was the pretreated POME after GAC adsorption

while the second type of feed was the permeate collected from the first-pass RO membrane system.

The pretreated POME was placed in the feed tank of the RO membrane system and was pumped through the membrane module using a piston type pump (CAT 1056). The RO membrane system was operated in the similar manner as the UF membrane system and the cross-flow velocity, trans membrane pressure and permeate flux were measured using the Eqs. (5.1) – (5.3). Each of the experiment was repeated twice and the average values were recorded. The data were reproducible within an error of $\pm 5\%$.

6.2 POME Characteristic Analysis and Correlations

30 samples of raw POME collected from the United Oil Palm Industries Sdn. Bhd., Sungai Kecil, Nibong Tebal, Penang throughout the year of 2005 were analyzed and the characteristics of the raw POME are tabulated in Table 6.1. Based on the characteristic of the raw POME as listed in Table 6.1, the parameters of suspended solids, carbohydrate constituents, protein and ammoniacal nitrogen are utilized in all the transport models to predict and evaluate the performance of the processes or systems in the pilot plant. The concentration of these solutes are used to estimate the concentration of oil & grease, COD, BOD and total nitrogen based on the correlation equations of Eqs. (3.1) to (3.4).

Table 6.1: Average characteristics of POME from United Oil Palm Industries Sdn. Bhd.

Parameter	Range	Average Value
Feed Flow Rate (m^3/hr)	26-27	27
pH	4.05 – 4.20	4.10
Temperature (^oC)	68 – 75	70
Total COD (mg/L)	38,000 – 43,500	40,000
Soluble COD (mg/L)	17,800 – 20,500	19,500
Total BOD (mg/L)	19,800 – 21,800	20,500
Soluble BOD (mg/L)	10,500 – 11,500	11,200
Suspended solids (mg/L)	13,400 – 15,400	14,800
Oil and grease (mg/L)	3,600 – 4,000	3,700
Carbohydrate Constituents (mg/L)	11,300 – 12,500	12,100
Protein (mg/L)	19,000 – 21,000	20,700
Ammoniacal Nitrogen (mg/L)	80 – 110	100
Total Nitrogen (mg/L)	730 – 800	750

By using the correlation equation of Eq. (3.1), the total COD concentration is correlated to the suspended solids concentration as shown in Fig. 6.1. A linear plot of total COD concentration against the suspended solids concentration shows that the intercept of

y-axis indicates the value of raw POME soluble COD ($COD_{soluble}$). The final correlation is obtained as:

$$COD_{total} = 1.4153\, C_{ss} + 18447 \tag{6.1}$$

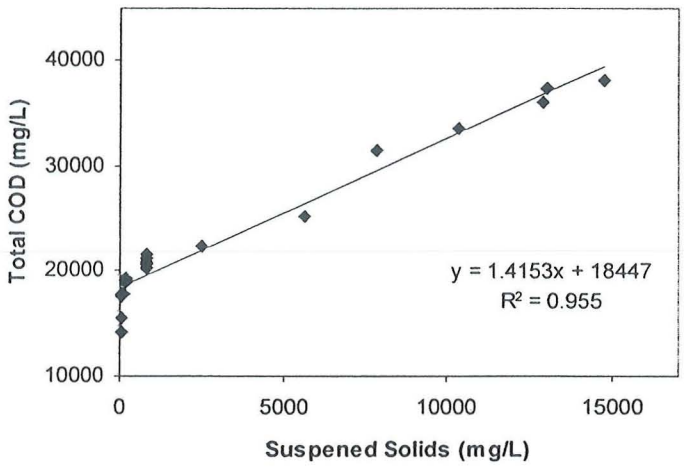

Fig. 6.1: Linear plot of total COD concentration against the suspended solids concentration

Since the oil & grease concentration is also dependant on the suspended solids concentration, the linear plot of oil & grease concentration against suspended solids concentration based on Eq. (3.2) is shown in Fig. 6.2. The slope of the plot give the value of $b_{O\&G} = 0.2573$. Thus, the final correlation is obtained as:

$$C_{O\&G} = 0.2573 C_{ss} \tag{6.2}$$

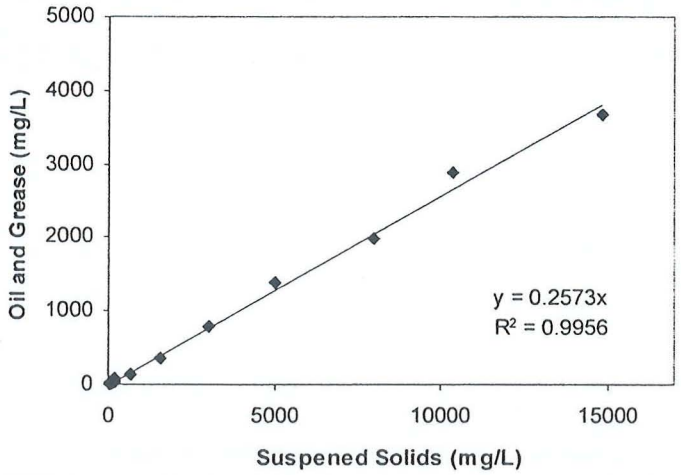

Fig. 6.2: Linear plot of oil and grease concentration against the suspended solids concentration

The soluble COD of raw POME is further reduced by means of GAC adsorption and membrane separation processes. The concentrations of all the dissolved organic solutes i in the system ($i = 1$ for carbohydrate constituents, $i = 2$ for protein and $i = 3$ for ammoniacal nitrogen) were used to correlate with the soluble COD value based on Eq. (3.3). The correlation was obtained by using the multivariable regression of Levenberg-Marquardt Method. As the soluble COD value examined fall in a wide range of 100 to 19,500 mg/L, the correlation was obtained based on the high range and low range correlation so that a linear plot can be obtained. For the high range correlation (working range 1900-19,500mg/L), the values of the dimensionless coefficients b_1, b_2 and b_3 were 1.2599, 0.2708 and 0.5595 respectively. The final correlation is given by:

$$COD_{soluble} = 1.2599\, C_1 + 0.2708\, C_2 + 0.5595\, C_3 \qquad (6.3)$$

For the low range correlation (working range 100-350mg/L), the values of the dimensionless coefficients b_1, b_2 and b_3 were 8.7891, 6.4598 and 0.0897 respectively. The final correlation is given by Eq. (6.4).

$$COD_{soluble} = 8.7891\, C_1 + 6.4595\, C_2 + 0.0897\, C_3 \qquad (6.4)$$

The comparison of the experimental data and the model predictions is shown in Fig. 6.3. It shows that the correlation was successfully applied in the prediction of soluble COD concentration with the coefficient of determination (R^2) of more than 0.9.

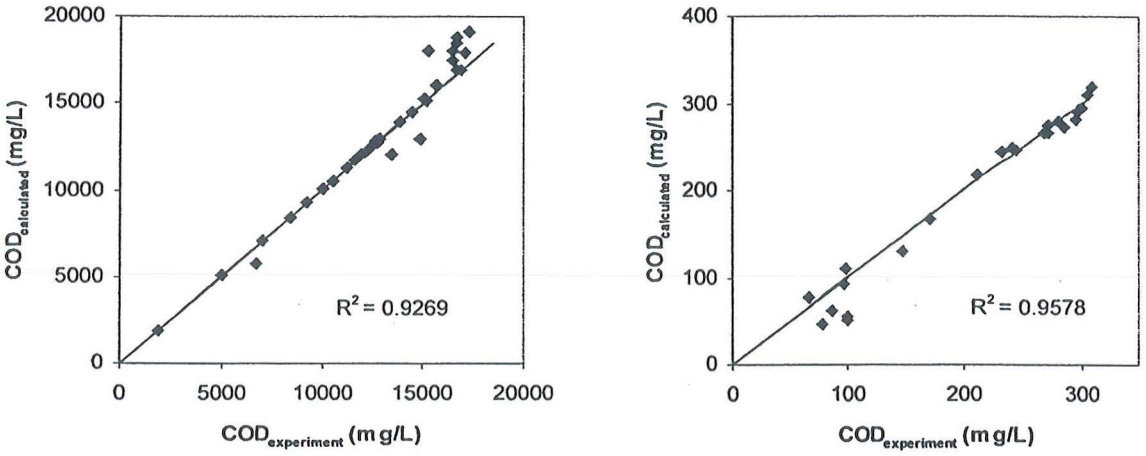

(a) (b)

Fig. 6.3: Comparison of experimental COD against calculated COD (a) high range correlation (b) low range correlation.

The substitution of Eq. (6.3) and Eq. (6.4) respectively into Eq. (6.1) gives the complete correlation of suspended solids and dissolved organic solutes (carbohydrate constituents, protein and ammoniacal nitrogen) with the total COD concentration. The correlation equation for high range total COD concentration is given as:

$$COD_{total} = 1.4153\, C_{ss} + 1.2599\, C_1 + 0.2708\, C_2 + 0.5595\, C_3 \quad (6.5)$$

The correlation equation for low range total COD concentration is given as:

$$COD_{total} = 1.4153\, C_{ss} + 8.7891\, C_1 + 6.4595\, C_2 + 0.0897\, C_3 \quad (6.6)$$

Based on the observation of the present study, the rate of degradation is strongly dependant on the soluble and insoluble component of the sample to be examined. The insoluble component (suspended solids) of the sample is more difficult to be digested by the bacteria (lower rate of degradation) than the soluble component (dissolved organic

solutes). Thus, both correlations of insoluble BOD with insoluble COD and soluble BOD with soluble COD are needed. The summation of insoluble and soluble BOD will give the total BOD value. The linear plot of insoluble BOD concentration against insoluble COD concentration based on Eq. (3.4) is shown in Fig. 6.4. The slope of the plot give the value of $b_{BOD} = 0.4327$. Thus, the final correlation is obtained as:

$$BOD_{inso\,lub\,le} = 0.4327\,COD_{inso\,lub\,le} \tag{6.7}$$

where the term $BOD_{inso\,lub\,le}$ is the insoluble BOD concentration and $COD_{inso\,lub\,le}$ is the insoluble COD concentration.

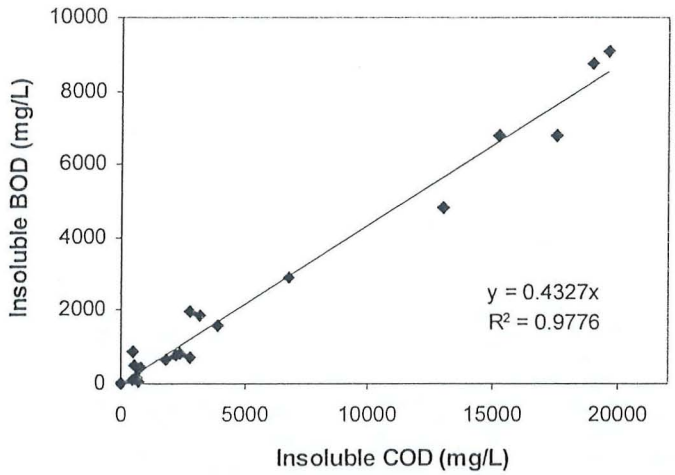

Fig. 6.4: Linear plot of insoluble BOD concentration against the insoluble COD concentration

The correlation of soluble BOD, $BOD_{so\,lub\,le}$ with soluble COD is obtained based on the high range and low range correlation so that a linear plot can be obtained. For the high range correlation (working range 2000-12,000mg/L), the value of the dimensionless coefficient, b_{BOD} as shown in Fig. 6.5(a) was 0.6240 and the final correlation is:

$$BOD_{so\,lub\,le} = 0.6240\,COD_{so\,lub\,le} \tag{6.8}$$

For the low range correlation (working range 25-110mg/L), the value of the dimensionless coefficient, b_{BOD} as shown in Fig. 6.5(b) was 0.3338 and the final correlation is:

$$BOD_{soluble} = 0.3338 COD_{soluble} \tag{6.9}$$

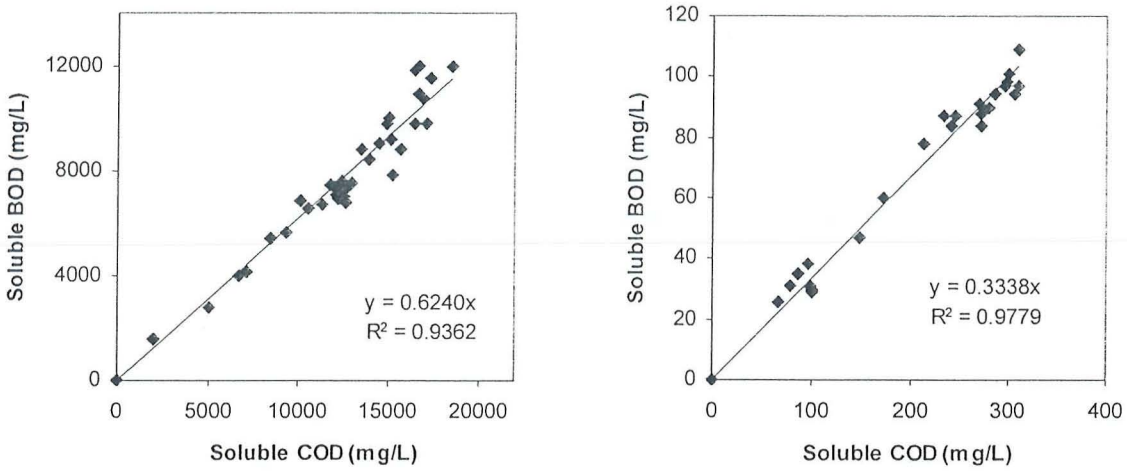

Fig. 6.5: Linear plot of soluble BOD concentration against the soluble COD concentration (a) high range correlation (b) low range correlation

The summation of Eq. (6.8) and Eq. (6.9) respectively with Eq. (6.7) gives the total BOD concentration, BOD_{total}. The correlation equation for high range total BOD concentration is given as:

$$BOD_{total} = 0.4327 COD_{insoluble} + 0.6240 COD_{soluble} \tag{6.10}$$

The correlation equation for low range total BOD concentration is given as:

$$BOD_{total} = 0.4327 COD_{insoluble} + 0.3338 COD_{soluble} \tag{6.11}$$

The value of insoluble and soluble COD can be calculated from Eqs. (6.1), (6.3)-(6.4).

6.2 Flocculation Process

In the study of the flocculation process, the jar test analysis was used to evaluate the performance of different type of cationic and anionic polymers at different operating

condition. The results obtained from the jar test analysis were corresponding with the results obtained from the pilot plant study at the variation not more than 5%. The performance of the flocculation process was also evaluated by using the Population Balance Model (PBM) in term of suspended solids removal.

6.2.1 Jar Test Analysis

In the jar test analysis, the most suitable type of cationic and anionic polymers at the optimum dosage was evaluated. Based on the selected type of polymers and dosage, the operating parameters of temperature, stirring speed, stirring time and pH were optimized. The efficiency of the flocculation process was evaluated based on the important responses in term of suspended solids removal, COD removal, ratio of suspended solids concentration in the filtrate to the supernatant and water recovery.

6.2.1(a) Single Polymer System

In the single polymer system, only cationic polymer was added in the flocculation process. Five types of cationic polymers as shown in Table 6.2 were evaluated.

Table 6.2: The supplier and price of cationic polymer

Type of cationic polymer	Supplier	Price (RM/kg)
KP1200H	Euro Chemo Pharma Sdn. Bhd.	19.80
Polyfloc KP9650	Dia-Chemical Sdn. Bhd.	13.50
KP7000	Euro Chemo Pharma Sdn. Bhd.	33.00
Envifloc 70KS	Envilab Sdn. Bhd.	16.50
FO 4190SH	Exotic Chemical Sdn. Bhd.	16.00

Fig 6.6(a) shows the effect of dosage for the cationic polymers on the suspended solids removal. The suspended solids removal, R_{ss} was calculated as:

$$R_{ss} = 1 - \frac{C_{ss,out}}{C_{ss,in}} \tag{6.12}$$

where the term $C_{ss,in}$ is the inlet/feed suspended solids concentration and $C_{ss,out}$ is the outlet/supernatant suspended solids concentration. For all the cationic polymers, the highest suspended solids removal (>99.4%) with the concentration less than 100mg/L was achieved at the dosage of 300-600mg/L. The COD removal, R_{COD} as shown in Fig. 6.6(b) is evaluated based on the equation as follows:

$$R_{COD} = 1 - \frac{COD_{out}}{COD_{in}} \tag{6.13}$$

where the term COD_{in} is the inlet/feed COD concentration and COD_{out} is the outlet/supernatant COD concentration. The COD removal is highest for all cationic polymers at the dosage of 300-600mg/L. However, the range of COD removal is small as it varied only from 53-61% for all the cationic polymers.

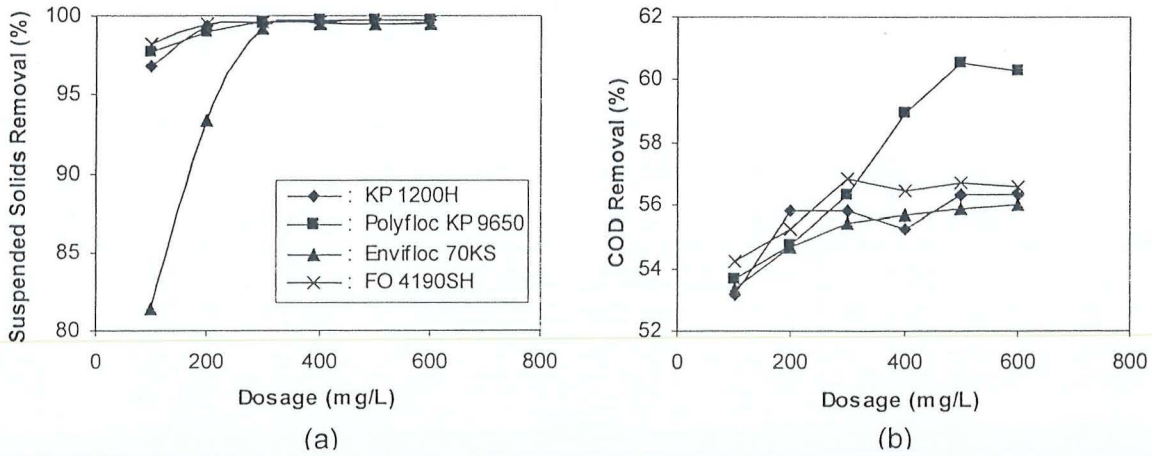

Fig 6.6: Effect of cationic polymer dosage on (a) suspended solids removal and (b) COD removal of POME for different type of cationic polymers.

The flocculation efficiency based on filtration study is measured in term of the water recovery and the ratio of suspended solids concentration in the filtrate to the supernatant, $R_{F/S}$ which is defined as:

$$R_{F/S} = \frac{C_{ss,F}}{C_{ss,S}} \tag{6.14}$$

where the term $C_{ss,F}$ is the suspended solids concentration in the filtrate and $C_{ss,S}$ is the suspended solids concentration in the supernatant. An efficient flocculation should have $R_{F/S} \approx 1$. If the $R_{F/S} > 1$, this indicates that some fine flocs have been carried over to the filtrate, the flocs obtained is easy to break and thus it is not suitable to be dewatered.

Fig. 6.7(a) shows the effect of cationic polymers dosage on the $R_{F/S}$ value. For all the polymers, the filtrate suspended solids concentration at the dosage of 200mg/L and below increased tremendously with the $R_{F/S}$ from 6 to 61. The filtrate suspended solids concentration increased tremendously at all the dosage for KP 1200H and FO 4190SH. This indicates that flocs generated were soft, weak, easy to break and were not suitable for dewatering process. Thus, KP 1200H and FO 4190SH can not be used in this system. For Polyfloc KP 9650 and Envifloc 70KS, the $R_{F/S}$ value at the dosage of 300mg/L and above was close to unity (filtrate suspended solids remained below 100mg/L) and this indicates that flocs breakage do not occur during filtration. This shows that the flocs is dense and therefore, suitable for dewatering. Based on the observed results, the dosage of 300mg/L is the optimum dosage for the cationic polymer flocculation.

Fig. 6.7(b) shows the water recovery for the cationic polymers at the dosage of 300mg/L. Polyfloc KP 9650 gives the highest percentage of water recovery (56%) at 10s.

This shows that Polyfloc KP 9650 has the best dewatering capability followed by Envifloc 70KS. Between Polyfloc KP 9650 and Envifloc 70KS, Polyfloc KP 9650 is chosen for the cationic polymer flocculation system as it offers lower price. Though Polyfloc KP 9650 demonstrates the best dewatering capability, the water recovery of 56% was still very low compared to the desired water recovery of 75%. In addition, though the maximum suspended solids removal of >99.4% with the concentration of <100mg/L was achieved, the performance was still poor compared to the desired suspended solids concentration of <50mg/L. Therefore, addition of anionic polymer flocculation is needed to enhance the suspended solids removal and dewatering capability of the flocculation system.

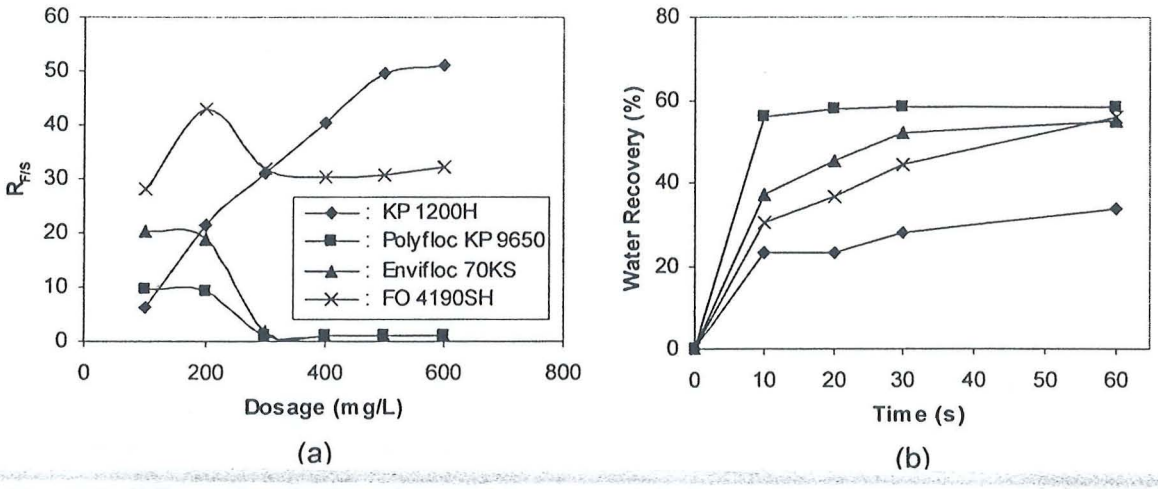

Fig. 6.7: Effect of cationic polymer dosage on (a) $R_{F/S}$ and (b) water recovery of POME for different type of cationic polymers.

6.2.1(b) Dual Polymer System

In the dual polymer system, the cationic polymer was first added and followed by anionic polymer to enhance the performance of flocculation process. The flocculation of POME by using anionic polymer is aimed to achieve the suspended solids concentration of less than 50mg/L and water recovery of more that 75% to meet the physical constraint of

the dewatering and membrane systems. The anionic polymers as shown in Table 6.3 were evaluated.

Table 6.3: The supplier and price of anionic polymer

Type of anionic polymer	Supplier	Price (RM/kg)
AN 350M	Euro Chemo Pharma Sdn. Bhd.	16.00
Polyfloc AP 8350	Dia-Chemical Sdn. Bhd.	12.70
Polyfloc AP 8300	Dia-Chemical Sdn. Bhd.	12.70

Fig. 6.8(a) shows that the suspended solids removal increased when the anionic polymer dosage increased. The suspended solids concentration of less than 50mg/L with the removal of more than 99.7% is achieved at the dosage of 50-60mg/L for AN 350M and Polyfloc AP 8350. Fig. 6.8(b) shows that the COD removal increased when the anionic polymer dosage increased with the Polyfloc AP 8350 gave the highest COD removal. However, the range of COD removal is small as it is varied only from 53-61% for all the anionic polymers.

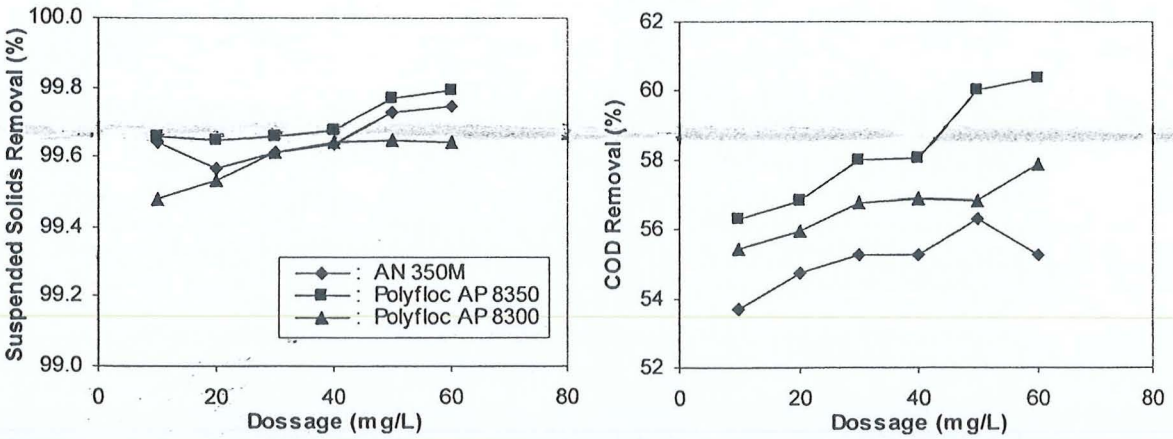

Fig 6.8: Effect of anionic polymer dosage on (a) suspended solids removal and COD removal of POME for different type of anionic polymers.

Fig. 6.9(a) shows that the $R_{F/S}$ remained at the value close to unity for the dosage of 50-60mg/L. This indicates that the floc breakage during filtration at the dosage of 50mg/L and above is very minimal. It shows that, the floc formed is dense and suitable for the dewatering process. Based on these findings, the anionic polymer dosage of 50mg/L is recommended. Fig. 6.9(b) shows the water recovery of the anionic polymers at the dosage of 50mg/L. Both AN 350M and Polyfloc AP 8350 gave the highest water recovery with 78% achieved in just 10s. Based on the price of anionic polymers shown in Table 6.3, the anionic polymer chosen is Polyfloc AP 8350. The optimum operating conditions for the flocculation of POME obtained based on the jar test analysis is summarized in Table 6.6.

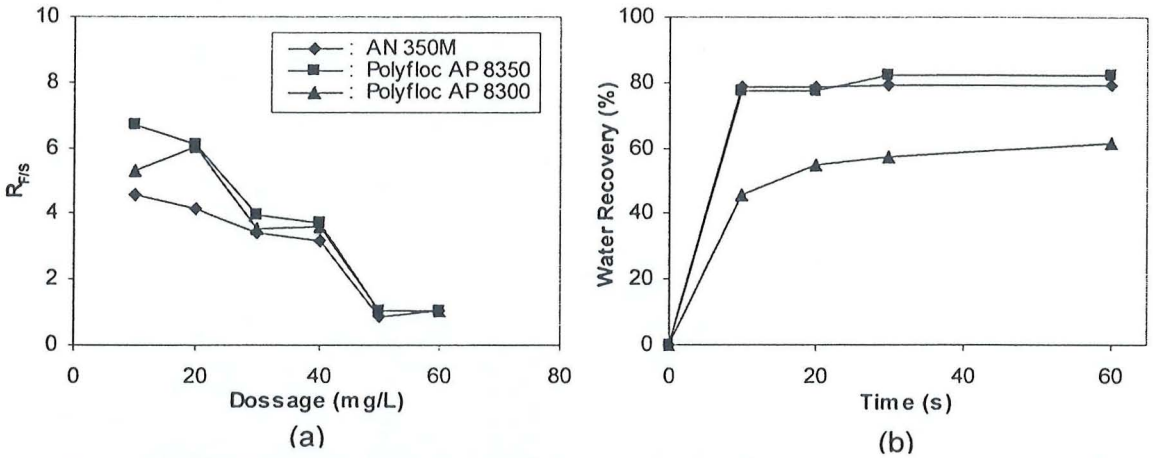

Fig. 6.9: Effect of anionic polymer dosage on (a) $R_{F/S}$ and (b) water recovery of POME for different type of anionic polymers.

Table 6.4: The proposed optimum parameters for chemical treatment of POME

Parameters	Cationic Polymer	Anionic Polymer
Polymer Type	Polyfloc KP 9650	Polyfloc AP 8350
Polymer Prepared Concentration (%)	0.4	0.1
Unit Cost (RM/kg)	13.50	12.70
Dosage (mg/L)	300	50
Temperature (°C)	No adjustment needed	No adjustment needed
pH	No adjustment needed	No adjustment needed
Stirring Speed (rev/min)	200	150
Stirring Time (min)	3	1

6.2.3 Population Balance Model for Flocculation Process

The performance of the jar test for the single and dual polymer systems can be evaluated and predicted by using the Population Balance Model (PBM). The PBM predicts the time evolution of the aggregate/floc size distribution which is required to estimate the suspended solids removal. Once the suspended solids removal is obtained, the COD and oil & grease concentration can be calculated based on Eqs. (6.1) and (6.2) respectively. The BOD concentration can be estimated by using Eq. (6.10).

Prior to the implementation of PBM, the physical properties of initial flocculating suspension (raw POME) have to be evaluated. The primary particle mean diameter as shown in Table 6.5 is obtained based on the particle size distribution data which is measured by injecting the raw POME into the laser granulometer (Mastersizer, Malvern).

Table 6.5: Physical properties of initial flocculating suspension (raw POME)

Parameter	Value
Particle concentration (no./ m^3)	2.334×10^{11}
Primary particle mean diameter (micron)	64.2
Particle density (kg/ m^3)	600
Suspension Density (kg/m^3)	1000
Viscosity (Pa.s)	1.0240×10^{-3}

6.2.2(a) Single Polymer System

For the single polymer system analysis based on PBM, the direct flocculation of POME was investigated by using medium charge density with high molecular weight cationic polymer (Polyfloc KP 9650) at the dosage of 100, 200 and 300mg/L respectively under constant shear of 200rev/min. The raw POME was flocculated at its initial pH (without pH adjustment) and the floc size distribution data, pretreated POME suspended solids, COD, oil & grease concentrations were obtained for each reaction time of 1-6 minute.

The flocculation efficiency of POME is investigated based on PBM. The discretized PBM of Eq. (3.5) forms a set of nonlinear ODEs and were solved numerically by the orthogonal collocation technique (Constantinides and Mostoufi, 1999). During the integration of the PBM equations, the calculated floc size distribution was tested for conservation of solid volume at each reaction time. The results obtained in the present investigation had the loss of total solid volume of less than 1%. The initial estimation of parameters in the Eq. (3.11) due to adsorbed polymer layers (bridging attraction) can be obtained from the literature as shown in Table 6.6.

Table 6.6: Model parameters used in PBM for cationic polymer induced flocculation.

Parameter	Value
Boltzmann Constant, K_B	1.3807×10^{-23} J/K
Avogadro's number, N_{AV}	6.022×10^{23}
Elementary charge, e	1.6×10^{-19} Columb
Kinematic viscosity, ν	$1.0 \times 10^{-6}\ m^2 s^{-1}$
Hamaker constant of the solids across a vacuum, A_p	6.0×10^{-20} J*
Hamaker constant of the solvent across a vacuum, A_m	3.7×10^{-20} J
Hamaker constant of the polyacrylamide across a vacuum, A_s	8.0×10^{-20} J**
Dielectric constant of the vacuum	8.85×10^{-9} C/mV
Polymer volume fraction at a single saturated surface, Φ_{So}	0.18
Scaling length, D_{Sc}	4 nm
The term $\alpha_{Sc} K_B T / a_m^3$ of Eq. (3.17)	3×10^5 N/m^2
Adsorbed polymer layer thickness, δ	90 nm
Fractional polymer surface coverage, Γ / Γ_0	0.60 - 0.65
Surface potentials, ψ_{oi}	-87.2 – 12.5 mV

*Data from Van Oss (1994); **Data from Israelachvili (1991)

Table 6.7 shows the experimental data and the model parameters used in the simulation studies. The surface potential of particles is difficult to measure and is normally assumed approximately equal to its zeta potential. However, when particles have adsorbed polymer layers, surface potential could be quite different from zeta potential.

Nevertheless, fitted surface potentials turn out to be fairly close to measured zeta potentials as shown in Table 6.7.

Table 6.7: Experimental data and model parameters employed in the simulation studies.

Polymer concentration (mg/L)		d_F*	Water recovery	Suspended solids removal	COD removal	Oil and Grease Removal	Measured zeta potential	Fitted surface potential
Cationic	Anionic		(%)	(%)	(%)	(%)	(mV)	(mV)
100	--	1.74	13.33	98.20	53.69	95.12	-92.4	-87.2
200	--	1.80	45.65	98.99	54.74	98.10	-31.0	-32.6
300	--	1.82	58.07	99.59	56.32	99.74	+16.8	+12.5
300	10	1.82	61.87	99.66	56.30	99.66	+13.5	+12.1
300	30	1.83	69.81	99.65	56.81	99.85	+10.7	+11.7
300	50	1.85	82.08	99.66	57.96	99.74	-6.2	-4.4

* d_f is the aggregate fractal dimension which were obtained by dynamic scaling

The simulation results shown in Fig. 6.10 follow the experimental trend closely. Thus, the correlation of suspended solids, COD, oil & grease with the floc size distribution based on the PBM has been successfully applied. Fig. 6.10 and Table 6.7 shows that the suspended solids, COD, oil & grease removal increased as the fractal dimension and cationic polymer dosage increased. This implies that at higher cationic polymer dosage, more suspended solids were captured to produce larger and denser flocs (indicated by higher fractal dimension value) and thus the suspended solids concentration in the pretreated POME was greatly reduced. Once the suspended solids concentration was reduced, the COD, oil & grease concentration of pretreated POME was also reduced.

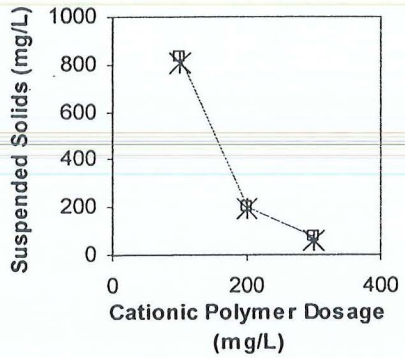

(a)

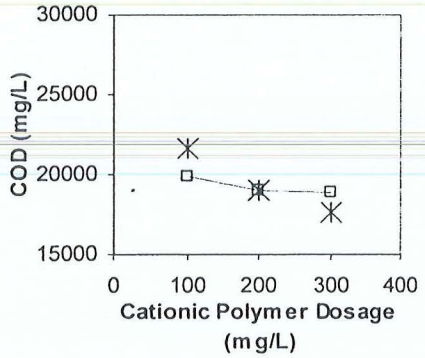

(b)

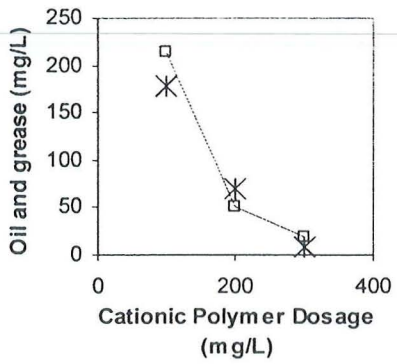

(c)

Fig. 6.10: Effect of cationic polymer dosage on (a) suspended solids (b) COD (c) oil & grease concentration of pretreated POME. Experimental: ⁎ Simulation: —□— .

6.2.2(b) Dual Polymer System

For the dual polymer system, the direct flocculation of POME was investigated by first adding the medium charge density with high molecular weigh cationic polymer (Polyfloc KP 9650) at the dosage of 300mg/L under constant shear of 200rev/min. After stirring for 3min, the high charge density with high molecular weigh anionic polymer (Polyfloc AP8350) was added under constant shear of 150rev/min. The raw POME was flocculated at its initial pH (without pH adjustment) and the floc distribution data, pretreated POME suspended solid, COD, oil & grease concentration were obtained for each reaction time of 1-6 minutes.

The PBM of Eq. (3.5) was solved and implemented in a similar manner as presented in the pervious section. At the flocculation time of 3-6min after the anionic polymer addition, the PBM was implemented by using the identical model parameters of cationic polymer except those presented in Table 6.8.

Table 6.8: Model parameters used in PBM for anionic polymer.

Parameter	Value
Hamaker constant of the polyacrylic acid across a vacuum, A_s	8.0×10^{-20} J*
Polymer volume fraction at a single saturated surface, Φ_{So}	0.15
Adsorbed polymer layer thickness, δ	90 nm
Fractional polymer surface coverage, Γ / Γ_0	0.70 - 0.75
Surface potentials, ψ_{oi}	-4.4 – 12.1 mV

*Data from Vincent (1973)

Fig. 6.11 shows the comparison of simulation results of suspended solids, COD, oil & grease concentration in pretreated POME by using the correlation of Eq. (6.1)-(6.2) with the experimental results based on the average values taken after the anionic polymer was added. The simulation results followed the experimental trend closely and the correlation of suspended solids, COD, oil & grease with the floc size distribution based on the PBM was successfully applied in the dual polymer system. Fig. 6.11 and Table 6.7 indicate that suspended solids, COD, oil & grease removal increases slightly as the fractal dimension and anionic polymer dosage increase.

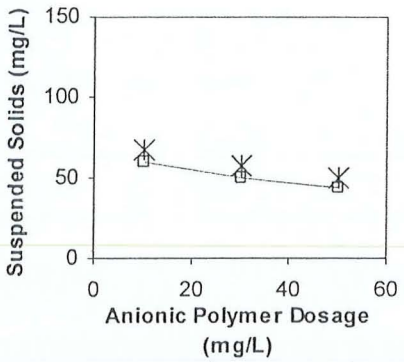

(a)

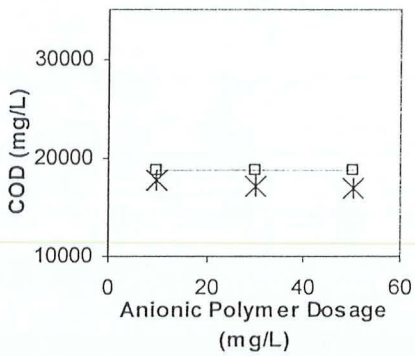

(b)

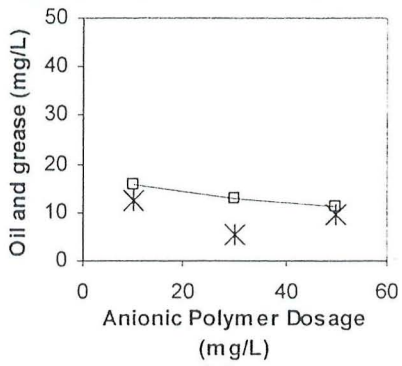

(c)

Fig. 6.11: Effect of anionic polymer dosage on (a) suspended solids (b) COD (c) oil and grease concentration of pretreated POME. Experimental: ✳ Simulation: —⊟—.

Although additional of anionic polymer did not give significant effect on flocs growth, suspended solids, COD and oil & grease removal, the percent of water recovery increased tremendously as the fractal dimension and anionic polymer dosage increased as shown in Table 6.4. This shows that additional of anionic polymer produced dense flocs of high fractal dimension which gave high water recovery as less water was captured inside the flocs.

6.2.2 (c) Preliminary Cost Analysis

A preliminary cost analysis presented in Table 6.9 was carried out to evaluate and compare the treatment costs between the direct flocculation of POME in the present study and the conventional coagulation-flocculation process presented in the literature (Ahmad *et al.*, 2003; Ahmad *et al.*, 2005). Without even considering the cost of chemical used in pH adjustment for the conventional pretreatment, the total treatment cost of conventional pretreatment is 3.6 times higher than the total treatment cost of direct flocculation. Thus, the present study proves that direct flocculation is more cost effective than the conventional pretreatment of POME.

Table 6.9: Comparison of the treatment costs between the direct flocculation of POME and the conventional coagulation-flocculation process

	Parameters	Direct flocculation	Conventional pretreatment*
1st stage	Type of coagulant/flocculent	Cationic polymer	Alum
	Dosage of coagulant/flocculent	300 mg/L POME treated	15 000mg/L POME treated
	Unit cost of coagulant/flocculent	RM 15.50/kg	RM 1.00/kg
	Total cost of coagulant/flocculent	RM 4.65/m^3 POME treated	RM 15.00/m^3 POME treated
2nd stage	pH adjustment	Not needed	Needed
3rd stage	Type of flocculent	Anionic polymer	Cationic polymer
	Dosage of flocculent	50 mg/L POME treated	300 mg/L POME treated
	Unit cost of flocculent	RM 9.00/kg	RM 11.00/kg
	Total cost of flocculent	RM 0.45/m^3 POME treated	RM 3.30/m^3 POME treated
	Total treatment cost	RM 5.10/m^3 POME treated	RM 18.30/m^3 POME treated
	Suspended solids removal	99.66%	>99%
	COD removal	55.79%	>50%
	Oil and grease removal	99.66%	>99%
	Water recovery	80.78%	78%

* The literature data obtained from Ahmad *et. al.* (2003) and Ahmad *et. al.* (2005).

6.3 Granular Activated Carbon (GAC) Adsorption Process

The breakthrough curves of the GAC adsorption was predicted based on the coupled model of Homogeneous Surface Diffusion Model (HSDM) with Ideal Adsorbed Solution Theory (IAST). The simulation results were compared with the experimental breakthrough curves obtained from the fixed bed adsorption study.

The pretreated POME used as the feed in the fixed bed adsorption study was the supernatant collected from the flocculation process. The pretreated POME formed a ternary solutes system containing carbohydrate constituents, protein and ammoniacal nitrogen by ignoring the present of suspended solids. The fixed-bed adsorption tests were conducted using the complex solution of pretreated POME (ternary system) containing carbohydrate constituents (10600 ± 210mg/L), protein (18300 ± 370mg/L) and ammoniacal nitrogen (80 ± 2mg/L) at 28°C and pH of 4.1. The experimental conditions are shown in Table 6.10.

Table 6.10: Experimental conditions for pretreated POME fixed-bed adsorption tests.

Run	τ (min)	Q (mL/min)	Re	L (m)	$k_{fi} \times 10^7$ (m/s)			$D_{si} \times 10^{10}$ (m^2/s)		
					(1)*	(2)*	(3)*	(1)*	(2)*	(3)*
1	10	9.43	0.3319	0.10	8.76	7.39	416	1.59	1.07	0.0075
2	20	9.43	0.3319	0.20	8.76	7.39	416	1.50	1.01	0.0067
3	30	9.43	0.3319	0.30	8.76	7.39	416	1.50	1.01	0.0063
4	10	18.86	0.6638	0.20	11.04	9.31	543	1.78	1.26	0.0078
5	30	6.29	0.2213	0.20	7.65	6.46	364	1.33	1.00	0.0047

*(1) Carbohydrate constituents; (2) Protein; (3) Ammoniacal nitrogen

The simulation model based on the incorporation of IAST into the kinetic HSDM for breakthrough curves prediction of multiple solutes system (Eqs. (3.18), (3.13)-(3.16)) is written in Mathlab 7.0. The input parameters of the simulation model for defining the adsorption bed are bed diameter, bed length, feed flow rate and bed porosity. The input parameters defining the GAC are particle radius and density. The other input parameters required are the initial concentrations, external mass transfer coefficient and the Freundlich parameters for each adsorbate of carbohydrate constituents, protein and ammoniacal nitrogen present in the ternary system of pretreated POME.

The breakthrough curves of carbohydrate constituents, protein and ammoniacal nitrogen of pretreated POME for each experimental conditions regressed with the simulation model were compared with the experimental breakthrough curves as shown in Figs. 6.12-6.13. The coefficient of determination (R^2) for all the breakthrough curves as shown in Figs. 6.12-6.13 are fall in the range of 0.92 - 0.99. This indicates that the simulation results are in good agreement with the experimental data. Thus, the kinetic HSDM has been successfully applied in the prediction of breakthrough curves for the complex system of pretreated POME by using the incorporation of IAST.

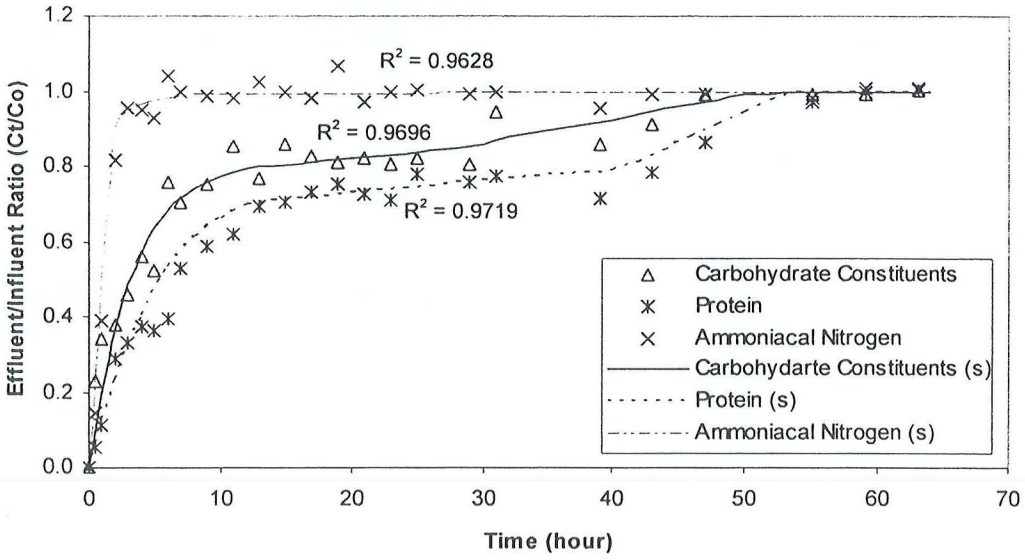
1.2
1.0
0.8
0.6
0.4
0.2
0.0
Effluent/Influent Ratio (Ct/Co)
R² = 0.9628
R² = 0.9696
R² = 0.9719
Carbohydrate Constituents
Protein
Ammoniacal Nitrogen
Carbohydarte Constituents (s)
Protein (s)
Ammoniacal Nitrogen (s)
0
10
20
30
40
50
60
70
Time (hour)

(a)

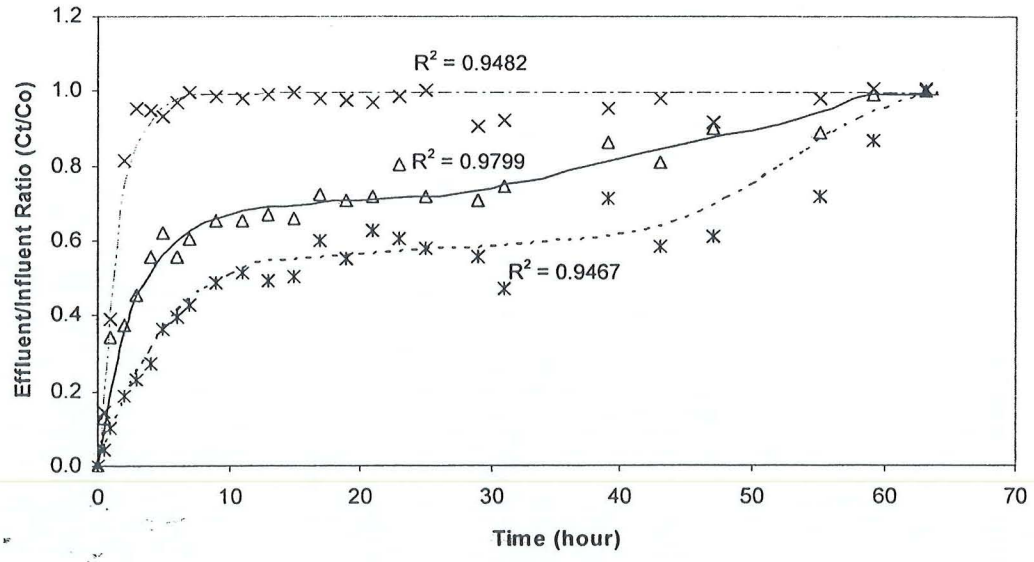
1.2
1.0
0.8
0.6
0.4
0.2
0.0
Effluent/Influent Ratio (Ct/Co)
R² = 0.9482
R² = 0.9799
R² = 0.9467
0
10
20
30
40
50
60
70
Time (hour)

(b)

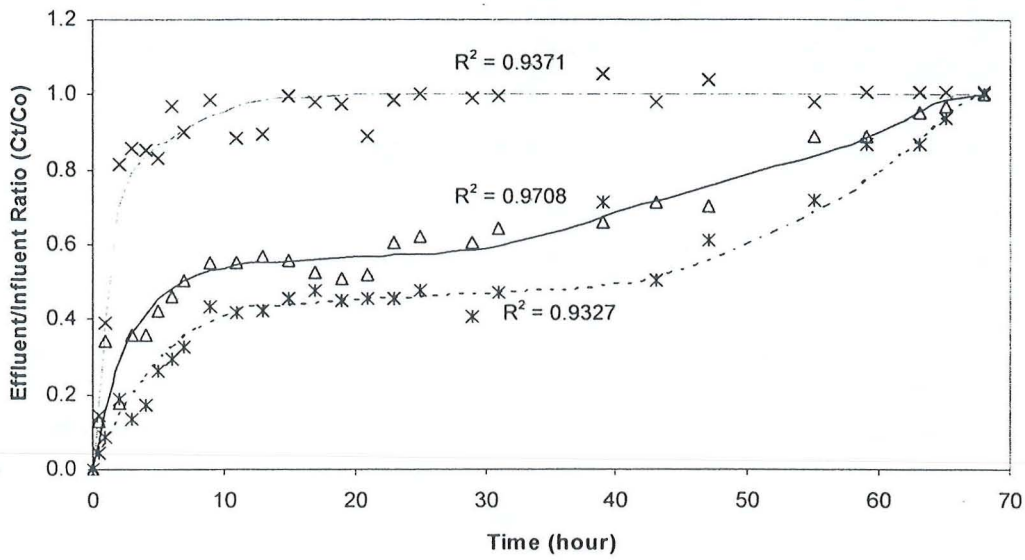

(c)

Fig. 6.12. The breakthrough curves of carbohydrate constituents, protein and ammoniacal nitrogen in pretreated POME system with changing bed length of (a) 10cm, (b) 20cm, (c) 30cm at constant feed flow rate of 9.43 mL/min. The notation (s) means simulation results.

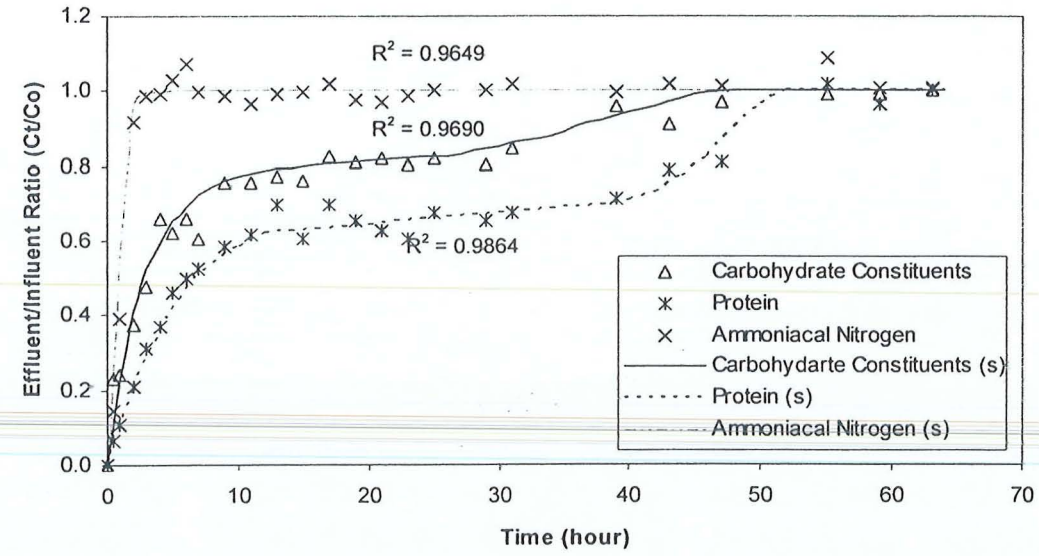

(a)

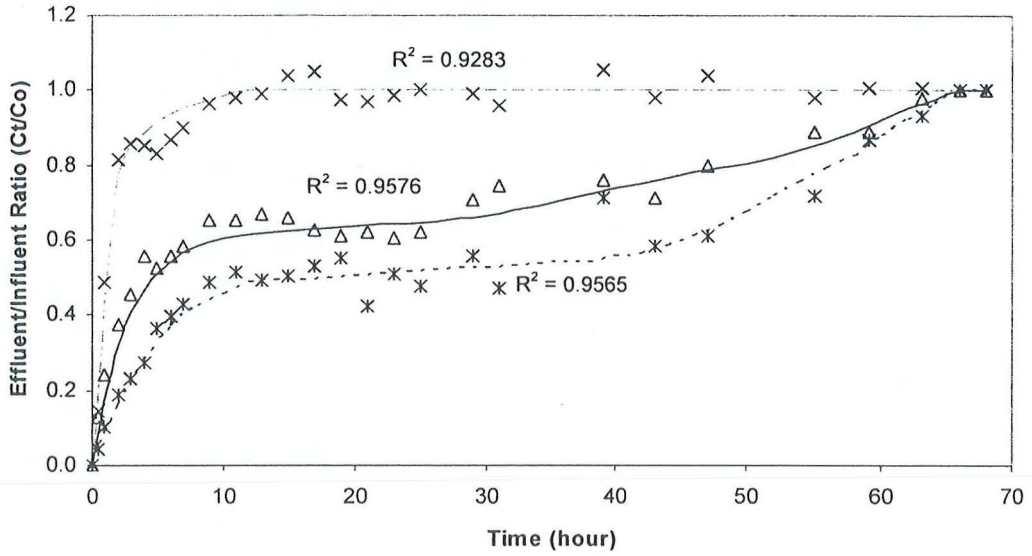

(b)

Fig. 6.13. The breakthrough curves of carbohydrate constituents, protein and ammoniacal nitrogen in pretreated POME system with changing feed flow rate of (a) 18.86 mL/min and (b) 6.29 mL/min. The notation (s) means simulation results.

Both experimental data and simulation results for this ternary system show that protein is a strongly adsorbed species and followed by carbohydrate constituents compared to the ammoniacal nitrogen. Therefore, in the complex system of pretreated POME, the adsorption of ammoniacal nitrogen has been inhibited in the presence of carbohydrate constituents and protein.

Fig. 6.14 shows the breakthrough curves of COD for the pretreated POME adsorption on GAC based on the experimental conditions shown in Table 6.10. The simulation results based on the correlation of Eq. (6.5) show a good agreement with the experimental data with coefficient of determination, R^2 of 0.96 – 0.99 for Run 1-5. This demonstrates that in the ternary system of pretreated POME, the solutes of carbohydrate constituents, protein and ammoniacal nitrogen had successfully correlated to its COD value.

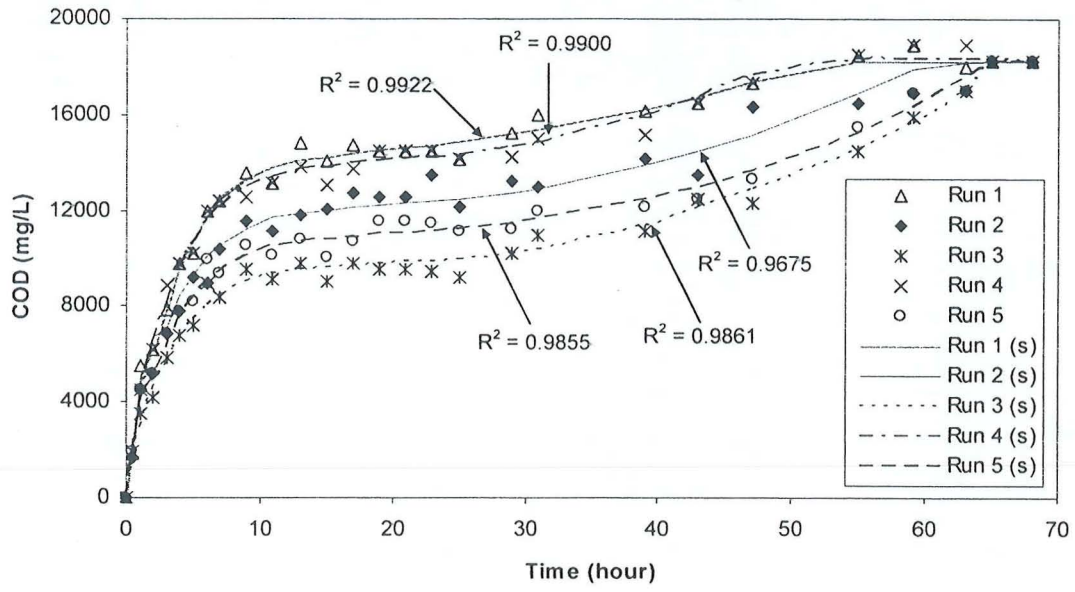

Fig. 6.14. The breakthrough curves of COD for the pretreated POME adsorption on GAC. The notation (s) means simulation results.

The breakthrough curves achieved saturation in term of COD at 55hr, 59hr, 65hr, 55hr, 66hr for Run 1-5 respectively. Most of the COD was removed in the first hour as most of the organic solutes were also removed in the first hour as indicated in Figs 6.12-6.13.

6.4 Ultrafiltration (UF) Membrane System

In the present study, both types of UF membrane from the pilot plant; which were the ceramic and polymeric tubular module were investigated to obtain the experimental data by using the pretreated POME collected from the GAC adsorption unit as the feed. During the implementation of the Coupled Model of Back Transport Analysis with Filtration Theory for UF system, the calculation was based on the ternary solutes system (pretreated POME) consist of carbohydrate constituents (8000mg/L ± 210), protein (10,100mg/L ± 370) and ammoniacal nitrogen (90mg/L ± 2).

6.4.1 Flux and Fouling Behavior of the UF Membrane

Fig. 6.15 considers the effect of trans membrane pressure on the volume flux of permeate for both UF ceramic and polymeric membranes. The simulation results show a good agreement with the experimental data with the coefficients of determination (R^2) of more than 0.89 were obtained for both ceramic and polymeric membranes at the trans membrane pressure of 1 to 4bar.

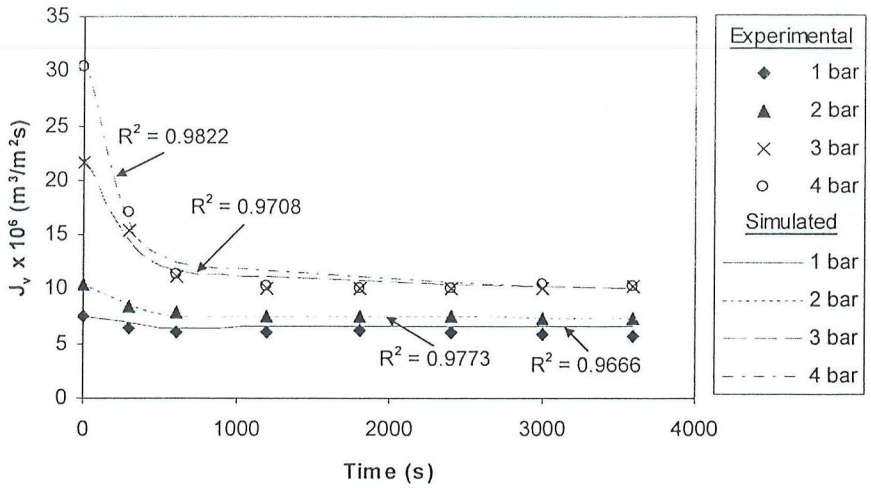

(a)

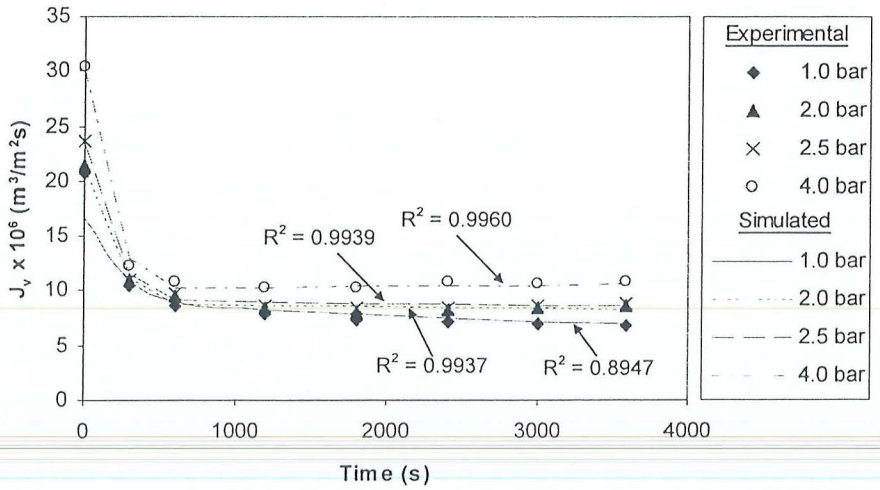

(b)

Fig. 6.15: Volume flux of permeate against filtration time at different trans membrane pressure (a) UF ceramic membrane (b) UF polymeric membrane

Fig. 6.16 considers the effect of feed flow rate on the volume flux of permeate for both UF ceramic and polymeric membranes. The coefficients of determination (R^2) of more than 0.95 for both membranes at all the feed flow rates indicate that the simulated results are able to represent the experimental data.

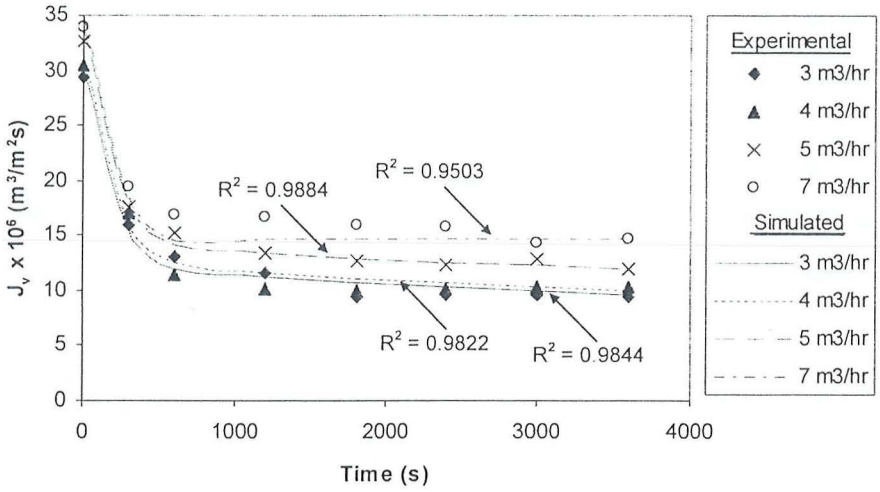

(a)

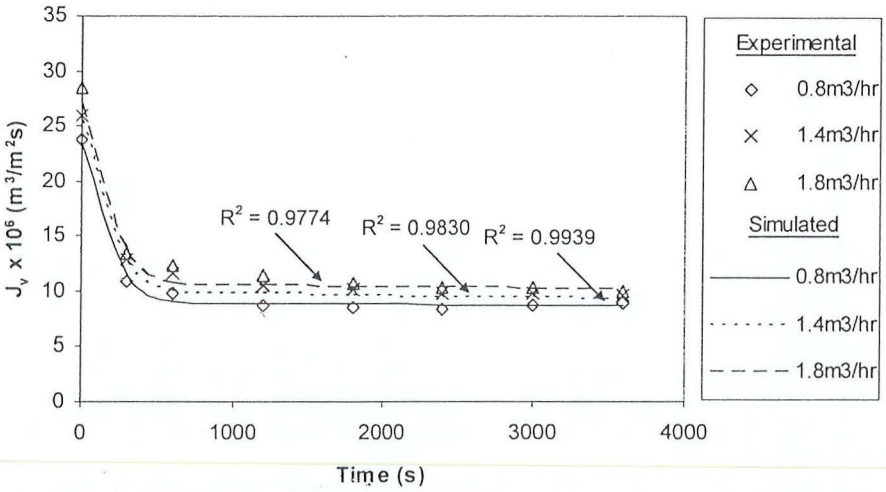

(b)

Fig. 6.16: Volume flux of permeate against filtration time at different feed flow rate (a) UF ceramic membrane, (b) UF polymeric membrane

Fig. 6.17 shows the gel layer resistance as a function of time for UF ceramic and polymeric membrane at various trans membrane pressure. The gel layer resistance is calculated from Eq. (6.15).

$$R_g = \frac{\Delta P - \Delta \pi}{\mu J_v} - R_m \qquad (6.15)$$

To obtain the experimental and simulation value of R_g, the experimental and simulation values of J_v were used in the calculation respectively.

Fig. 6.17 demonstrates that the resistance due to the deposition of solutes increased with the trans membrane pressure. High trans membrane pressure resulted in the higher volume flux of permeate due to the increase in driving force. This would result in the more accumulation of retained solutes and hence the gel layer resistance increased. The developed model was successful in predicting the gel layer resistance, R_g as a function of time at different trans membrane pressures. The coefficients of determination (R^2) were more than 0.91 for both types of membranes at trans membrane pressure of 1 to 4bar.

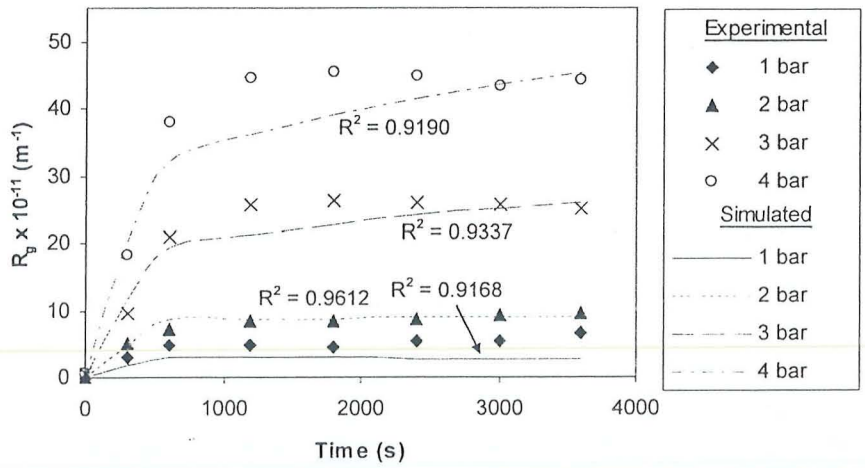

(a)

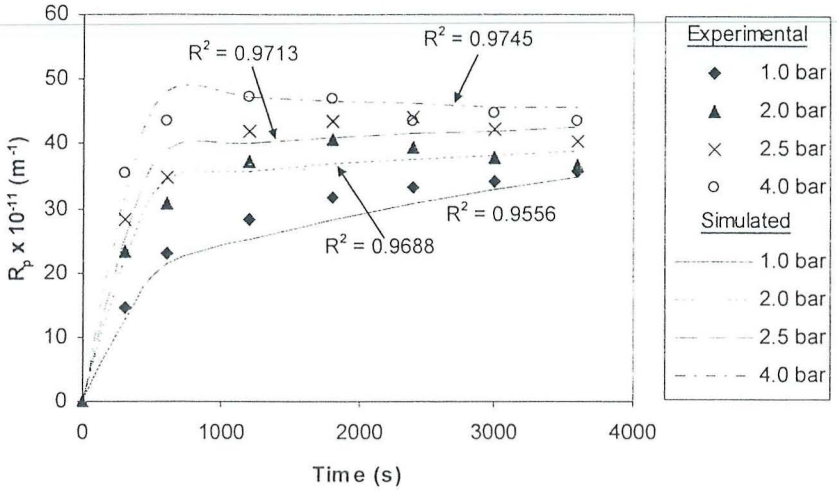

(b)

Fig. 6.17: Gel layer resistance against the filtration time at different trans membrane pressure. (a) UF ceramic membrane and (b) UF polymeric membrane.

Fig. 6.18 depicts the variation of gel layer resistance with increasing feed flow rate for both UF ceramic and UF polymeric membranes under the same bulk feed concentration. With the increase in feed flow rate (or cross flow velocity), the gel layer resistance decreases because more solutes were removed from the deposited layer to bulk by the action of back transport mechanism. Simulation results show a good agreement with the experimental data by having coefficients of determination, R^2 of more than 0.80 for both membranes at the varying feed flow rates.

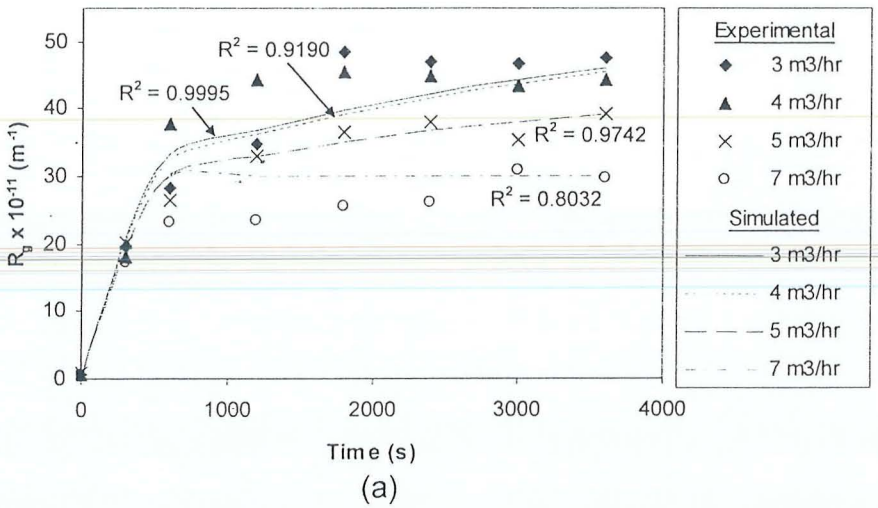

(a)

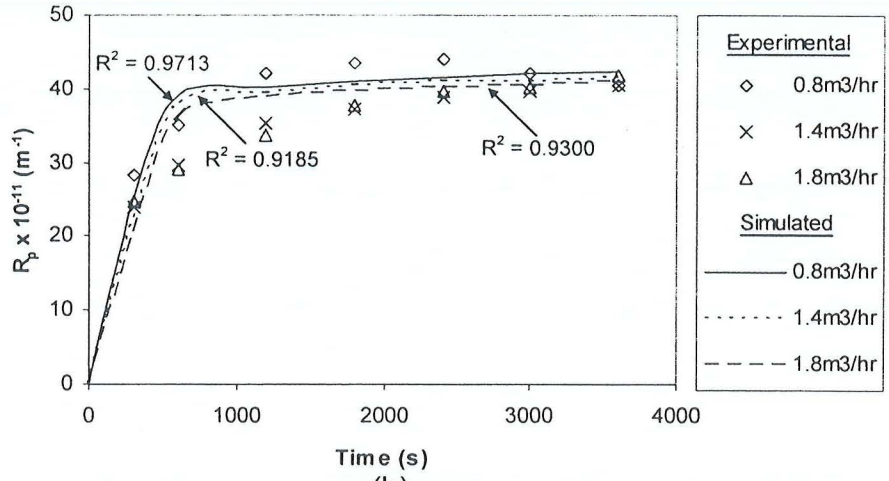

(b)

Fig. 6.18: Gel layer resistance against the filtration time at different feed flow rate (a) UF ceramic membrane and (b) UF polymeric membrane.

6.4.2 Permeate Quality for the Ternary Solutes System

Fig. 6.19 shows the rejection of each individual solute (carbohydrate constituents, protein and ammoniacal nitrogen) against the increasing trans membrane pressure. The simulation results by using Eq. (3.27) gave a good agreement with the experimental data. At higher trans membrane pressure, the higher driving force would force more solvent (water) of lower molecular weight to pass through the pores of the membrane.

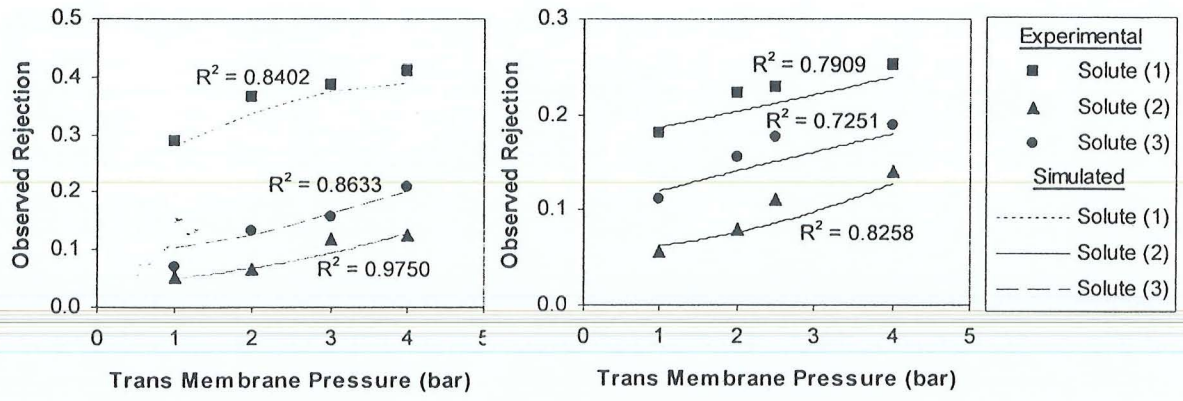

(a) (b)

Fig. 6.19: The steady-state observed rejection for individual solute against the trans membrane pressure (a) UF ceramic membrane and (b) UF polymeric membrane. The notation (1) carbohydrate constituents, (2) protein and (3) ammoniacal nitrogen

Fig. 6.20 shows the rejection curves of each individual solute against increasing feed flow rate at constant bulk feed concentration and trans membrane. Comparisons made between the simulation results and the experimental data show that the model is in good agreement with the experimental data. The results from Fig. 6.20 indicated that the rejection of each solute increased when the feed flow rate increased. Increasing feed flow rate (or cross flow velocity) lead to lower gel layer resistance (Fig. 6.18) and thus higher rejections were observed.

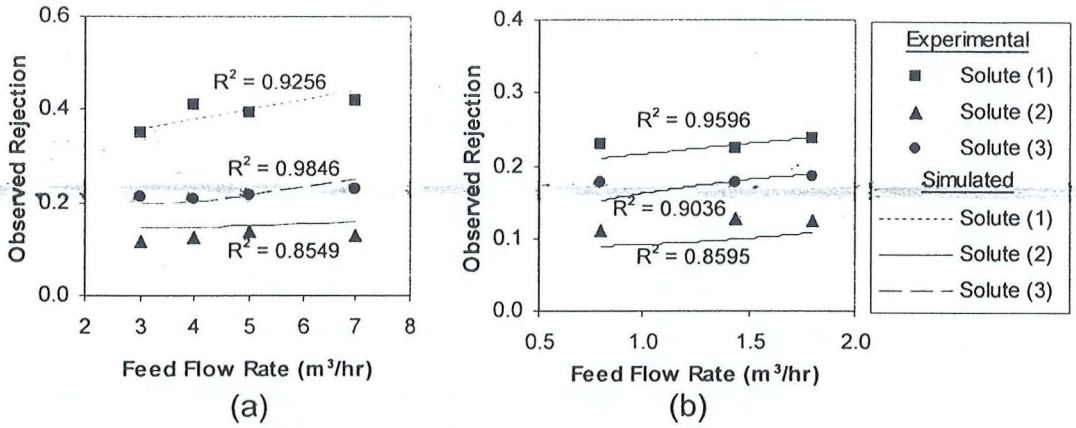

Fig. 6.20: The steady-state observed rejection for individual solute against the feed flow rate (a) UF ceramic membrane and (b) UF polymeric membrane.

Fig. 6.21 shows the COD concentration of the permeate against increasing trans membrane pressure for UF ceramic and UF polymeric membrane at constant bulk feed concentration and feed flow rate. Fig. 6.22 shows the COD concentration of the permeate against increasing feed flow rate for UF ceramic and UF polymeric membrane at constant bulk feed concentration and trans membrane pressure.

The simulation values obtained from Eq. (6.5) showed a good fit with the experimental data in Figs. 6.21 and 6.22. Both figures demonstrate a decrease of COD concentration in the permeate stream when the trans membrane pressure and feed flow

rate increased, respectively. This is in line with the observed rejection shown in Figs. 6.19 and 6.20. The increase of observed rejection at the increasing trans membrane pressure and feed flow rate resulted more solvent to pass through the pores of membrane compared to the solutes and thus lower COD concentration was obtained.

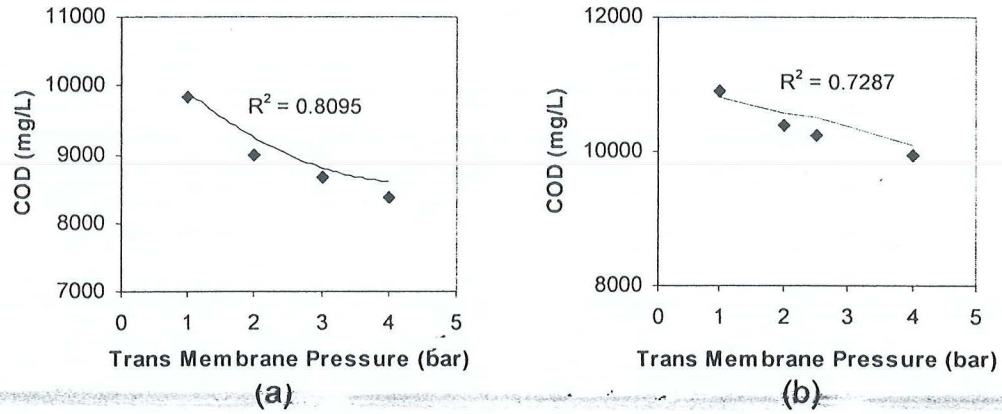

Fig. 6.21: Variation of steady-state COD concentration in the permeate with trans membrane pressure (a) UF ceramic membrane and (b) UF polymeric membrane. The solid lines are the simulation results while the dotted points are the experimental results.

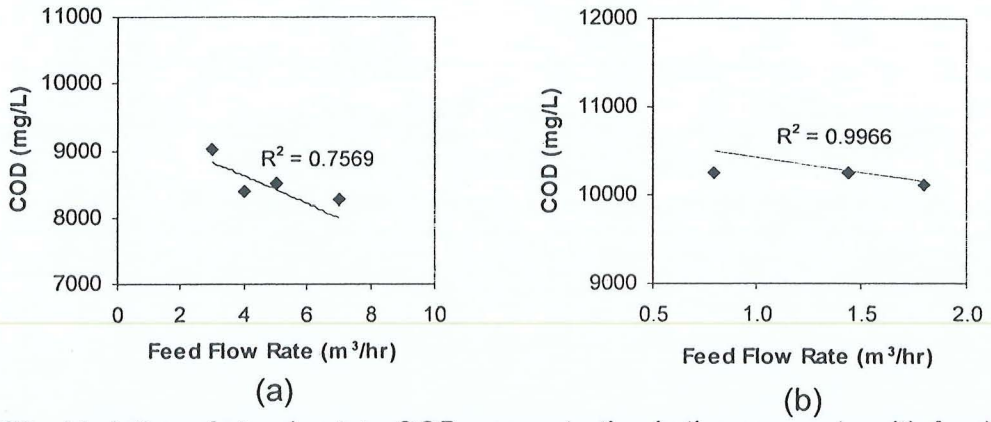

Fig. 6.22: Variation of steady-state COD concentration in the permeate with feed flow rate (a) UF ceramic membrane and (b) UF polymeric membrane. The solid lines are the simulation results while the dotted points are the experimental results.

Figs. 6.21 and 6.22 show that the efficiency of COD removal using both UF ceramic and UF polymeric membrane was low (10-20% of COD removal). The low rejection of carbohydrate constituents (15-45%), protein (5-15%) and ammoniacal nitrogen

(7-23%) showed in Figs. 6.19 and 6.20 indicated that most of the solutes were able to pass through the membrane and thus contributed to low efficiency of COD removal. Therefore, the carbohydrate constituents, protein and ammoniacal nitrogen contained large portion of micromolecules which need to be further removed by RO membrane system.

6.5 Reverse Osmosis (RO) Membrane System

In the present study, the RO polymeric membrane from the pilot plant was investigated to obtain the experimental data by using the pretreated POME as the feed. The experimental data was compared with the simulation results obtained from the Coupled Model of Extended Spiegler-Kedem Model with Concentration Polarization Model for RO membrane system. During the implementation of the model for the RO membrane system, the calculation was based on the ternary solutes system (pretreated POME) consist of carbohydrate constituents, protein and ammoniacal nitrogen.

Three types of feed (Feed A, B and C) to the RO membrane system were investigated in the present study and were summarized in Table 6.11. The RO membrane system performance was investigated by the variation of trans membrane pressure, feed flow rate and feed type/concentration.

Table 6.11: Type of RO feed based on different mode of operation

RO Feed Type	Feed A	Feed B	Feed C
Operation Mode	GAC-RO-RO	GAC-UF-RO	GAC-RO-RO
Feed Source	GAC Adsorption	UF Membrane	First-pass RO Membrane
Solute Feed Concentration*			
C_1, mg/L	8,500	5,800	15
C_2, mg/L	11,000	9,200	25
C_3, mg/L	100	80	4
C_{total}, mg/L	19,600	15,080	44
COD_{total}, mg/L	13,900	9,950	303

*(1) carbohydrate constituents, (2) protein and (3) ammoniacal nitrogen

6.5.1 Flux and Concentration Polarization Behavior of the RO Membrane

Fig. 6.23 shows the volume flux of permeate versus filtration time at varying trans membrane pressure, feed flow rate and feed type. The simulation results show a good agreement with the experimental data with the coefficient of determination (R^2) more than 0.88. Fig. 6.23 indicates that the fouling of the membrane caused the volume flux of permeate decreased until the system reached a steady-state value.

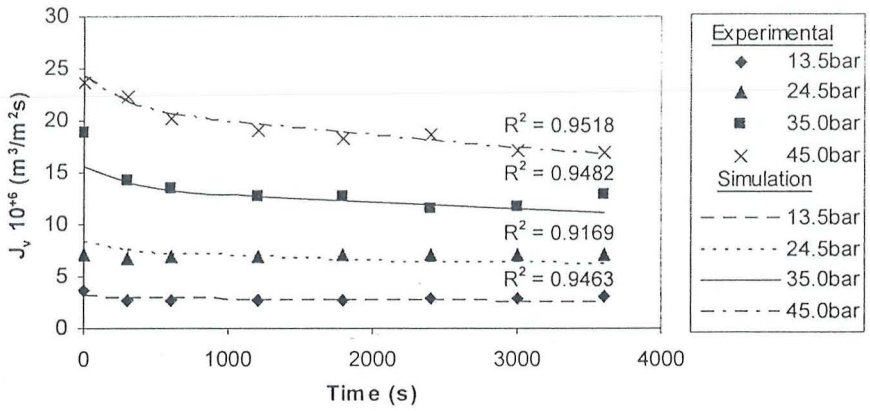

(a)

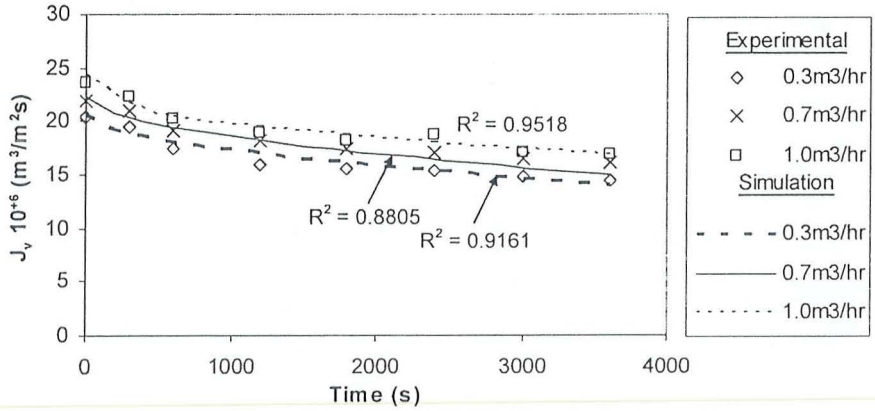

(b)

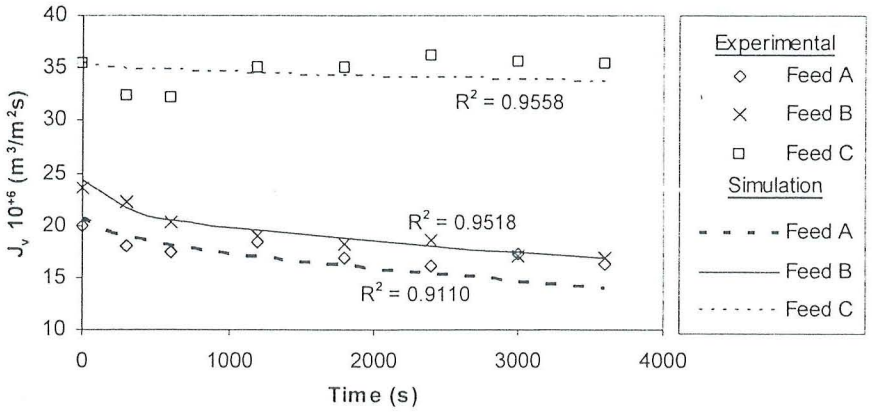

(c)

Fig. 6.23: Volume flux of permeate against filtration time at different (a) trans membrane pressure (b) feed flow rate and (c) feed type.

Fig. 6.23(a) shows the volume flux of permeate versus filtration time with the increasing trans membrane pressure. The feed concentration was based on the RO feed collected from the permeate stream of UF membrane system based on GAC-UF-RO mode (Feed B) as shown in Table 6.11. Although the permeate fluxes were greater at higher trans membrane pressures (due to the greater driving force), the fractional permeate flux reductions were quantitatively increased at higher trans membrane pressures. A qualitative explanation for this observed behavior is that at higher trans membrane pressures, higher concentrations build up in the boundary layer resulted higher wall concentrations and consequently, leading to a higher deterioration rate in permeate flux.

Fig. 6.23(b) shows the volume flux of permeate versus filtration time with the increasing feed flow. As it can be seen from Fig. 6.23(b), higher feed flow rate resulted an increase in the volume flux of permeate. It must be noted that at a higher feed flow rate, the superficial velocity at the membrane surface was greater and this lead to greater turbulence and mass transfer coefficient; resulting lower wall concentrations which enhanced the permeate flux.

Fig. 6.23(c) shows the volume flux of permeate versus filtration time with the decreasing total feed concentration based on Table 6.11. Fig. 6.23(c) shows that lower volume flux of permeate and greater fractional permeate flux reductions were experienced at higher total feed concentration. This can be attributed to the fact that when the membrane was exposed to the higher total feed concentration at the similar operating condition, faster concentrations build up in the boundary layer resulted higher wall concentration.

Fig. 6.24 shows the extent of concentration polarization in terms of total solute concentration buildup at the membrane wall against the filtration time which is measured as the concentration factor, CF :

$$CF = \frac{C_m}{C_b} \tag{6.16}$$

For all the Figs. 6.24(a), 6.24(b) and 6.24(c), the concentration factor increased sharply at the initial filtration time (within few seconds). After a sharp increase during the initial filtration time, this increase became more sluggish. At the initial filtration time, the rate of rejected solutes accumulation on the membrane wall at negligible back-diffusion mass transfer was high due to the high filtration rate at the initial condition as depicted in Fig. 6.23. As time progress, the accumulation of the rejected solutes on the membrane wall lead to the flux deterioration and at the same time, higher back-diffusion mass transfer rate of the rejected solutes was encountered. Thus, the concentration factor increase became more sluggish as time progressed.

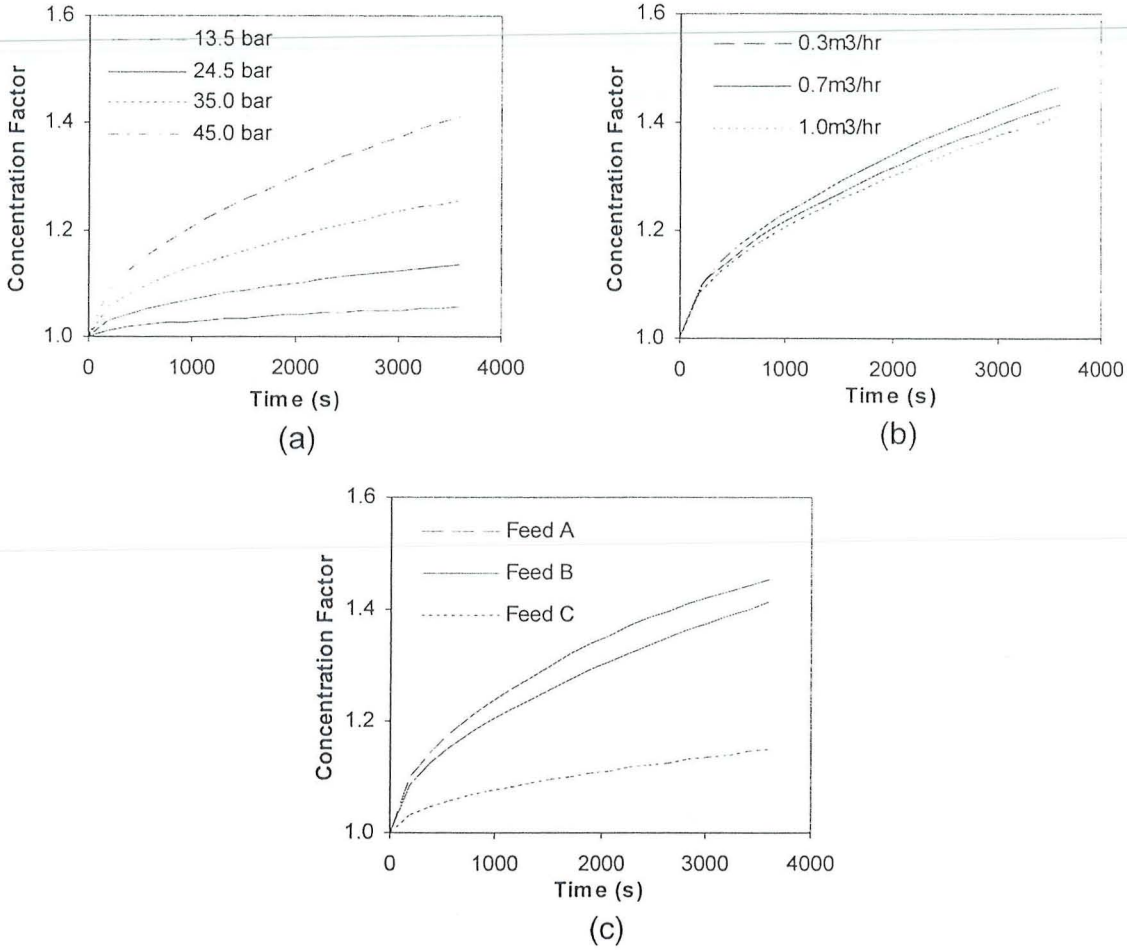

Fig. 6.24: Simulation results of concentration factor profile against filtration time for different (a) trans membrane pressure (b) feed flow rate and (c) feed type.

6.5.2 Permeate Quality for the Ternary Solutes System

Fig. 6.25 shows the comparison of the simulation and experimental results of the observed rejection for each solute (carbohydrate constituents, protein and ammoniacal nitrogen) at different trans membrane pressure, feed flow rate and feed type. The simulation results showed a good agreement with the experimental data with the coefficient of determination (R^2) more than 0.87. The outcome of the experiment demonstrates that the higher molecular weight of solutes (carbohydrate constituents and protein) gave a higher observed rejection compared to the solute which had the lower molecular weight (ammoniacal nitrogen).

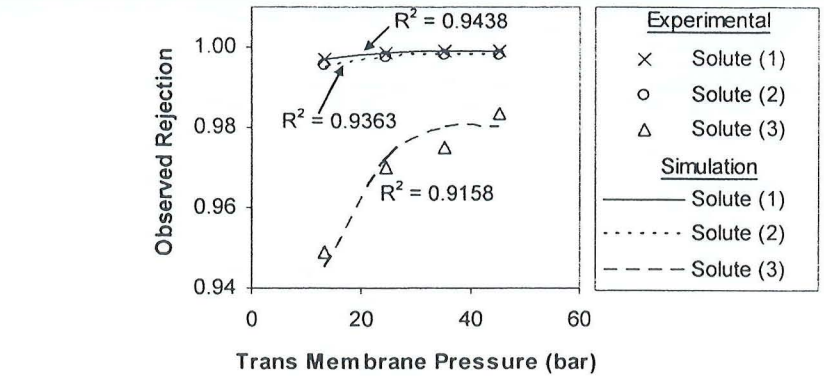

(a)

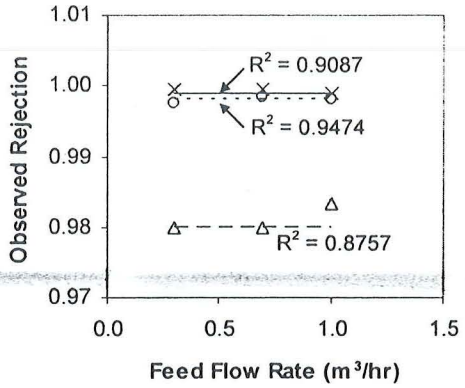

(b)

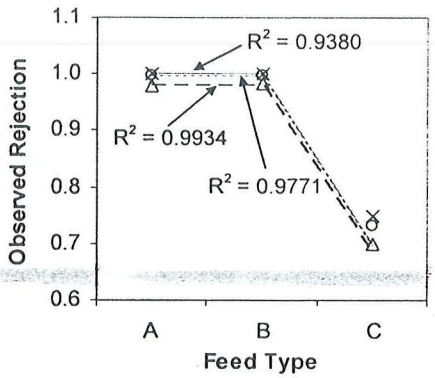

(c)

Fig. 6.25: The observed rejection for each solute at the different (a) trans membrane pressure (b) feed flow rate and (c) feed type. The notation (1) is carbohydrate constituents, (2) is protein and (3) is ammoniacal nitrogen.

Fig. 6.25(a) shows the simulation and experimental results of the observed rejection for each solute (carbohydrate constituents, protein and ammoniacal nitrogen) against the increasing trans membrane pressure. Figs. 6.25(a) depicts that the observed rejection for each solutes increased at increasing trans membrane pressure. This phenomenon resulted lower concentration in the permeate stream for each solutes at higher trans membrane pressure due to the higher driving force which would force more solvent (water) to diffuse through the membrane.

Fig. 6.25(b) shows the simulation and experimental results of the observed rejection for each solute against the increasing feed flow rate. Based on the results depicted in Fig. 6.25(b), the observed rejection for all solutes remained constant with slight increase at the increasing feed flow rate. Though higher turbulence was created at higher feed flow rate which resulted greater permeate flux and lower concentration factor, the effect of feed flow rate on the observed rejection was minimal.

Fig. 6.25(c) shows the simulation and experimental results of the observed rejection for each solute against the decreasing feed concentration based different type of feed as shown in Table 6.11. As shown from Fig. 6.25(c), the observed rejection of all the solutes obtained for Feed C were lower (at the range of 0.70-0.75) compared to Feed A and B although Feed C had a much lower feed concentration. As shown from Table 6.11, the Feed C was collected from the permeate stream of the first-pass RO membrane system. As all of the solutes were passed through the pores of the first-pass RO membrane system, thus, some of these solutes will also pass through the pores of the second-pass RO membrane system.

Fig. 6.26 shows the COD concentrations of the RO permeate for different trans membrane pressure, feed flow rate and feed type. The simulation values obtained from Eq. (6.6) showed a good fit with the experimental data with the coefficient of determination (R^2) more than 0.88. Fig. 6.26(a) demonstrates a decrease of COD concentration in the permeate stream when the trans membrane pressure increased. The increase of observed rejection at the increasing trans membrane pressure resulted lower permeate concentration and thus lower COD concentration was obtained.

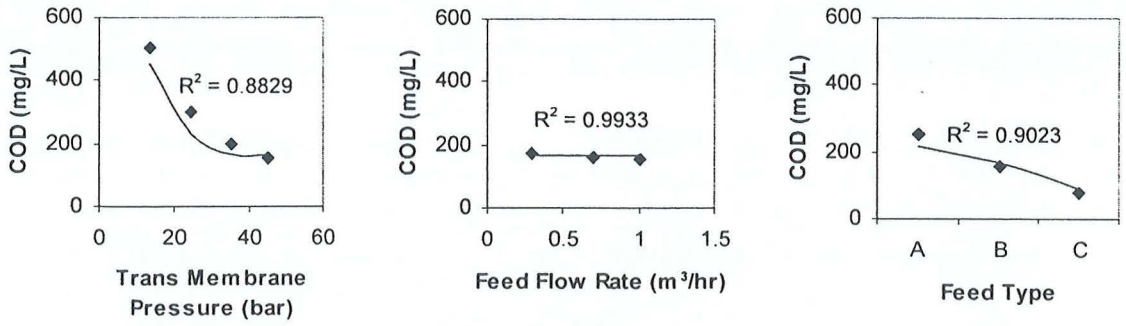

Fig. 6.26: COD concentration in the permeate stream with different (a) trans membrane pressure (b) feed flow rate and (c) feed type. The solid lines are the simulation results while the dotted points are the experimental results.

Fig. 6.26(b) shows the COD concentrations of the RO permeate for increasing feed flow rate. The COD concentration in the permeate stream was quite constant due to the constant observed rejection for all solutes based on Fig. 6.25(b). Fig. 6.26(c) shows that the COD concentrations of the RO permeate decrease for lower feed concentration based on three types of RO feed (Feed A, B and C). As shown from Fig 6.25(c), the RO membrane system rejected the solutes at a similar observed rejection for Feed A and B. Thus the COD concentration of the permeate stream was higher for Feed A as the total feed concentration of Feed A was higher than Feed B. Although the observed rejection for Feed C was the lowest (Fig. 6.25(c)), COD concentration in the permeate stream for Feed C was also the lowest because the total feed concentration for Feed C was much lower than the total feed concentration for Feed A and B as shown in Table 6.11.

The low COD concentration in the permeate stream (Fig. 6.26) compared to the COD concentration in the feed stream (Table 6.11) shows that the efficiency of COD removal using RO was high (94%-98% of COD removal for Feed A and B; 70% of COD removal for Feed C). The high rejection of carbohydrate constituents, protein and

ammoniacal nitrogen indicated that most of the solutes were unable to diffuse through the membrane and thus contributed to high efficiency of COD removal.

6.6 Design and Optimization of Treatment Plant

The uniqueness of each Design A, B and C is distinguished by the membrane system. The membrane system for Design A consists of UF membrane of ceramic type and followed by the RO membrane of polymeric type whereas for Design B, the membrane system consist of UF membrane of polymeric type followed by RO membrane of polymeric type. In the Design C, two-pass RO membrane system of polymeric type is employed.

6.6.1 Mass Balance Analysis

The mass balance, sizing and costing results presented in the present research are based on the optimum conditions. To avoid accumulation in the recycle stream, >90% suspended solids removal is assumed in the mass balance calculation. In addition, the volumetric flow rates for both cationic and anionic polymer solution are calculated based on the polymer concentration of 0.4% wt and 0.1% wt respectively. Throughout the mass balance calculation, the overall water recovery for the first and second membrane system was fixed at 70% in order to obtain the optimum water recovery for each stage of the membrane system.

The quality of the recovered water for S25, S23 and S18 in the Designs A, B and C respectively as shown in Tables 6.12-6.14 is meeting the constraints listed in Table 4.5 imposed by the DOE. The BOD concentration obtained for the Design A and B is quite close with the maximum allowable value. Though this situation is acceptable, it is quite undesirable because it provides limited rooms for the case when the characteristic of the raw POME fluctuates.

Table 6.12: Summary of the mass balance result at the optimum condition for Design A

Operating Conditions	Optimum Value**		
Pretreatment			
i) Cationic Polymer Flocculation			
- Polymer dosage, d_s	300 mg/L		
- Stirring speed, N	2.5 rev/s		
- Stirring time, t	3 min		
ii) Anionic Polymer Flocculation			
- Polymer dosage, d_s	50 mg/L		
- Stirring speed, N	2.4 rev/s		
- Stirring time, t	1 min		
iii) Sludge Dewatering using Dry Solids Decanter			
- Angular velocity, ω	230 1/s		
- G-force	1289G		
iv) GAC Adsorption			
- Residence time, τ	22.5 min		
First Membrane System			
i) UF Membrane Ceramic Type	Stage 1	Stage 2	Stage 3
- Trans Membrane Pressure, ΔP	4 bar	4 bar	4 bar
- Cross flow velocity, v	0.5055 m/s	0.5093 m/s	0.6201 m/s
- Water recovery, r	36%	36%	27%
Second Membrane System			
i) RO Membrane Polymeric Type	Stage 1	Stage 2	
- Trans Membrane Pressure, ΔP	45 bar	45 bar	
- Cross flow velocity, v	0.3126 m/s	0.3917 m/s	
- Water recovery, r	53%	36%	

Mass Balance Results

Cationic Polymer Flow rate = 2.03 m^3/hr @ 0.4%wt solution concentration
Anionic Polymer Flow rate = 1.35 m^3/hr @ 0.1%wt solution concentration
Sludge Cake from Decanter = 1631 kg/hr @ 25%wt solids content
Fertilizer Generated = 583 kg/hr @ 70%wt solids content (1679tons of fertilizer generated per year)

Parameter	Feed	Decanter	Recycle	GAC	UF Ceramic		RO Polymeric	
	S1	S7	S9	S11	S19	S18	S25	S24
T, °C	70	70	30	30	30	30	30	30
Q, m^3/hr	27.00	28.74	29.92	58.66	41.06	17.60	28.74	12.32
C_1, kg/m^3	12.07	10.73	24.55	12.52	8.74	21.35	0.01	29.11
C_2, kg/m^3	20.66	18.36	21.75	11.10	10.20	13.22	0.03	33.94
C_3, kg/m^3	0.10	0.09	5.18	2.67	2.29	3.56	0.06	7.49
C_{ss}, kg/m^3	14.80	0.04	4.6×10^{-3}	2.4×10^{-3}	3.3×10^{-6}	7.9×10^{-3}	4.2×10^{-10}	1.1×10^{-5}
$O\&G$, kg/m^3	3.70	0.01	1.2×10^{-3}	6.0×10^{-4}	8.6×10^{-7}	2.0×10^{-3}	1.1×10^{-10}	2.9×10^{-6}
Total-N, kg/m^3	<20.76	<18.45	<26.93	<13.77	<12.49	<16.78	<0.09	<41.43
COD, mg/L	38091	18600	39720	20283	15055	32482	263	50060
BOD, mg/L	12697	11595	24784	12656	9394	20267	88	31238

**Optimum value obtained based on minimization of the objective function of Eq. (4.15).

Table 6.13: Summary of the mass balance result at the optimum condition for Design B

Operating Conditions*		**Optimum Value	
First Membrane System			
i) UF Membrane Polymeric Type		Stage 1	Stage 2
- Trans Membrane Pressure, ΔP		4 bar	4 bar
- Cross flow velocity, v		0.2042 m/s	0.2388 m/s
- Water recovery, r		50%	40%
Second Membrane System			
i) RO Membrane Polymeric Type		Stage 1	Stage 2
- Trans Membrane Pressure, ΔP		45 bar	45 bar
- Cross flow velocity, v		0.3126 m/s	0.3917 m/s
- Water recovery, r		53%	36%

Mass Balance Results*								
Parameter	Feed	Decanter	Recycle	GAC	UF Polymeric		RO Polymeric	
	S1	S7	S9	S11	S17	S16	S23	S22
T, °C	70	70	30	30	30	30	30	30
Q, m^3/hr	27.00	28.74	29.92	58.66	41.06	17.60	28.74	12.32
C_1, kg/m^3	12.07	10.73	24.54	12.52	10.15	18.05	0.01	33.82
C_2, kg/m^3	20.66	18.36	21.75	11.10	10.03	13.60	0.03	33.39
C_3, kg/m^3	0.10	0.09	5.16	2.66	2.29	3.52	0.06	7.50
C_{ss}, kg/m^3	14.80	0.04	$4.6x10^{-3}$	$2.4x10^{-3}$	$3.0x10^{-6}$	$7.9x10^{-3}$	$3.9x10^{-10}$	$1.0x10^{-5}$
$O\&G$, kg/m^3	3.70	0.01	$1.2x10^{-3}$	$6.1x10^{-4}$	$7.8x10^{-7}$	$2.0x10^{-3}$	$9.9x10^{-11}$	$2.6x10^{-6}$
Total-N, kg/m^3	<20.76	<18.45	<26.91	<13.76	<12.32	<17.12	<0.09	<40.89
COD, mg/L	38091	18600	39703	20275	16792	28403	275	55846
BOD, mg/L	12697	11595	24773	12651	10478	17721	92	31848

* The optimum operating conditions for the pretreatment and the mass balance results for cationic and anionic flow rate, sludge cake and fertilizer flow rate is same as Design A listed in Table 6.12.

**Optimum value obtained based on minimization of the objective function of Eq. (4.15).

Table 6.14: Summary of the mass balance result at the optimum condition for Design C

Operating Conditions*	**Optimum Value	
First Membrane System		
i) RO Membrane Polymeric Type	Stage 1	Stage 2
- Trans Membrane Pressure, ΔP	45 bar	45 bar
- Cross flow velocity, v	0.3107 m/s	0.4167 m/s
- Water recovery, r	53%	36%
Second Membrane System		
i) RO Membrane Polymeric Type	Stage 1	
- Trans Membrane Pressure, ΔP	45 bar	
- Cross flow velocity, v	0.5002 m/s	
- Water recovery, r	70%	

Mass Balance Results*								
Parameter	Feed	Decanter	Recycle	GAC	RO first pass		RO second pass	
	S1	S7	S9	S11	S17	S16	S18	S19
T, °C	70	70	30	30	30	30	30	30
Q, m^3/hr	27.00	28.74	29.92	58.66	41.06	17.60	28.74	12.32
C_1, kg/m^3	12.07	10.73	24.57	12.53	0.02	41.74	$4.6x10^{-3}$	0.04
C_2, kg/m^3	20.66	18.36	21.78	11.11	0.03	36.98	0.01	0.07
C_3, kg/m^3	0.10	0.09	8.75	4.48	0.11	14.68	0.04	0.30
C_{ss}, kg/m^3	14.80	0.04	$4.6x10^{-3}$	$2.4x10^{-3}$	$3.0x10^{-7}$	$7.9x10^{-3}$	$3.0x10^{-11}$	$1.0x10^{-6}$
$O\&G$, kg/m^3	3.70	0.01	$1.2x10^{-3}$	$6.1x10^{-4}$	$7.7x10^{-8}$	$2.0x10^{-3}$	$7.7x10^{-12}$	$2.6\ x10^{-7}$
Total-N, kg/m^3	<20.76	<18.45	<30.53	<15.59	<0.14	<51.66	<0.05	<0.37
COD, mg/L	38091	18600	41754	21309	322	70818	114	810
BOD, mg/L	12697	11595	26053	13296	108	44189	38	270

* The optimum operating conditions for the pretreatment and the mass balance results for cationic and anionic flow rate, sludge cake and fertilizer flow rate is same as Design A listed in Table 6.12.
**Optimum value obtained based on minimization of the objective function of Eq. (4.15).

6.6.2 Equipment Sizing and Costing

The sizing of the pump is estimated based on the pump efficiency, n_p and motor efficiency, n_m of 0.83 and 0.94 respectively. Conservatively, the costing of the pumps is calculated based on two pumps per stream; with one pump in stand by while the other is operating.

Based on the optimum operating conditions and design, the treatment cost for a plant capacity of 27m^3/hr is estimated and the summary of the cost breakdown is displayed in Table 6.15. All the Designs A, B and C which are operating at the optimum conditions

are meeting the requirements and constraints as stated in Table 4.5. The results clearly shows that the total capital cost is strongly depend on the cost of the membrane system which accounts for 95.2%, 83.2% and 67.3% of the total direct capital cost for Designs A, B and C respectively as displayed in Fig. 6.27. In other words, the unit cost and the type of the membrane used as well as the total membrane area needed are the important parameters that will determine the total capital cost.

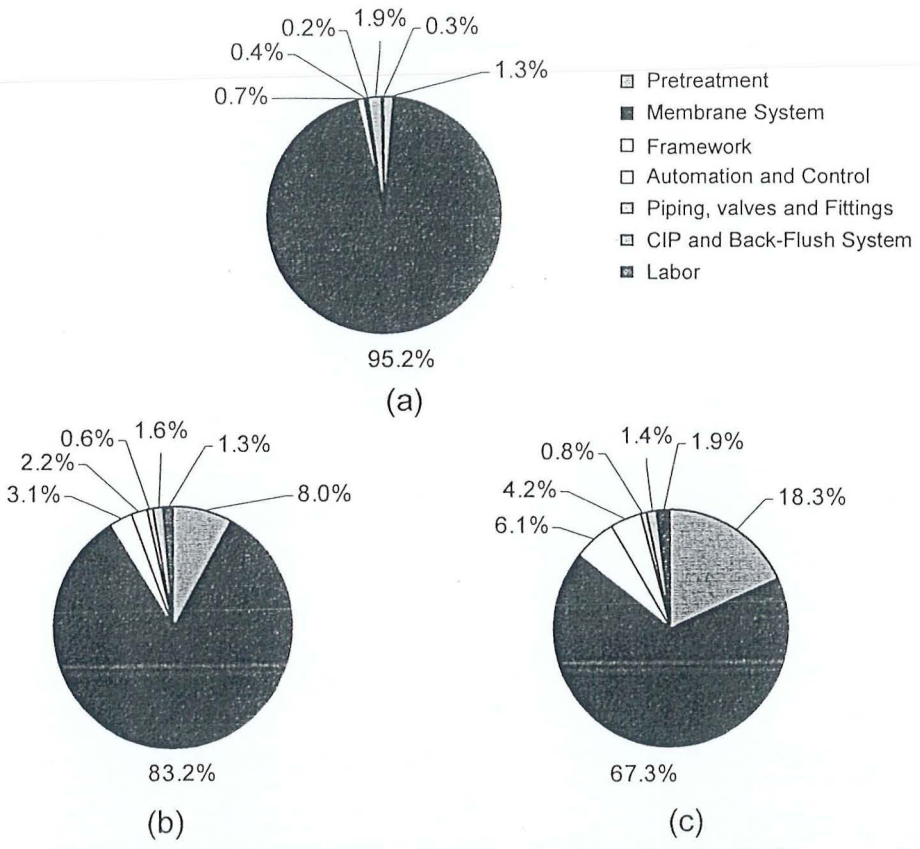

Fig. 6.27: Cost breakdown in term of percentage for the total direct capital cost of (a) Design A (b) Design B and (c) Design C.

Table 6.15: Summary of the estimated cost breakdown for Design A, B and C

	Design A	Design B	Design C
Direct Capital Cost (10^6 RM)			
Pretreatment	0.66	0.66	0.66
membrane system	49.36	6.87	2.43
framework	0.35	0.26	0.22
automation and control	0.21	0.18	0.15
piping, valves and fittings	0.10	0.05	0.03
CIP and back-flush system	0.98	0.13	0.05
Labor	0.18	0.11	0.07
Total	51.82	8.26	3.61
Indirect Capital Cost (10^6 RM)	5.16	0.81	0.34
Total Capital Cost (10^6 RM)	56.98	9.06	3.95
Annualized Capital Cost (10^6 RM/yr)	4.19	0.67	0.29
Operating Cost (10^6 RM/yr)			
Electrical	0.22	0.22	0.38
Maintenance	0.25	0.04	0.02
Chemical	0.64	0.64	0.64
GAC replacement	0.04	0.04	0.04
Chemical cleaning	0.10	0.02	0.0013
Membrane replacement	11.11	2.48	0.48
total	12.35	3.43	1.55
Profit gained from fertilizer sales (10^6 RM/yr)	0.88	0.88	0.88
Cost per cubic meter (RM/m^3)			
Capital cost	30.81	4.90	2.13
Operating cost	90.77	25.22	11.37
Profit gained from fertilizer sales	6.47	6.47	6.47
Total cost (RM/m^3)	115.11	23.64	7.03

The membrane replacement cost gives the most significant influence to the operating cost for the Designs A and B which account for 89.9% and 72.1% of the total operating cost respectively (Fig. 6.28). However, the chemical cost used for pretreatment (namely cationic and anionic polymers cost) gives the most significant influence to the operating cost for Design C (41.0%). This indicates that the chemical cost used for pretreatment become dominant when the RO membrane system with cheaper membrane unit cost is used.

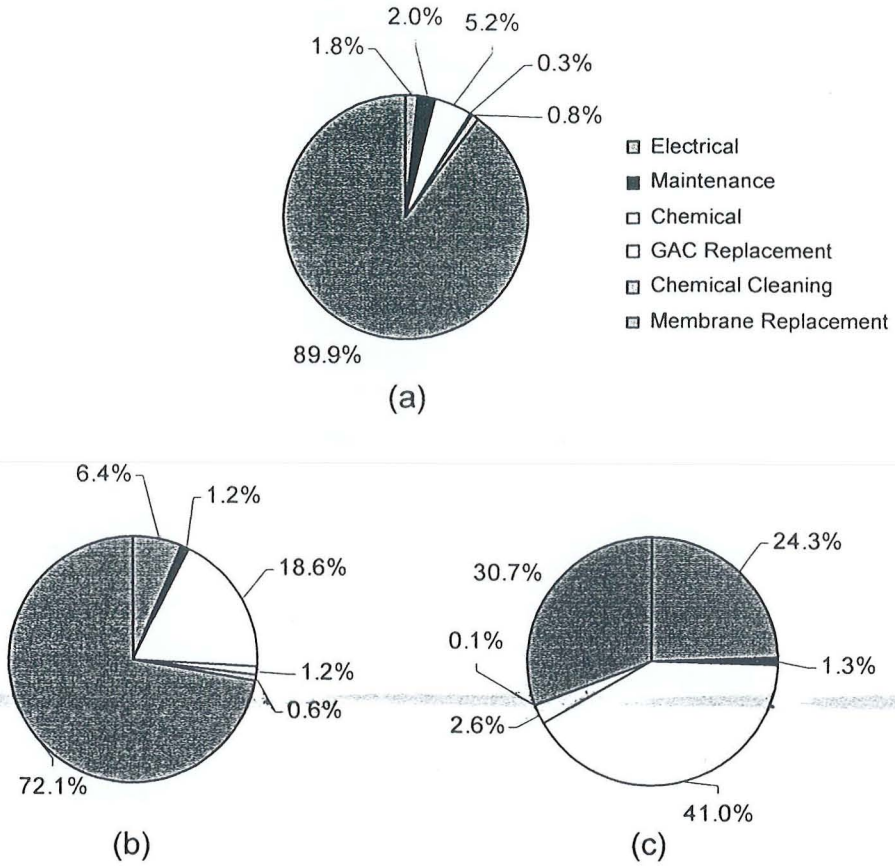

Fig. 6.28: Cost breakdown in term of percentage for the total operating cost of (a) Design A (b) Design B and (c) Design C.

6.6.3 Final Design for Membrane based POME Treatment Plant

The optimum design for the membrane based POME treatment system is the design with two-pass RO membrane system. As increasing operating pressure achieves greater cost reduction than increasing membrane area, the membrane system is operated at the maximum allowable pressure to reduce the total membrane area needed. The minimum total cost obtained for the proposed design is 7.03 RM/m^3 and the recovered water quality is well below the maximum allowable value imposed by the DOE. The summary of the overall operating condition, design and performance for the optimum membrane based POME treatment system of Design C is shown in Table 6.16.

Table 6.16: The summary of the overall optimum operating conditions for Design C

Operating Conditions	Optimum Value	
Pretreatment		
i) Cationic Polymer Flocculation		
- Polymer dosage, d_s	300 mg/L	
- Stirring speed, N	2.5 rev/s	
- Stirring time, t	3 min	
ii) Anionic Polymer Flocculation		
- Polymer dosage, d_s	50 mg/L	
- Stirring speed, N	2.4 rev/s	
- Stirring time, t	1 min	
iii) Sludge Dewatering using Dry Solids Decanter		
- Bowl diameter, d	0.5m	
- Bowl length, L	2.035m	
- Angular velocity, ω	230 1/s	
- G-force	1290G	
iv) GAC Adsorption		
- Residence time, τ	22.5 min	
First Pass RO Membrane System	Stage 1	Stage 2
- Trans Membrane Pressure, ΔP	45 bar	45 bar
- Number of pressure vessels in parallel	23	8
- Number of small modules in series	25	22.5*
- Cross flow velocity, v	0.3107 m/s	0.4167 m/s
- Water recovery, r	53%	36%
Second Pass RO Membrane System	Stage 1	
- Trans Membrane Pressure, ΔP	45 bar	
- Number of pressure vessels in parallel	10	
- Number of small modules in series	24.1*	
- Cross flow velocity, v	0.5002 m/s	
- Water recovery, r	70%	
Treatment cost		
Total capital cost	RM 3.95 x 10^6	
Annualized capital cost	RM 0.29 x 10^6 /yr	
Total operating cost	RM 1.55 x 10^6 /yr	
Profit gained from fertilizer sales	RM 0.88 x 10^6 /yr	
Total cost	RM 0.96 x 10^6 /yr	
Treatment cost per cubic meter		
Total capital cost	RM 2.13 /m^3	
Total operating cost	RM 11.37 /m^3	
Profit gained from fertilizer sales	RM 6.47 /m^3	
Total cost	RM 7.03 /m^3	

* The number with decimal is allowed as long as the total number of modules is an integer

The treated water based on optimum design for the membrane based POME treatment system of Design C with two-pass RO membrane system not only comply with the standard discharge limit imposed by the DOE, the treated water is clear as crystal which meeting the drinking water quality standard set by the USEPA (U.S. Environment Protection Agency). The chemical analyses of the second pass RO permeate water in the Table 6.17 showed that the quality of the treated water was well below the Maximum Contaminant Level (MCL) for drinking water quality standard set by USEPA and thus the treated water is suitable to be recovered and recycled.

Table 6.17: The POME characteristic of every stage of treatment and the drinking water standard set by U.S. Environmental Protection Agency (USEPA).

Parameter	POME	Flocculation	GAC Adsorption	Reverse Osmosis	USEPA Standard
pH	4.1	4.1	4.1	7.0	6.5-8.5
Color, color units	151	128	84	ND	15
Odor, threshold odor number	300	150	100	ND	3
Turbidity, NTU	11 000	21	2	<0.01	<0.5
COD, mg/L	40 000	18 000	13 900	114	NR
Total Dissolved Solids, mg/L	33 000	29 000	20 000	130	500
Oil and Grease, mg/L	3 700	10	ND	ND	0.3
Nitrogen (organic), mg/L	750	660	400	50	NR
Ammoniacal Nitrogen, mg/L	100	80	80	40	NR
Al, mg/L	3.9	0.52	0.34	ND	0.05-0.2
K, mg/L	1219	1309	1169	5.45	NR
Mg, mg/L	615	589	481	ND	150
Ca, mg/L	439	421	389	ND	NR
Fe, mg/L	58.53	13.72	13.53	ND	0.3
Mn, mg/L	3.09	1.43	1.24	ND	0.05
Cu, mg/L	0.13	0.11	0.09	ND	1.3
Zn, mg/L	0.74	0.08	0.04	ND	5

ND=Not Detectable; NR=Not Required

Though Design C is found to be the optimum design compared to Designs A and B with the minimum total cost of 7.03 RM/m^3, the feasibility of the proposed design based on the optimum total cost have to be evaluated. As the recovered water is clean and meeting the drinking water quality standard of USEPA, the recovered water can be recycled back to

the process plant as utility water, boiler feed water and process water. Based on the mass balance calculation, the total water recovery achieved by using the membrane technology as shown in Fig. 6.29 is 94%. By considering the cost saving due to water recycling, the total treatment cost of 4.28 RM/m^3 is needed if the Design C is adopted in the palm oil mills (calculation based on the Johor's industrial water tariff of RM 2.93/m^3 (Ministry of Energy, Water and Communications, 2007) as most of the palm oil mills in the peninsular of Malaysia (with more than 27%) are located in the state of Johor (Malaysian Palm Oil Board, 2005)).

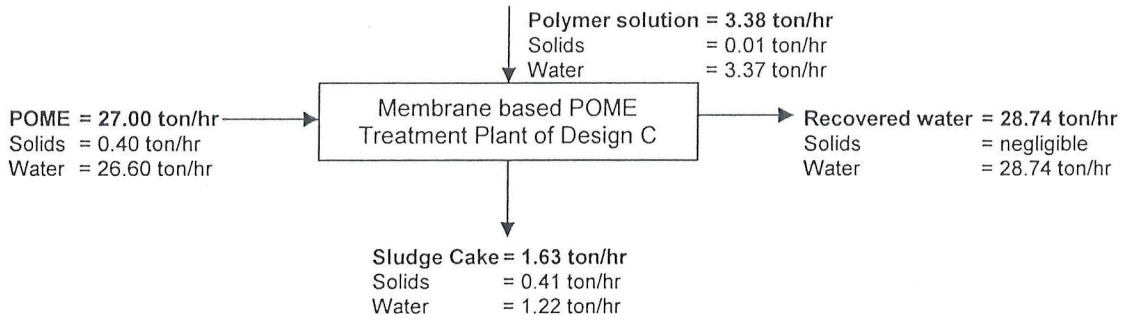

Fig. 6.29: Overall mass balance for membrane based POME treatment plant.

Based on the statistics of IOI Corporation Berhad as per year ending of 30 June 2005, the operating profit gained per ton of Fresh Fruit Bunch (FFB) processed is RM 209.77 (Plantation Statistics, 2006). Conservatively, for every ton of FFB processed, 0.75 ton of POME is generated and thus approximately 0.71 ton of clean water is recovered and recycled (based on 94% water recovery). By considering the cost saving due to water recycling, the total treatment cost of RM 3.21 per ton of FFB processed (inclusive capital and operating cost) is needed. In other words, for every ton of FFB processed, the corporation only needs 1.5% of their profit to recover and recycle clean water with drinking water quality standard from POME and thus the proposed membrane based POME treatment plant of Design C is feasible as the treatment cost is acceptable and affordable.

7.2 Conclusions

1. Based on the investigation on the pilot plant fabricated from the earlier Yayasan Felda grant, reliable and reproducible process data over a wide range of conditions within the error of ± 5% was obtained. This data was used throughout the study to verify the simulation data of the transport models developed for direct flocculation, GAC adsorption, UF and RO membrane system.

2. The fouling problem for both UF and RO membrane system is investigated based on the gel layer resistant and concentration factor. A simple three-step pretreatment system to overcome membrane fouling problem is proposed as below:

   i) Direct Flocculation Process

   - The direct flocculation using the water-soluble organic polymers without the need of pH adjustment is proposed to replace the inorganic coagulant of Alum which was proposed in the earlier Yayasan Felda grant in POME pretreatment.
   - The direct flocculation has significantly reduced the treatment cost by a factor of 3.6 compared to the conventional coagulation-flocculation process with comparable treatment efficiency.
   - In the single polymer system, the optimum cationic polymer dosage was 300mg/L at stirring of 200rpm for 3min to give 99.60%, 56.32%, 99.74% and 58.07% of suspended solids, COD, oil & grease removal and water recovery respectively. The flocs breakage was minimal with the fractal dimension of 1.82 but the percent of water recovery was still low compared to the targeted water recovery of at least 75%.

- In the dual polymer system, the anionic polymer was added after the cationic polymer flocculation. The optimum anionic polymer dosage was obtained as 50mg/L at stirring of 150rpm for 1min to give 99.66%, 57.96%, 99.74% and 82.08% of suspended solids, COD, oil & grease removal and water recovery respectively. High water recovery was achieved as the anionic polymer bridged those initially loose flocs to produce compact, dense and shear resistant flocs of higher fractal dimension (1.85).

ii) Sludge Dewatering Using Decanter/Filter Press

- In the pilot plant analysis, the flocculated sludge is dewatered by using the filter press in batch mode operation.
- In the industrial scale design, a Dry Solids Decanter is employed due to the continuous high solids loading and high cake solids concentration needs to be achieved.
- The sizing of Dry Solids Decanter is obtained as: bowl diameter 0.5 m, bowl length 2.035 m, angular velocity 230 1/s and G-Force 1290 G with the dry cake produced at 25% solids content.

iii) GAC Adsorption Process

- The pretreated POME adsorption on GAC was effective in removing the COD as most of the COD was removed in the first hour and the adsorbent achieved saturation only after 55hrs.
- The results for fixed-bed adsorption found that the protein was a strongly adsorbed species, followed by carbohydrate constituents and ammoniacal nitrogen.
- The results also proved that the saturation time increased with increasing residence time as the breakthrough curves for all the solutes shifted gradually to the right.

3. Transport models for the processes used in pilot plant are developed and verified based on the experimental data obtained from pilot plant analysis, as:

i) Flocculation process - Population Balance Model (PBM).

- The proposed model has considered the charge neutralization and bridging attraction under shear induced flocculation and the model predictions reflected the experimental results adequately.
- The correlation of indirect indicators (suspended solids, COD, oil & grease) with the floc size distribution based on the PBM was successfully applied.

ii) Granular activated carbon (GAC) adsorption - coupled model of Homogeneous Surface Diffusion Model (HSDM) with Ideal Adsorbed Solution Theory (IAST).

- The comparisons between the simulated and the experimental breakthrough curves showed a good agreement.
- The present study proved that when complex organic solutions were used, the model needed only representative solutes and the model allowed multiple solutes calculations to be performed.

iii) Ultrafiltration (UF) membrane system - coupled model of Back Transport Analysis with Filtration Theory.

- The comparisons between the simulation results and the experimental data for the continuous cross-flow UF membrane system showed a good agreement and proved its utility in predicting the performance of the multiple solutes system, even solute-solute interactions were ignored in the model.
- The volume flux of permeate increased with the increasing trans membrane pressure and feed flow rate. The observed rejection for each solute in the system increased when the trans membrane pressure and feed flow rate increased.

- The UF ceramic membrane gave higher rejections for all the solutes and COD as compared to the UF polymeric membrane.
- The UF membrane system gave low efficiency of COD removal (10-20%) for pretreated POME due to the low rejection of carbohydrate constituents (15-45%), protein (5-15%) and ammoniacal nitrogen (7-23%).
- Thus, the RO membrane system was needed to remove the remaining micro-molecules to achieve the desired water quality where the UF membrane system served as the pretreatment to the RO membrane process.

iv) Reverse osmosis (RO) membrane system - coupled model of Extended Spiegler-Kedem Model with Concentration Polarization Model.

- The simulation results has proven the model's utility in predicting the performance of the multiple solutes system with the consideration of solute-solute interactions.
- The simulation and experimental results prove that the volume flux of permeate was quite constant with filtration time at minor permeate flux reduction (less than 32.8%).
- The volume flux of permeate increased with the increasing trans membrane pressure and feed flow rate but with decreasing total feed concentration.
- The simulation and experimental results show that the observed rejection for each solute increased at increasing trans membrane pressure, feed flow rate and total feed concentration.
- The RO membrane system gave high efficiency of COD removal for pretreated POME (70-98%) due to the high rejection of carbohydrate constituents (75-99.9%), protein (73-99.8%) and ammoniacal nitrogen (69-99%). Thus, the RO

membrane system is effective to remove the remaining micro-molecules in the pretreated POME to achieve the desired water quality.

4) The optimization via total treatment cost minimization by using sequential quadratic programming method was used to obtain the optimum operating and design parameters for all the Designs A, B and C.

   i) The optimization for the designs arrived at an optimum condition that maximizes the water recovery by maximizing the trans membrane pressure and minimizing the membrane area because maintaining a high supply pressure is less costly than increasing the membrane area. At the optimum condition, the cross flow velocity was maintained close to the minimum allowable value for all the designs.

   ii) The results obtained at optimum condition showed that the quality of the recovered water for Designs A, B and C met the effluent discharge standards imposed by the Department of Environment (DOE) of Malaysia.

   iii) The sizing and costing analysis based on the optimum condition show that the total capital cost for Design A was the highest (RM56.98 millions), followed by Design B (RM9.06 millions) and Design C (RM3.95 millions).

   iv) The total operating cost at optimum condition for Design A was the highest (RM12.53 millions/year), followed by Design B (RM3.43 millions/year) and Design C (RM1.55 millions/year).

   v) Consequently, total treatment cost per cubic meter of POME treated at the optimum condition for Design A was the highest (RM115.11/m^3), followed by Design B (RM23.64/m^3) and Design C (RM7.03/m^3).

5) Design C was chosen as an optimal design for the industrial scale membrane based POME treatment system due to its lowest total treatment cost.

   i) The treated water obtained from the membrane based POME treatment system of Design C with two-pass RO system not only complied with the effluent discharge standards imposed by the DOE of Malaysia, but also met the drinking water quality standard of the U.S. Environment Protection Agency (USEPA).

   ii) The recovered water can be recycled back to the process plant as utility water, boiler feed water and process water.

   iii) The total treatment cost is only 1.5% of their profit gained from every ton of Fresh Fruit Bunch (FFB) processed to recover and recycle clean water with drinking water quality standard from POME.

   iv) The POME treatment with the membrane technology was feasible and promising as the treatment cost was affordable and the results were encouraging. Therefore, a complete industrial scale membrane based POME treatment plant design can be readily to be commercialized and applied in the palm oil mills in Malaysia to meet the discharge standards laid down by the Department of Environment (DOE).

7.2 Recommendations

1. A demonstration plant according to the Design C can be installed in one of the palm oil mills in Malaysia for long term evaluation on the performance of the system. This demonstration plant will lead a step closer to the full commercialization of the membrane based POME treatment system which is environmental friendly with zero discharge.

2. The investigation on the different types of cationic and anionic polymers from different chemical suppliers for direct flocculation can be carried out to find the possibility of treatment cost reduction. Flocculent from natural resources such as Moringa Oleifera can be used to substitute the commercial flocculent for cost reduction because the natural flocculent can be synthesized easily and the raw material can be found abundantly in Malaysia at low cost.

3. The research on different types of membranes available in the market can be carried out for the possibility of cost reduction. Lower cost can be obtained by selecting the membrane which produces the highest volume flux of permeate with the lowest membrane unit cost. The membrane also can be operated at the lowest possible trans membrane pressure and requires only minimal chemical cleaning reagents for membrane regeneration.

YAYASAN FELDA

LAPORAN KEWANGAN GERAN PENYELIDIKAN

(Tempoh : NOV 2004 hingga MEI 2007)

Tajuk Projek : Pilot plant studies for treatment of palm oil mill effluent (POME) using Membrane Technology.

A. Kedudukan Geran

(a) Jumlah Geran Penyelidikan Diluluskan : RM 220,000.00

(b) Amaun Geran Penyelidikan Diterima Sehingga Mei 2007 : RM 219,000.00

(c) Baki Geran Penyelidikan : RM 1000.00

B. Rekod Perbelanjaan

Perkara	Perbelanjaan (RM)		
	Peruntukan	Kumulatif sehingga Mei 2007	Baki
(i) Kos Penggajian Kakitangan Sokongan			
a) Pegawai Penyelidik : 2 (Pelajar PhD)	58,000.00	92,754.26	-34,754.26
(ii) Perjalanan / Pengangkutan	8050.00	16,977.65	-8,927.65
(iii) Penyewaan	750.00	0.00	750.00
(iv) Bahan/Bekalan Penyelidikan	21,150.00	58,080.24	-36,930.24
(v) Pengubahsuian dan baik Pulih Makmal/Kelengkapan	19,500.00	280.00	19,220.00
(vi) Peralatan Khas dan Aksesori	83,700.00	30,611.00	53,089.00
(vii) Lain-Lain			
b) Seminar Antarabangsa	24,450.00	19,179.50	5270.50
c) Komunikasi dan perhubungan	4400.00	1,117.35	3282.65
JUMLAH	220,000.00	219,000.00	1000.00

C. Jumlah dana yang diterima tetapi belum digunakan sehingga Mei 2007 – RM 0.00

D. Catatan :

RESEARCH ACHIEVEMENTS

This research project has an outstanding achievement and output due to its significant in environmental issues as well as introducing a new alternative technology for the treatment of POME. The outputs are categorized into three parts that are recognition in awards received, publication to international journals and conferences and finally the number of research students involved.

9.3 Awards

1. International Exhibition, Ideas-Inventions- New Products (IENA 2005), Nuremberg Exhibition Center, Nuremberg, Germany, 3 – 6 November 2005, Gold Medal.
2. 16th International Invention, Innovation, Industrial Design & Technology(I-TEX 2005), organized by Malaysian Invention and Design Society (MINDS), PWTC, Kuala Lumpur, 19 – 21 May 2005, Silver Medal.
3. 15th International Invention, Innovation, Industrial Design & Technology(I-TEX 2004), organized by Malaysian Invention and Design Society(MINDS), Mid Valley, K.L, 20-22 May 2004, Gold Medal.
4. Invention, Innovation, Industrial Design Technology 2002, I-TEX 2002 organized by Malaysian Invention and Design Society (MINDS), Mid Valley Exhibition Centre, KL, 29-31 March 2002, Silver Medal.
5. EXPO Science & Technology 2002, organized by Ministry of Science and Technology, Malaysia, PWTC, KL, 2-4 November 2002, Gold Medal
6. International Exhibition Ideas, Inventions, New Products, IENA 2003, Nuremberg Exhibition Center, Nuremberg, Germany, 30 October – 2 November 2003, Silver Medal
7. Most Outstanding Research Project in Universiti Sains Malaysia 2003, December 2003, Second Prize (Silver Medal).

URKUNDE

INTERNATIONALE FACHMESSE »IDEEN-ERFINDUNGEN-NEUHEITEN« NÜRNBERG 2005

Assoc. Prof. Abdul Latif Ahmad
Universiti Sains Malaysia
Research & Innovation (R&I)

wurde für hervorragende Leistungen eine

Goldmedaille verliehen.

Erfindung / Neuheit

CHITEC: Umweltfreundliches bio-abbaubares Polymer für flockige Öl-absorber Rückstände

CHITEC: An environmental friendly and biodegradable polymer for residue oil flocsorb

Nürnberg, 5. November 2005

Die internationale Jury der IENA 2005

MINISTRY OF SCIENCE, TECHNOLOGY & INNOVATION

ITEX Invention · Innovation Industrial Design · Technology

MINDS

Certificate of Award

This is to certify that

Assoc. Prof. Dr. Abdul Latif Ahmad, Prof. Subhash Bhatia, Zalina Binti Othman

has been awarded the

ITEX Silver Medal

for the invention

Moringa Oleifera Seed: A Biodegradable, Environmental Friendly and Healthier Coagulants

at the

16th International Invention Innovation Industrial Design & Technology Exhibition 2005 (ITEX 2005)
Kuala Lumpur, Malaysia

19th – 21st May 2005

Academician Tan Sri Datuk Dr Augustine S. H. Ong
President
Malaysian Invention and Design Society

I•TEX

Certificate of Award

This is to certify that

ABDUL LATIF AHMAD, BASSIM H HAMEED AND
SUMATHI SETHUPATHI

has been awarded the

GOLD MEDAL

for the Invention

CHITEC: A Biodegradable Polymer for Residue Oil Flocsorb

at the 15th
International Invention Innovation
Industrial Design & Technology Exhibition
I•TEX 2004

on 20 – 22 MAY 2004

MINDS

Tan Sri Datuk Dr. Augustine S. H. Ong
President
Malaysian Invention and Design Society

EHREN-URKUNDE

INTERNATIONALE AUSSTELLUNG »IDEEN-ERFINDUNGEN-NEUHEITEN« NÜRNBERG 2003

Deputy Registrar
Research Creativity&Management
Office Chancellory
Ass. Prof. Abdul Latif Ahmad, Prof. Subhash Bhatia, Ms. Suzylawati Ismail
Malaysia

wurde für hervorragende Leistungen eine

Silbermedaille verliehen.

Erfindung/ Neuheit

Ein neues Verfahren der Membrantechnologie zur Behandlung des ausströmenden Faulgases
A novel process of membrane technology for the treatment of effluent (POME) gas

Nürnberg, 2. November 2003

Die internationale Jury der IENA 2003

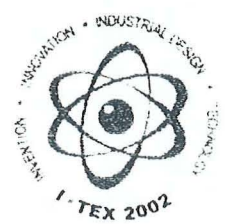

Certificate of Award

This is to certify that a

SILVER MEDAL

has been awarded to

Dr. Abdul Latif Ahmad

Prof. Subhash Bhatia &

Suzylawati Ismail

for the Invention

A novel process based on membrane technology for treatment of palm oil mill effluent (POME)

at I·TEX 2002

Dated This 30th Day of March 2002

MINDS

Tan Sri Datuk Dr. Augustine S.H. Ong
President of MINDS

Ministry of Science,
Technology and the Environment
of Malaysia

Gold Medal

This Certificate of Award
is presented to

Assoc. Prof. Abdul Latif Ahmad
Prof. Subhash Bhatia
Suzylawati Ismail

For the invention/innovation
of

A Novel Process Based on Membrane Technology for Treatment of Palm Oil Mill Effluent (POME)

At
Expo S&T 2002
2-4 November 2002
Kuala Lumpur

YB Dato' Seri Law Hieng Ding
Minister of Science, Technology and the Environment of Malaysia

OUTSTANDING PROJECT AWARD 18 DECEMBER 2003

UNIVERSITI SAINS MALAYSIA
INSTITUTE OF GRADUATE STUDIES

This is to certify that the following project has been awarded

Second Prize

for the quality of the contribution made
by a Graduate Student towards the success of the Project

Project Title : Membrane Based Process for Treatment of Palm Oil Mill Effluent

Project Head : Prof. Madya Abdul Latif Ahmad

Graduate Student : Suzylawati Ismail
School of Chemical Engineering

PROFESSOR DATO' DZULKIFLI ABDUL RAZAK
Vice Chancellor

PROFESSOR RAMLI MOHAMED
Dean, Institute of Graduate Studies

9.4 International Publications

1. Ahmad, A.L., Chong, M.F. and Bhatia, S. (2007). Mathematical modeling of multiple solutes system for reverse osmosis process in palm oil mill effluent (POME) treatment. Chemical Engineering Journal [In Press].

2. Subhash Bhatia, Zalina Othman and Abdul Latif Ahmad (2007) Coagulation – Flocculation Process for POME Treatment using *Moringa oleifera* Seeds Extract: Optimization Studies. Chemical Engineering Journal, [In Press].

3. Ahmad, A.L., Sumathi, S. & Hameed, B.H. (2006). Coagulation of residue oil and suspended solid in palm oil mill effluent by chitosan, alum and PAC. Chemical Engineering Journal Vol. 118, Issues 1-2 (2006) pp. 99-105.

4. Ahmad, A.L., Chong, M.F. and Bhatia, S. (2006). Prediction of Breakthrough Curves for Adsorption of Complex Organic Solutes Present in Palm Oil Mill Effluent (POME) On Granular Activated Carbon. Industrial and Engineering Chemistry Research Vol. 45, Issues 20 (2006) pp. 6793-6802.

5. A.L. Ahmad, Chong Mei Fong and Subhash Bhatia (2006). Ultrafiltration Modeling of Multiple Solutes System for Continuous Cross-Flow Process. Chemical Engineering Science Vol. 61, Issues 15 (2006) pp. 5057-5069.

6. A.L. Ahmad, M.F. Chong and S. Bhatia (2005) Drinking *Water Reclamation From Palm Oil Mill Effluent (POME) Using Membrane Technology*. Desalination Journal, Vol. 191, Issues 1-3 (2006) pp 35-44.

7. A.L. Ahmad, S. Sumathi and B.H. Hameed (2006). *Coagulation of Residue Oil and Suspended Solid in Palm Oil Mill Effluent by Chitosan, Alum and PAC.* Chemical Engineering Journal, Vol. 118, Issue 1-2, (2006), pp 99-105.

8. A.L. Ahmad, S. Ismail And S. Bhatia (2005) *Optimization Of Coagulation-Flocculation Process For Palm Oil Mill Effluent Using Response Surface Methodology*. Journal Of Environmental Science And Technology, Vol. 39(8) (2005), pp 2828-2834.

9. A.L. Ahmad, S. Ismail And S. Bhatia (2005). *Membrane Treatment For Palm Oil Mill Effluent: Effect Of Transmembrane Pressure And Crossflow Velocity*. Desalination Journal, Vol. 179 Issues 1-3 (2005), pp 245-255.

10. A.L. Ahmad, S. Ismail and S. Bhatia (2005). *Ultrafiltration Behavior In The Treatment Of Agro-Industry Effluent: Pilot Scale Studies*. Journal Of Chemical Engineering Science, Vol. 60 Issue 19 (2005), pp 5385-5394.

11. A.L. Ahmad, S. Sumathi and B.H. Hameed (2005). *Adsorption of Residue Oil from Palm Oil Mill Effluent using Powder and Flake Chitosan: Equilibrium and Kinetics Studies*. Water Research Journal, Vol. 39 Issue 12 (2005), pp 2483-2494.

12. A.L. Ahmad, S. Sumathi and B.H. Hameed (2005). *Residue Oil and Suspended Solids Removal using Natural Adsorbents Chitosan, Bentonite and Activated Carbon: A Comparative Study*. Chemical Engineering Journal, Vol. 108 Issues 1-2 (2005), pp 179-185.

13. A.L. Ahmad, M.F. Chong and S. Bhatia (2005). *Mathematical Modelling and Simulation of Multiple Solutes System for Nanofiltration Process*. Journal of Membrane Science, Vol. 253 Issues 1-2 (2005), pp 103-115.

14. A.L. Ahmad, S. Bhatia, N.Ibrahim and S.Sumathi (2004). *Adsorption of Residual Oil from Palm Oil Mill Effluent using Rubber Powder*. Brazilian Journal of Chemical Engineering. (July-Sept. 2005) Vol 22, No.3, pp 371 – 379.

15. Abdul Latif bin Ahmad, S. Sumathi and Bassim H. Hameed (2004). Coagulation-Adsorption of Suspended Solids and Residual Oil from Palm Oil Mill Effluent Using Chitosan. ASEAN Journal of Chemical Engineering, Vol. 4 No.2, (2004) pp 48-57.

16. A.L. Ahmad, S. Sumathi and B. Hameed (2004). *Chitosan: A Natural Biopolymer for the Adsorption of Residue Oil from Oily Wastewater*. Adsorption Science and Technology Journal, Vol. 22, No. 1, 2004, pp 75 – 88

7. A.L. Ahmad, K. Shitamparam, S. Ismail and M.M. D. Zulkali (2003). *Extraction of Residue Oil from palm Oil Mill Effluent (POME) using Organic Solvent.* ASEAN Journal of Sciences and Technology for Development, Vol. 20, No. 3&4, December 2003, pp 385-394

9.3 International Conferences

1. Ahmad, A. L., Choi Yee Chan, Syamsul Rizal Abd Shukor and Mat Don Mashitah, Recovered oil from palm oil mill effluent and separation of its carotene by adsorption chromatography, International Conference on Environment (ICENV 2006), 13-15 November 2006, Penang, Malaysia.

2. A.bdul Latif Ahmad, Subhash Bhatia, Mei Fong Chong & Suzy Ismail, *Drinking Water Reclaiming From Palm Oil Mill Effluent Using Membrane Technology*, International Congress on Membranes and Membrane Processes 2005 (ICOM 2005), 21-26 August 2005, Seoul, Korea. (Korea Selatan)

3. A.L. Ahmad, S. Bhatia and S. *Ismail. Treatment of Agro Based Industrial Effluent Using Ceramic Ultrafiltration Membrane: Effect of Pressure and Crossflow Velocity.* Conference on Membrane in Drinking Water Production, L'Aquila, Italy, 15-17 November 2004

4. Norliza Ibrahim, Abdul Latif Ahmad and Subhash Bhatia. *Removal of Suspended Solids and Residual Oil using membrane Separation Technology.* Regional Symposium on Membrane Sciences & Technology. 21 – 25 April 2004, Johor.

9.4 National Conferences

1. S. Bhatia, A. L. Ahmad and Z. Othman, *A Jar Test Studies on Pretreatment Process of Palm Oil Mill Effluent (POME) Using Moringa Oleifera Seeds Extract.* National Postgraduate Colloqium(NAPCOL 2004), Penang, 8-9 December 2004, pp244 – 248.

2. A.L. Ahmad, M.F. Chong and S. Bhatia. *Extended Spiegler Kadem Model for Nanofiltration.* National Postgraduate Colloqium(NAPCOL 2004), Penang, 8-9 December 2004, pp 318 -324

9.5 Research Students

1. Postgraduate student
   - 2 PhD (Graduated)
   - 1 PhD (In Progress)
   - 2 Master (Graduated)
2. Undergraduate student
   - 3 Final Year Student (Graduated)

Ahmad, A.L., Ismail, S. and Bhatia, S. (2003) Water recycling from palm oil mill effluent (POME) using membrane technology, *Desalination*, 157, p.87-95.

Ahmad, A.L., Ismail, S. and Bhatia, S. (2005) Optimization of coagulation-flocculation process for palm oil mill effluent using response surface methodology, *Environ. Sci. Technol.*, 39, p.2828-2834.

American Public Health Association (APHA). (1999) *Standard Methods for The Examination of Water and Wastewater.* APHA, Washington, DC.

Bell, G.M., Levine, S. and McCartney, L.N. (1970) Approximate methods of determining the double-layer free energy of interaction between two charged colloidal spheres. *J. Colloid Interface Sci.*, 33, p.335-359.

Bhattacharjee, C. and Datta, S. (2003) Analysis of polarized layer resistance during ultrafiltration of PEG-6000: an approach based on filtration theory. *Separation and Purification Technology*, 33, p.115-126.

Bhattacharya A. and Ghosh, P. (2004) Nanofiltration and reverse osmosis membranes: theory and application in separation of electrolytes, *Reveiws in Chemical Engineering*, 20, p. 111-173.

Biegler, L.T., Grossmann, I.E. and Westerberg, A.W. (1999) *Systematic Methods of Chemical Process Design*, Prentice Hall PTR, New Jersey.

Bushell, G.C., Yan, Y.D., Woodfield, D., Raper, J. and Amal, R. (2002) On techniques for the measurement of the mass fractal dimension of aggregates. *Advances in Colloid and Interface Science*, 95, p.1-50.

Cheryan, M. (1998) *Ultrafiltration and Microfiltration Handbook*, Technomic Publishing, Lancaster, P.A.

Chow, M.C. (1991) *Palm Oil Mil Effluent Analysis*, Palm Oil Research Institute of Malaysia, Kuala Lumpur, p.11-18.

Constantinides, A. and Mostoufi, N. (2000) *Numerical Methods for Chemical Engineers with MATLAB Applications*, Prentice Hall PTR, New Jersey, p.502-522.

Crittenden, J.C., Luft, P., Hand, D.W., Oravltz, J.L., Loper, S.W. and Arl, M. (1985) Prediction of multicomponent adsorption equilibria using ideal adsorbed solution theory. *Environ. Sci. Technol.*, 19, p.1037-1043.

Ding, A., Hounslow, M.J. and Biggs, C.A. (2006) Population balance modeling of activated sludge flocculation: Investigating the size dependence of aggregation, breakage and collision efficiency, *Chemical Engineering Science*, 61, p. 63-74.

Dubois, M., Gilles, K.A., Hamilton, J.K., Rebers, P.A. and Smith, F. (1956) Colorimetric method for determination of sugars and related substances. *Analytical Chemistry*, 28, p.350-356.

Environmental Quality Act 1974 (2005) Compiled by Legal Research Board, International Law Book Services, p. 49-62.

Flesch, J. C., Spicer, P.T. and Pratsinis, S.E. (1999) Laminar and turbulence shear-induced flocculation of fractal aggregates. *AIChE J.*, 45, p.1114-1124.

Fukuda, T., Yang, W., and Yamauchi, A. (2003) KCl transport mechanism across charged mosaic membrane in KCl-sucrose mixed system, *J. Membrane Sci.*, 212, p. 255-261.

Gauwbergen, D.V. and Baeyens, J. (1998) Modelling reverse osmosis by irreversible thermodynamics, *Separation and Purification Technology*, 13, p.117-128.

Geankoplis, C.J. (1993) *Transport Processes and Unit Operations*. 3rd ed. Prentice-Hall International, Inc, New Jersey, USA.

Gehlert, G., Adbulkadir, M., Fuhrmann, J. and Hapke, J. (2005) Dynamic modeling of an ultrafiltration module for use in a membrane bioreactor. *J. Memb. Sci.*, 248, 63-71.

Genes, P.G. (1981) Polymer solutions near an interface. 1. Adsorption and depletion layers. *Macromolecules*, 14, p.1637-1644.

Genes, P.G. (1982) Polymer solutions near an interface. 2. Interaction between two plates carrying adsorbed polymer layers. *Macromolecules*, 15, p.492-500.

Geraldes, V., Pereira, N.E. and Pinho, M.N. (2005) Simulation and optimization of medium-sized seawater reverse osmosis processes with spiral-wound modules. *Ind. Eng. Chem. Res.*, 44, p. 1897-1905.

Gerstlauer, A., Gahn, C., Zhou, H., Rauls, M. and Schreiber, M. (2006) Application of population balances in the chemical industry—current status and future needs, *Chemical Engineering Science*, 61, p. 205 – 217.

Hand, D., Crittenden, J., Hokanson, D. and Bulloch, J. (1997) Predicting the performance of fixed-bed granular activated carbon adsorbers, *Water Sci. Technol.*, 35, p. 235–241.

Ho, C.C., Tan, Y.K., and Wang, C.W. (1984) The Distribution of Chemical Constituents Between The Soluble and The Particulate Fractions of Palm Oil Mill Effluent and Its Significance on Its Utilization/Treatment, *J. Agricultural Wastes*, 11, p. 61

Ismail, S. (2005) Membrane separation technology for palm oil mill effluent (POME) treatment: an integrated approach, Ph.D thesis, Universiti Sains Malaysia.

Jain, S. and Gupta, S.K. (2004) Analysis of modified surface pore flow model with concentration polarization and comparison with Spiegler-Kedem model in reverse osmosis system, *J. Membrane Sci.*, 232, p.45-61.

Karode, S.K. (2001) Unsteady state flux response: a method to determine the nature of the solute and gel layer in membrane filtration. *J. Memb. Sci.*, 188, p.9-20.

Kimura, S. (1995) Analysis of reverse osmosis membrane behaviors in a long-term verification test, *Desalination*, 100, p.77-84.

Ko, D.C.K., Porter, J.F. and McKay, G. (2005) Application of the concentration-dependent surface diffusion model on the multicomponent fixed-bed adsorption systems, *Chemical Engineering Science*, 60, p. 5472 – 5479

Kumar, N.S.K., Yes, M.K. and Cheryan, M. (2004) Ultrafiltration of soy protein concentrate: performance and modeling of spiral and tubular polymeric modules. *J. Memb. Sci.*, 244, p.235-242.

Kumar, S. and Ramkrishna, D. (1996) On the solution of population balance equations by discretization: I. A fixed pivot technique. *Chem. Eng. Sci.*, 51, p.1311-1332.

Lee, J.W., Yang T.H., Shimb, W.G., Kwon T.O. and Moon, I.S. (2006) Equilibria and dynamics of liquid-phase trinitrotoluene adsorption on granular activated carbon: Effect of temperature and pH, *Journal of Hazardous Materials*, In Press.

Lee, V.K.C., Porter, J.F. and Mckay, G. (2005) Application of solid-phase concentration-dependent HSDM to the acid dye adsorption system. *AIChE J.*, 51, p.323-332.

Leung, W.F. (1998) Torque requirement for high-solids centrifugal sludge dewatering. *Filtration + Separation*, 35/9, p. 883-887.

Lo, I.M.C. and Alok, P.A. (1996) Computer simulation of activated carbon adsorption for multi-component systems. *Environment International*, 22, p.239.

Ma, A.N. (2000) Environment management for the palm oil industry. *Palm Oil Developments*, 30, 1-10

Mahabot, S. and Harun, A.R. (1986) *Effluent Treatment System for FELDA's Palm Oil Mill*, Technical Service Department, Kuala Lumpur.

Malaysian Palm Oil Board (MPOB) (2005). [Online]. (Accessed on 11th January 2007). Available from World Wide Web: http://www.mpob.gov.my

Maskan, F., Wiley, D.E., Johnston, L.P.M. and Clements, D.J. (2000) Optimal design of reverse osmosis module networks. *AIChE J.*, 46 (5), p. 946-954.

Mathew, A.P. and Weber, W.J.J. (1976) Effects of external mass transfer and intraparticle diffusion on adsorption rates in slurry reactors, *AIChE Symposium Series*, 73, p. 91-107.

Ministry of Energy, Water and Communications (2007) [Online], (Assessed 3th January 2007). Available from World Wide Web: http://www.ktak.gov.my.

Miorin, A.F. (1997) *Wastewater Treatment Plant Design*, Water Pollution Control Federation, USA.

Nere, N.K. and Ramkrishna, D. (2006) Solution of population balance equation with pure aggregation in a fully developed turbulent pipe flow, *Chemical Engineering Science*, 61, p. 96 – 103.

Pastagia, K.M., Chakraborty, S., DasGupta, S., Basu, J.K., and De, S. (2003) Prediction of permeate flux and concentration of two-component dye mixture in batch nanofiltration, *J. Membrane Sci.*, 218, p.195-210.

Perry, R.H. (1997) *Perry's Chemical Engineers' Handbook*. 7th ed. The McGraw-Hill Companies, Inc., New York.

Plantation Statistics (2006) [Online], (Assessed 28th November 2006). Available from World Wide Web: http://www.ioigroup.com.

Runkana, V., Somasundaran, P. and Kapur, P.C. (2004) Mathematical modeling of polymer-induced flocculation by charge neutralization. *Journal of Colloid and Interface Science*, 270, p. 347-358.

Runkana, V., Somasundaran, P. and Kapur, P.C. (2006) A population balance model for flocculation of colloidal suspensions by polymer bridging. *Chem. Eng. Sci.*, 61, p.182-191.

Slezak, A., Turczynski, B. and Nawrat, Z. (1989) Modification of the Kedem-Katchalsky-Zelman model equations of the transmembrane transport, *J. Non-Equlib. Thermodyn.*, 14, p.205-218.

Somasundaran, P. and Runkana, V. (2003) Modeling flocculation of colloidal mineral suspensions using population balances. *Int. J. Miner. Process.*, 72, p.33-55.

Sotelo, J.L., Uguina, M.A., Delgado, J.A. and Celemin, L.I. (2004) Adsorption of methyl ethyl ketone and trichloroethene from aqueous solutions onto activated carbon fixed-bed adsorbers. *Separation and Purification Technology*, 37, p.149-160.

Spicer, P.T. and Pratsinis, S.E. (1996) Coagulation and fragmentation: universal steady-state particle size distribution. *AIChE J.*, 42, p.1612-1620.

Sutzkover, I., Hasson D. and Semiat, R. (2000) Simple technique for measuring the concentration polarization level in a reverse osmosis system, *Desalination*, 131, p.117-127.

Tansel, B., Bao, W.Y. and Tansel, I.N. (2000) Characterization of fouling kinetics in ultrafilration systems by resistance in series model. *Desalination*, 129, 7-14.

Thill, A., Moustier, S., Aziz, J., Wiesner, M.R. and Bottero, J.Y. (2001) Flocs restructuring during aggregation: experimental evidence and numerical simulation. *Journal of Colloid and Interface Science*, 243, p.171-182.

Tien, C. (1994) *Adsorption Calculations and Modeling*, Butterworth-Heinemann, Boston, p.155-158.

Tu, S.C., Ravindran, V., Den, W. and Pirbazari, M. (2001) Predictive membrane trasport model for nanofiltration processes in water treatment, *AIChE J.*, 47, p.6.

Vincent, B. (1973) The van der Waals attraction between colloid particles having adsorbed layers II. Calculation of interaction curves. *J. Colloid Interface Sci.*, 42, p.270-285.

Wadley, S., Brouckaert, C.J., Baddock, L.A.D. and Buckley, C.A. (1995) Modelling of nanofiltration applied to the recovery of salt from waste brine at a sugar decolourisation plant, *J. Membrane Sci.*, 102, p.163.

Walker, N.C. (2000) The dry solids decanter centrifuge: capacity scaling. *Filtration + Separation*, 37/4, p. 28-32.

Walker, N.C. (2000a) The dry solids decanter centrifuge: conveyor torque and differential. *Filtration + Separation*, 37/8, p. 18-23.

Wikipedia (2007) [Online], (Assessed 24th January 2007). Available from World Wide Web: http://en.wikipedia.org

YAYASAN FELDA

LAPORAN KEWANGAN GERAN PENYELIDIKAN

(Tempoh : NOV 2004 hingga MEI 2007)

Tajuk Projek : Pilot plant studies for treatment of palm oil mill effluent (POME) using Membrane Technology.

A. **Kedudukan Geran**

(a) Jumlah Geran Penyelidikan Diluluskan : RM 220,000.00

(b) Amaun Geran Penyelidikan Diterima Sehingga Mei 2007 : RM 219,000.00

(c) Baki Geran Penyelidikan : RM 1000.00

B. **Rekod Perbelanjaan**

Perkara	Perbelanjaan (RM)		
	Peruntukan	Kumulatif sehingga Mei 2007	Baki
(i) Kos Penggajian Kakitangan Sokongan			
a) Pegawai Penyelidik : 2 (Pelajar PhD)	58,000.00	92,754.26	-34,754.26
(ii) Perjalanan / Pengangkutan	8050.00	16,977.65	-8,927.65
(iii) Penyewaan	750.00	0.00	750.00
(iv) Bahan/Bekalan Penyelidikan	21,150.00	58,080.24	-36,930.24
(v) Pengubahsuian dan baik Pulih Makmal/Kelengkapan	19,500.00	280.00	19,220.00
(vi) Peralatan Khas dan Aksesori	83,700.00	30,611.00	53,089.00
(vii) Lain-Lain			
b) Seminar Antarabangsa	24,450.00	19,179.50	5270.50
c) Komunikasi dan perhubungan	4400.00	1,117.35	3282.65
JUMLAH	220,000.00	219,000.00	1000.00

C. Jumlah dana yang diterima tetapi belum digunakan sehingga Mei 2007 - RM 0.00

D. Catatan :